NEUROINFLAMMATION AND NEURODEGENERATION AS MECHANISMS FOR WORSENED OUTCOMES IN ELDERLY TRAUMATIC BRAIN INJURY

By

©2007
Gregory A. Onyszchuk

B.Eng, McGill University, 1986

M.Sc., University of Quebec at Montreal, 1991

Submitted to the graduate degree program in Molecular and Integrative Physiology
and the Graduate Faculty of the University of Kansas
in partial fulfillment of the requirements for the degree of
Doctor of Philosophy

_____
Nancy E.J. Berman, Ph.D. Co-Chair

_____
William M. Brooks, Ph.D., Co-Chair

_____
Paul Cheney, Ph.D.

_____
Diane Durham, Ph.D.

_____
Randolph Nudo, Ph.D.

_____
John Stanford, Ph.D.

Date Defended: _____

The Dissertation Committee for Gregory Onyszchuk certifies
that this is the approved version of the following dissertation:

NEUROINFLAMMATION AND NEURODEGENERATION AS MECHANISMS FOR WORSENED OUTCOMES IN ELDERLY TRAUMATIC BRAIN INJURY

Committee:

Nancy E.J. Berman, Ph.D., Co-Chair

William M. Brooks, Ph.D., Co-Chair

Paul Cheney, Ph.D.

Diane Durham, Ph.D.

Randolph Nudo, Ph.D.

John Stanford, Ph.D.

Date Approved: _____

ACKNOWLEDGEMENTS

I am so very grateful to all those who have helped me with my research and non-research activities. Those include but are not limited to Dr. Yong-Yue He, Amber Dowell, Jennifer French of the Hoglund Brain Imaging Center, the Faculty and Staff of the Department of Integrative and Molecular Physiology, the Faculty and Staff of the Department of Anatomy and Cell Biology, and the Faculty and Staff of the office of Graduate Studies and Research. I would like to thank my committee members for their guidance and support. I would like to thank the members of the Berman lab for all of their support and assistance, especially with imaging measurements. Finally, I would like to thank my mentors Drs. Nancy Berman and Bill Brooks, for their guidance, support, and advice.

DEDICATION

To my fellow students and lab-members, thanks for making this challenging journey so enjoyable.

To my children, Ethan and Zachary, thanks for your youthful energy and all of those questions about what I am doing “down at the lab”.

To my parents, Anastasia and Mario, thanks for your interest, encouragement and editing assistance.

To my wife and partner, Barbara, embarking on this journey and fulfilling this dream would not have been possible without your untiring support and love.

“Twenty years from now you will be more disappointed by the things you didn't do than by the ones you did do. So throw off the bowlines. Sail away from the safe harbor. Catch the trade winds in your sails. Explore. Dream. Discover.” – Mark Twain

"Personally, I am always ready to learn, although I do not always like being taught."

- Winston Churchill

TABLE OF CONTENTS

LIST OF ABBREVIATIONS

BBB ..... Blood-Brain Barrier

CCI ..... Controlled Cortical Impact

GFAP ..... Glial Fibrillary Acidic Protein

Iba1 ..... Integrated Calcium Binding Adapter Protein-1

IgG ..... Immunoglobulin type G

MR ..... Magnetic Resonance

MRI ..... Magnetic Resonance Imaging

TBI ..... Traumatic Brain Injury

LIST OF FIGURES

ABSTRACT

It is only recently that clinical and epidemiological data has been reported about the particularly heavy burden of traumatic brain injury (TBI) in the elderly. With the expected growth in the world population over age 65, and the continued trends towards physically active lifestyles in this group, it is likely that the burden of TBI in the elderly will worsen.

While some progress has been made, we are still very far behind in understanding the molecular and cellular mechanisms of damage and repair following TBI. This is especially true in elderly TBI, in which very little pre-clinical research has been conducted.

In the present study, a mouse model of sensorimotor controlled cortical impact (CCI) injury was developed, using a computer-controlled electromechanical striker. This model was first characterized with adult (4-6 month old) mice, using behavioral testing, magnetic resonance (MR) imaging and histological assessments. The model was then used for experiments with groups of adult and aged (21-24 month old) mice, in order to compare functional deficits and recovery, transient brain pathology and histology between the groups, and to identify age-related differences in outcomes and their potential mechanisms.

It was found that sensorimotor deficits were greater, and recovery poorer, in the aged animals compared to the adult. Acute edema was prolonged, compromise of the blood-brain barrier was greater and prolonged, and neurodegeneration was greater in the aged animals compared to the adult. Not only was significantly increased neurodegeneration found at the site of injury in the aged brains, but subtly increased neurodegeneration was found in the aged hippocampus and thalamus - brain structures remote from but connected with the injured aged cortex. Overall astrocyte response in the aged hippocampus was blunted, possibly reflecting an increased vulnerability or reduced functional capacity of aged hippocampal astrocytes. Microglial response was subtly increased in aged hippocampus and thalamus, and trends over time suggested that in the aged brain, the microglial response in these structures following cortical injury may be increased chronically, as compared to the response in the adult brain.

These studies demonstrate age-related differences in edema, blood-brain barrier permeability and neuroinflammation in the aged brain. All of these mechanistic elements may represent opportunities for interventions targeted specifically to elderly TBI patients.

Chapter 1 - BACKGROUND AND SIGNIFICANCE

Introduction - The Public Health Burden of TBI in the Elderly

Traumatic Brain Injury (TBI) affects over 1.5 million Americans every year, and claims over 50,000 American lives (Kraus et al., 1984; Conroy and Kraus, 1988; Thurman and Guerrero, 1999). Three age groups are most affected by TBI are: 0-4 years, 15-24 years, and 65+ years (Thurman et al., 1999). Recently-published data indicate the rate of incidence of TBI-related hospitalization in the 65 years and older U.S. population is 156 in 100,000, higher than in any other age group (Coronado et al., 2005). It is estimated that the U.S. population between 75 and 84 years of age will more than double between 2000 and 2050, and that the population 85 years old and older will more than quadruple in the same period (http://www.census.gov/). Taken with the trends of increasing life expectancy, and more active lifestyles in the elderly, it is clear that the significant burden represented by TBI in the elderly is likely to further increase.

It is surprising that there is so little research being conducted to explore TBI in the elderly, given the magnitude of its burden. While there are thousands of reports of human and animal research in TBI (keyword search of http://www.ncbi.nlm.nih.gov/entrez/query.fcgi, keywords "traumatic brain injury"), the literature on TBI and the elderly is far more scant, and most reports do not document research on TBI mechanisms, they describe retrospective analyses of

human injuries and outcomes. Clearly, TBI in the elderly is a very significant problem that deserves fundamental research.

Outcomes After TBI

The characteristic pattern of impairment and recovery after TBI is often as follows: there is loss of consciousness (LOC), followed by a period of acute confusion and disorientation – most commonly referred to as post traumatic amnesia (PTA), followed by a recovery period (Sherer et al., 2000). The most recent TBI Fact Sheet published by the Center for Disease Control, provides the following on TBI outcomes: "TBI can cause a wide range of functional changes affecting thinking, sensation, language, and/or emotions. It can also cause epilepsy and increase the risk for conditions such as Alzheimer's disease, Parkinson's disease, and other brain disorders that become more prevalent with age" (http://www.cdc.gov/).

Given the heterogeneity seen in TBI pathology, it is not surprising that there is great variation in the specific deficits seen in individual patients. Despite this, some of the deficits are well correlated with the specific region of the brain that is damaged:

- damage to the anterior portion of the frontal lobes often results in deficits in executive function, in the planning and execution of what were previously routine tasks, and in mental flexibility,
- damage to the posterior portion of the frontal lobes can result in reduced ability to carry out motor tasks, hemiparesis, plegia, spasticity and aphasia,

- damage to the temporal lobes can yield deficits in the storing of new short term memories, in visual and verbal memory, and can produce increased irritability and aggression,
- damage to the parietal lobes can lead to problems in processing sensory information, difficulty in understanding language, and to patients getting lost in familiar and unfamiliar surroundings,
- damage to the occipital lobes can yield visual deficits, inability to recognize objects, and blindness,
- damage to the cerebellum can impair walking and coordinated use of upper extremities,
- diffuse axonal injury is associated with a generalized slowness in thinking and difficultly in getting things done.

This material is adapted from the document entitled: Veterans Health Initiative: Traumatic Brain Injury, available at (http://www.va.gov). Other non-localized neurobehavioral symptoms reported by TBI patients include headache, anxiety, difficulty concentrating, restlessness, and depression (Satz et al., 1998). A small subset of patients also experience late complications, including post-traumatic epilepsy and post-traumatic hydrocephalus (Sherer et al., 2000).

The CDC, in their 1999 publication, Traumatic Brain Injury in the United States: A Report to Congress, the CDC estimated that 35% of TBI patients experience long

term disability (also at http://www.cdc.gov/). Estimates of non return to work rates include 71% after 2 to 7 years for severe TBI (Brooks et al., 1987) and 36% after 2 years for moderate TBI (Dikmen et al., 1990).

There is strong evidence of worse outcomes from TBI in the elderly population. A 2003 U.S. study of 5600 human patients with severe TBI indicated that patients younger than 36 years showed a 21% mortality rate and a 39% rate of unfavorable outcome, whereas patients older than 55 years showed a 52% mortality rate and 74% rate of unfavorable outcome (Hukkelhoven et al., 2003). A study of severe blunt brain injury published in 1993 reported that 79% of elderly (age 60 and over) patients died in the hospital, compared with 36% of the patients in the age range 20 to 40 years. Furthermore, this study showed dramatically lower favorable outcome rates in the elderly group – 2% versus 36% for the younger patients (Pennings et al., 1993). Another study, of Californian patients with non-fatal fall-related traumatic brain injury, found that hospitalization rates were more than 3 times greater in patients aged 65 and above, and the proportion of admitted patients ultimately discharged with only self-care or unskilled care required was 86% in the 0-64 year old group and only 41% in the 65 and older group (Cross and Trent, 2003).

Pathophysiology of TBI

Traumatic brain injuries can range widely in their cause and context, and especially in their biomechanical characteristics. Thus, diverse pathologies may result,

individually or in combination, from any specific traumatic event. The main biomechanical forces studied are those of contact – where the head is struck or strikes a fixed object or surface, and acceleration/deceleration – where the head is subject to violent linear and/or rotational motion (King et al., 1995). In contact injuries, the size, shape, composition and relative velocity of the striking or struck object are important, as are the location of the contact and the resulting head motion. In acceleration/deceleration injuries, the magnitude and orientation of the acceleration are the most important, and many believe that rotational acceleration/deceleration, especially in the coronal plane, results in the greatest degree of damage (McLean and Anderson, 1997).

The terms "primary" and "secondary" have been used for decades in the clinical and research settings to define damage from TBI (Graham and Adams, 1971; Cooper, 1992; Graham et al., 2000). It is useful to consider several points to understand the concept expressed by these terms. Mendelow and Crawford, writing from a clinical viewpoint, where time is often of the essence in determining treatment options, define primary brain damage as damage that occurs at the time of impact, produces its clinical effect almost immediately and is refractory to most treatment. In contrast, secondary brain damage occurs at some time after the primary impact and is largely preventable and treatable (Mendelow and Crawford, 1997). The authors also offer that "understanding this concept prepares the non-specialist clinician for the main challenge in head injury management: the prevention and treatment of secondary

damage. It is therefore essential that all the causes and consequences of secondary brain damage are known and understood" (Mendelow and Crawford, 1997).

Blumbergs, writing from an anatomical viewpoint, defines primary damage as "the result of mechanical forces producing tissue deformation at the moment of injury", and secondary damage as damage that occurs as a complication of the different types of primary brain damage (Blumbergs, 1997). Primary damage is subdivided into diffuse axonal injury, diffuse vascular injury, focal vascular injury, focal axonal injury, contusion and laceration. Secondary damage is divided into diffuse hypoxic-ischemic damage, diffuse brain swelling, focal hypoxic-ischemic damage, and focal brain swelling. McIntosh, writing from a mechanistic perspective, describes secondary injury very simply as "delayed cell damage and death" (McIntosh et al., 1996).

Our knowledge of TBI mechanisms and their temporal characteristics is not exact, but a common progression of events following the injury is as follows: intracranial hematoma, with or without contusions, damage to small vessels adjacent to the injury, astrocyte swelling, cellular migration, failure of energy substrate supply leading to increased cellular damage, cytotoxic cerebral edema, sensitization of the glutamate-NMDA-receptor-calcium cascade, elevated levels of excitatory amino acids, free radical production, and the release of inflammatory mediators (Guha, 2004). This long list highlights a key characteristic in TBI: that damage is often complex and

multifaceted, that there are potentially many inter-dependent mechanisms involved in the ultimate anatomical, physiological and behavioral results.

Figure 1-1 depicts some of the events that follow TBI in human patients, at the structural and cellular levels, in a fashion intended to emphasize their relative timing and progression.

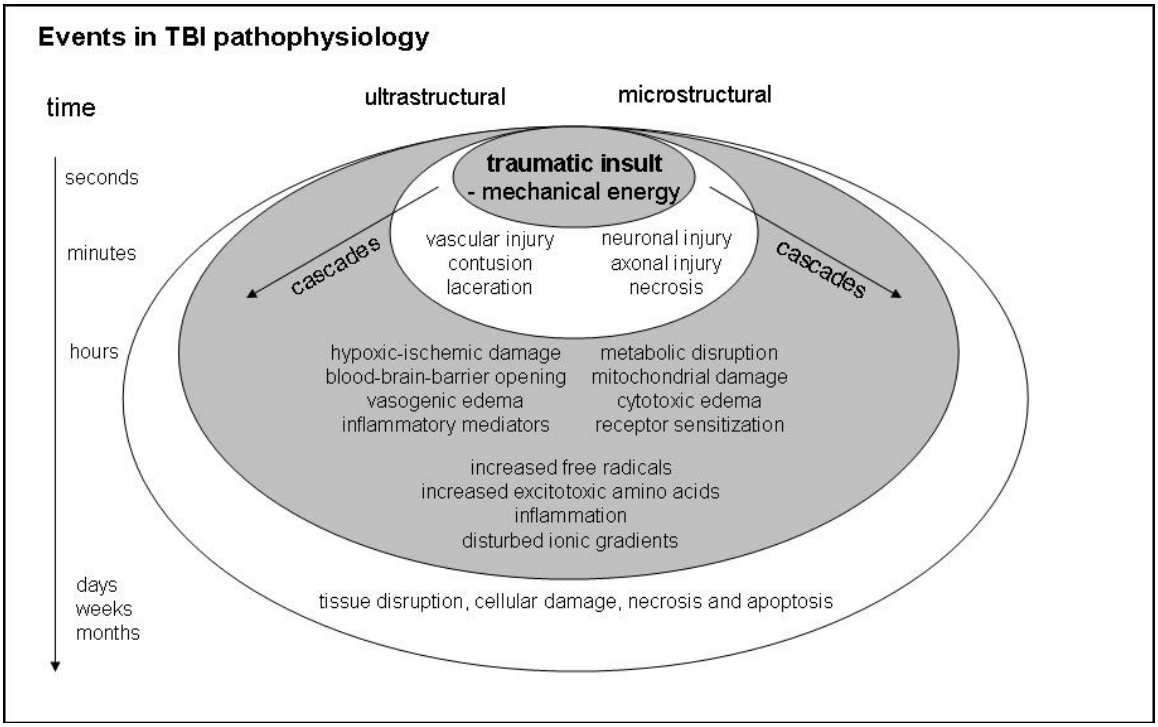

Figure 1-1: TBI Pathophysiology

Specific Damage Mechanisms

While a great many mechanisms have been implicated in the damage and cell death following TBI, a subset of these has received the most attention from the research

community. Here is a short summary of those mechanisms thought to play the most significant roles:

Ischemia, Disturbed Ionic Homeostasis, Excitoxicity

Most of what has been learned from animal models of focal ischemia has some relevance to necrotic cell death in TBI. In early work, it was found that ischemia stimulated anaerobic metabolism, lactate production, disruption of ionic gradients, the release of excitotoxic amino acids (including glutamate), cellular swelling and massive influx of Ca^{2+} into the cell (Tolias and Bullock, 2004). Calcium influx was followed by the release of reactive oxygen species, energy depletion and neuronal cell death. In fact calcium was, in earlier work, considered to be the "final common pathway" in cell death from central nervous system injury (Young, 1992). It is now understood that there are a number of other damage mechanisms that may be stimulated by changes in intracellular calcium levels, including the proteolysis of cytoskeletal proteins by calpains (Newcomb et al., 1997), and changes in mitochondrial permeability (Xiong et al., 1997).

There have been significant efforts in clinical trials to address excitoxicity and calcium-related mechanisms, including calcium channel blockers (European Study Group, 1994) and N-methyl-d-aspartate (NMDA)-receptor antagonists (Bullock et al., 1992), with limited success. Management of cerebral perfusion pressure (CPP) has been studied in TBI, particularly in the context of attempting to prevent secondary

ischemic insults. One study completed in 1999 found no significant difference in outcome between a group of patients with CPP maintained above 70mm Hg and a group with CPP kept above 50mm Hg (McKinley et al., 1999).

Reactive Oxygen Species

In addition to calcium-mediated release of the reactive oxygen species (ROS) from the mitochondria, it is thought that, after TBI, ROS can be produced by arachidonic acid cascade, by cytoplasmic generation, through activation of monoamine oxidase, cyclo-oxygenase or nitric oxide synthase or even by excitatory amino acids (McIntosh et al., 1998b). ROS can cause peroxidative destruction of the cell membrane, they can oxidize cellular proteins and nucleic acids, and they can attack the cerebrovasculature (McIntosh et al., 1998a).

Some of the compounds targeting ROS, peroxidative and oxidative damage mechanisms that have undergone clinical trials include corticosteroids (Roberts, 2001), superoxide dismutases (Narayan et al., 2002) and lipid membrane peroxidase inhibitors (Marshall et al., 1998).

Edema

Edema is one of the most commonly seen and earliest-described consequences of TBI. Brain edema is very simply defined as the abnormal accumulation of fluid within the brain parenchyma. In the context of TBI, brain edema is said to be

"influenced by a concert of complex molecular and cellular, structural and functional changes in blood–brain barrier (BBB) function, microcirculation, cell volume regulation and autodestructive mediators" (Unterberg et al., 1997). Vasogenic edema after TBI, especially after BBB compromise in the acute post-traumatic period from focal injuries, has been extensively studied. It is characterized by "protein-rich exudate derived from plasma resulting from an increased permeability of the capillary endothelial cells to albumin and other plasma proteins (Betz et al., 1989). Cytotoxic edema, as mentioned above, can follow directly from intracellular Ca^{2+} influx, and is characterized by sustained intracellular water accumulation involving both astrocytes and neurons that occurs independently of the BBB integrity (Unterberg et al., 1997).

Some of the compounds targeting edema in clinical trials include corticosteroids and a non-psychotropic cannabinoid, dexanabinol. Dexanabinol acts as a NMDA receptor antagonist, an antioxidant and as a cytokine inhibitor (Lavie et al., 2001). A recently completed randomized, placebo-controlled worldwide clinical trial (CRASH), involving over 10,000 patients found that corticosteroid injection within 48 hours of injury actually increased the risk of death (Roberts et al., 2004).

Diffuse Axonal Injury

Among the first studies of diffuse axonal injury (DAI) or traumatic axonal injury (TAI) are the works of Holbourn in 1943 and Strich in 1956, in which evidence was developed to show that acceleration/deceleration forces could cause widespread

damage by the stretching and shearing of blood vessels and neurons (Gaetz, 2004). While originally associated with severe TBI, more recent evidence suggests that DAI is present in over 90% of TBI cases (Gentleman et al., 1995). Although early work suggested that axons were actually torn by the mechanical energy at the moment of trauma, there is more recent evidence to the contrary, suggesting that a progressive disruption of the axonal membrane occurs, mediated by mitochondrial events (Pettus et al., 1994; Maxwell et al., 1997). If a progressive disruption occurs, then perhaps a window for intervention exists, and so several compounds targeting mitochondrial mechanisms are being advanced toward human trials, including N-type voltage-sensitive calcium channel blockers (Verweij et al., 2000) and mitochondrial transition pore formation blockers (Okonkwo and Povlishock, 1999).

Inflammation

Inflammatory mechanisms continue to be a significant focus of research into TBI mechanisms. In fact, some researchers have begun to describe TBI as an inflammatory condition (Schmidt et al., 2005). There is strong evidence of intracerebral accumulation of leukocytes and lymphocytes after TBI, presumably facilitated by BBB disruption (Perry et al., 1997). Equally, there is strong evidence for macrophages, microglia, natural killer cells, helper T-cells and T-cytotoxic suppressor cells in the brain parenchyma after TBI (Holmin et al., 1997; Holmin et al., 1998; Lenzlinger et al., 2001b). Macrophages and microglia are thought to be key players in the resulting inflammatory cascade, releasing ROS and pro-inflammatory

cytokines (Thomas, 1992). Perhaps most interesting about inflammation in the context of TBI is that there is emerging evidence of a "duality", in which it is thought that inflammation may play a damaging role early on in the progression of neuron damage and death, and then a beneficial role in initiation of the regenerative response (Lenzlinger et al., 2001a; Schmidt et al., 2005).

Despite focused efforts to study inflammation after TBI, and despite the identification of key cytokine molecules, such as TNF-α, IL-1, IL-6 and TGF-β, our knowledge of the detailed nature and timing of the inflammatory mechanisms has not yet advanced sufficiently to yield clinical trials of inflammation-specific compounds, although there have been trials in stroke for IL-1 receptor agonists (Emsley et al., 2005).

In the context of this project, inflammation is of particular interest, not only for its potential role in neuron death, but also as a potential mechanism for impairment of neural function. There is evidence that inflammatory cytokines are involved in normal neural function, including synaptic plasticity and neural transmission (Vitkovic et al., 2000). The potential mechanisms by which cytokines may be involved in behavioral and cognitive impairment include demyelination, impaired nutrient intake, neurotransmitter dysregulation, reactive oxygen and nitrogen species, RAGE receptor activation, apoptosis, vascular insult (Wilson et al., 2002).

Current Clinical Trials

As of October 15, 2007, only 5 open trials of specific therapies/agents are listed at the NIH clinical trials website (http://www.clinicaltrials.gov) within the "brain injury" category: hypothermia, enriched oxygen, hypertonic saline, diclofenac, and ketamine.

Hypothermia is interesting in TBI for its potential to reduce excitotoxicity, reduce inflammation, and increase antioxidant activity. A large U.S. trial failed to show benefit, but a new trial (NABIS:H2) is underway with a much more restrictive protocol, testing only if outcome is improved by surface-induced moderate hypothermia in patients aged 16-45 with low admission temperature (Clifton, 2004; Adelson et al., 2005).

Hyperbaric oxygen treatment (HBOT), in early work, was found, in patients with severe TBI, to improve cerebral aerobic metabolism and reduce elevated intracranial pressure. HBOT may allow the brain to make more efficient use of increased amounts of oxygen (Rockswold et al., 2007; Zhou et al., 2007). In early clinical studies, increased inspired oxygen concentration has been found to improve mitochondrial function and improve neurobehavioral outcome (Menzel et al., 1999). A Phase II trial is evaluating the effects of there two treatments seperately and in combination.

Hypertonic saline, administered to counteract is already in limited use for its potential to increase blood pressure, reduce increased intracranial pressure (ICP) and restore

blood flow in trauma patients with substantial blood loss (Tyagi et al., 2007). Current trials are focused on studying different dose and infusion methods.

Diclofenac acts to reduce pyrexia and fever and may, for patients with acute cerebral injury, improve intracranial pressure and limit secondary damage (Cormio and Citerio, 2007).

Ketamine, a short-acting anesthetic drug, is in use for a variety of pediatric emergency department procedures, including for the treatment of burn victims and for fracture reduction (Tobias, 2005). Ketamine is thought not to decrease blood pressure, and may actually decrease intracranial pressure, a common complication in head trauma (Leone et al., 2006). In a small non-randomized, non-control interventional trial with pediatric TBI patients, single doses of ketamine are being evaluated for their effect on ICP and cerebral perfusion pressure (CPP).

Interestingly, there are no current or completed clinical trials listed for TBI interventions that have specifically targeted the elderly population.

Relevance and review of rodent models of TBI

Animal models have been used to study TBI for over 50 years. The goal of any animal model of TBI is to replicate one or more of the clinically-relevant features of human TBI, and to allow for straightforward evaluation, analysis, and interpretation

(Finnie, 2001). Implicit in the use of a model is the assumption that the mechanism of injury is not of primary importance as long as the lesion or damage created is of sufficient similarity to that found in human TBI patients.

For impact injury models, pioneering work was published by Denny-Brown and Russell (Denny-Brown and Russell, 1941). For acceleration/deceleration injury models, Ommaya and Gennarelli were among the early innovators, with Ommaya the first to publish (Ommaya, 1963). More recently, rodent models have become the most popular for TBI research, given the economy and availability of these animals, and the opportunity for the use of genetically modified strains.

Gennarelli, in his seminal review of animal models or TBI (Gennarelli, 1994), describes the most common types of injuries seen in human patients, and provides a view on the utility of ten different animal models for study of those injury types. The injury types cited by Gennarelli are: concussion, axonal injury, brain swelling, contusion, acute subdural hematoma, intracerebral hematoma, and skull fracture. Gennarelli's review emphasizes the point that human TBI patients often present with multiple injuries, and the complexity and heterogeneity of the injuries are well accounted for in simpler animal models. This review also shows how, in 1993, there were few models judged effective for the study of focal contusions in TBI, a need that has since been addressed with the increase in popularity of the controlled cortical impact model.

Laurer, Lenzinger and McIntosh, in their more recent review of "mechanical energy" animal models of TBI (Laurer and McIntosh, 1999), classify human head injury into "focal" and "diffuse". "Focal" describes injuries that involve contusions and lacerations, often with hematoma, in the direct vicinity of the site of mechanical impact. The popular animal models that mimic focal injury are: weight drop closed head, fluid percussion, and rigid indentation / controlled cortical impact. "Diffuse" is used to describe diffuse brain swelling, ischemic brain damage and diffuse axonal injury, occurring primarily from tissue distortion and shear, caused by inertial forces present at the moment of injury. Here the popular models cited are inertial acceleration and impact acceleration. These authors claim that there is growing evidence that many animal models, unlike previously thought, produce some form of primary or secondary diffuse injury. Thus, animal models do involve a greater degree of complexity than originally believed.

There has been some controversy over the use of rodent models for the study of TBI and its mechanisms, particularly since so many therapeutic interventions tested in these animals have failed to translate successfully in human trials. Cenci, Whishaw and Schallert write in defense of rat models of TBI (and stroke), that, similar to human cases, the models can produce "focal and widespread secondary damage to the brain, which can yield acute and chronic impairments of sensory, motor and cognitive functions" (Cenci et al., 2002). The authors also make a very strong case that it is

vital to select sensitive and reliable behavioral measurements for any study, especially if results are to be translated to the human context. These points are likely all valid for mouse models of TBI.

Mouse controlled cortical impact TBI model

Controlled cortical impact was first described by Lighthall in 1988, as a model for focal contusions in the ferret (Lighthall, 1988). Originally, the model used a pneumatically actuated cylinder to deliver a very short duration direct mechanical impact to the animal's exposed dura mater via a small diameter polished metal tip.

Subsequently, this model was adapted for other species, by Dixon for the rat (Dixon et al., 1991) and by Smith for the mouse (Smith et al., 1995). Different impactor devices have been implemented in order to improve consistency and to control more effectively the mechanical parameters of the impact. Most uses of CCI today involve a lateral model, in contrast to Lighthall's original experiments where a midline injury was performed.

Our understanding of the damage produced by CCI in mice and rats has continued to progress over the last 10 years. With the availability and economy of laboratory mice, and the opportunity to use genetically engineered mice, mouse models of TBI have continued to grow in popularity.

Early studies established that there is cortical damage proportional to the velocity of impact and the depth of cortical penetration (ref Dixon, ref Smith). In addition, damage was noted in the hippocampal and thalamic areas. For moderate and severe CCI, damage in the contralateral cortex and hippocampus has been reported (Kochanek et al., 1995; Baskaya et al., 1996). Motor, sensory and cognitive deficits have been measured, with different degrees and latencies, according to injury severity and location (Smith et al., 1995; Fox et al., 1998; Hannay et al., 1999).

Work very recently published by Hall (Hall et al., 2005), highlights the value of the mouse CCI model, including its potential to yield detailed data on neurodegeneration. The authors established a comprehensive time course of ipsilateral and contralateral damage for severe TBI, documenting for 6 time points from 6 to 168 hours after injury, the neurodegeneration seen in cortex, in the CA1, CA3 and dentate gyrus regions of the hippocampus, in the thalamus, and the corpus callosum. This study used de Olmos silver staining to examine deteriorating neurons and their processes. The study did not include any behavioral assessments, but the authors provide a solid analysis of their results and make many convincing arguments for potential correlations between the damage they observed and the behavioral deficits that have been documented in other mouse CCI studies.

Background on MRI, Image Contrast and Edema

In some of the earliest work on human brain MRI, published in 1982, images from 13 normal individuals and 140 patients with a wide variety of neurological disorders were examined and compared with computed tomography (CT) scans. In this work, it was recognized and reported that spin echo sequences were of "particular value in demonstrating acute and space-occupying lesions as well as cerebral edema" (Bydder et al., 1982). Work in cats, dogs and non-human primates was published shortly thereafter, using different experimental models of brain edema and ischemia (Spetzler et al., 1983; Brant-Zawadzki et al., 1984; Bartkowski et al., 1985; Shirakuni et al., 1985). Here, the ability of MRI, and specifically spin echo T2-weighted images, to detect edema was further confirmed. Measurements taken from MR images were compared with water content measurements obtained from microgravimetric assays of excised tissues to establish the definitive correlation between T2-weighted signal hyperintensity and edema.

The reason that edema appears bright in a T2-weighted image of the brain is explained by the mechanisms of contrast in MRI images. Image contrast, or the appearance of areas of greater (white or brighter grey) and lesser (black or darker grey) signal, is a result of fundamental biological properties of living tissue: the hydrogen spin density, T1 and T2 values (Hendrick, 1999). T1 and T2 values (relaxation times) are time constants that describe how the longitudinal and transverse

magnetization of the hydrogen nuclei in the imaged tissue return to equilibrium after being perturbed by a radio frequency (RF) pulse (Wood and Wehrli, 1999).

In a T2-weighted image, tissues with greater T2 values appear bright, whereas in a T1-weighted image, tissues with shorter T1 values appear bright. Since water has a relatively long transverse relaxation time (higher T2 value), and a relatively long relaxation time (higher T1 value) than those of the brain parenchyma, water (and edematous tissue with its increased water content) appears bright on T2-weighted images and dark on T1-weighted images. Detailed equations that relate inherent tissue contrast and image contrast with T1, T2 and hydrogen spin density values are given in (Hendrick, 1999).

Aging and the brain

The study of changes and degeneration in the human brain with aging is an active field of research. While many questions remain unanswered, several broad concepts have emerged that may be important in a study of TBI and aging.

In the aging brain, there is "progressive accumulation of damaged molecules and impaired energy metabolism in brain cells" (Mattson et al., 2002a). There is also evidence of neuronal loss, of reduced dendritic complexity and of "synaptic compromise" (Hof, 1997). There is also evidence for altered levels of neurotrophins, neurotransmitters, and cytokines (Mattson et al., 2002b). There is increased oxidative

stress (Floyd and Hensley, 2002), altered calcium homeostasis mechanisms, increased mitochondrial function and altered regulation of apoptosis (Benn and Woolf, 2004).

Aging and the inflammatory response

Inflammation in the brain, and especially the role of cytokines as inflammatory mediators, are active fields of research, as are aging and inflammation. Linkages between neurodegenerative disorders, inflammation and aging are becoming clearer. There is strong evidence that inflammation plays a key role in Alzheimer's disease, Parkinson's disease, Amyotrophic Lateral Sclerosis (ALS), Multiple Sclerosis (MS) and Huntington's disease (Beal, 1995). There is also strong evidence that certain inflammatory mediators and markers are in greater abundance in older brains (Gomez et al., 2005). The term "inflamm-aging" has been used to describe the pro-inflammatory status that characterizes aging (Franceschi et al., 2000).

Recent evidence by Berman and Sandhir (Sandhir et al., 2004), from a cortical lesion mouse model, highlights the importance of inflammation and of the cytokine MCP-1 in damage seen from cortical injury in the aged brain. If inflammation is an important mechanism in the damage associated with TBI, and if the inflammatory response is increased in aged brains, it is possible that differences in inflammation could explain the differences in damage and outcome from TBI in elderly patients.

Study Rationale

The financial and social costs associated with TBI are enormous. Surprisingly, few interventions are available to reduce damage and improve outcome after TBI. As yet, there have been few successes in clinical trials of new pharmacological compounds and medical therapies. It is likely that the failure of clinical trials is as least partly due to our lack of a sufficiently detailed understanding of the many and complex mechanisms of TBI damage and repair.

TBI incidence has a tri-modal age distribution, with peaks in the following age groups: 0-4 years, 15-24 years and over 65 years. Although some research in pediatric TBI is underway, little work has been done to explore how TBI damage at the tissue, cellular and molecular levels may be different in the elderly population, in which incidence and outcomes are worse than in any other age group.

Because we are in the very early stages of using animals in research to study age-related TBI, this study will have a significant descriptive element, in addition to the mechanistic investigations that are outlined. It is expected that this work will provide a strong foundation for additional studies of mechanisms of TBI in the elderly.

There is strong evidence from human patients showing that inflammation is an important mechanism in the pathophysiology after TBI. Likewise, there is growing evidence that the aged brain is more susceptible to inflammation. Therefore, it is the

overall intent of this study to explore the age-related effects of the inflammatory response after TBI.

REFERENCES

Adelson PD, Ragheb J, Kanev P, Brockmeyer D, Beers SR, Brown SD, Cassidy LD, Chang Y, Levin H (2005) Phase II clinical trial of moderate hypothermia after severe traumatic brain injury in children. Neurosurgery 56:740-754; discussion 740-754.

Bartkowski HM, Pitts LH, Nishimura M, Brant-Zawadzki M, Moseley M, Young G (1985) NMR imaging and spectroscopy of experimental brain edema. J Trauma 25:192-196.

Baskaya MK, Rao AM, Prasad MR, Dempsey RJ (1996) Regional activity of ornithine decarboxylase and edema formation after traumatic brain injury. Neurosurgery 38:140-145.

Beal MF (1995) Aging, energy, and oxidative stress in neurodegenerative diseases. Ann Neurol 38:357-366.

Benn SC, Woolf CJ (2004) Adult neuron survival strategies--slamming on the brakes. Nat Rev Neurosci 5:686-700.

Betz AL, Iannotti F, Hoff JT (1989) Brain edema: a classification based on blood-brain barrier integrity. Cerebrovasc Brain Metab Rev 1:133-154.

Blumbergs P (1997) Pathology. In: Head Injury (Reilly P, Bullock R, eds). London: Chapman.

Brant-Zawadzki M, Bartkowski HM, Ortendahl DA, Pitts LH, Hylton NM, Nishimura MC, Crooks LE (1984) NMR in experimental cerebral edema: value of T1 and T2 calculations. AJNR Am J Neuroradiol 5:125-129.

Brooks N, McKinlay W, Symington C, Beattie A, Campsie L (1987) Return to work within the first seven years of severe head injury. Brain Inj 1:5-19.

Bullock R, Kuroda Y, Teasdale GM, McCulloch J (1992) Prevention of post-traumatic excitotoxic brain damage with NMDA antagonist drugs: a new strategy for the nineties. Acta Neurochir Suppl (Wien) 55:49-55.

Bydder GM, Steiner RE, Young IR, Hall AS, Thomas DJ, Marshall J, Pallis CA, Legg NJ (1982) Clinical NMR imaging of the brain: 140 cases. AJR Am J Roentgenol 139:215-236.

Cenci MA, Whishaw IQ, Schallert T (2002) Animal models of neurological deficits: how relevant is the rat? Nat Rev Neurosci 3:574-579.

Clifton GL (2004) Is keeping cool still hot? An update on hypothermia in brain injury. Curr Opin Crit Care 10:116-119.

Conroy C, Kraus JF (1988) Survival after brain injury. Cause of death, length of survival, and prognostic variables in a cohort of brain-injured people. Neuroepidemiology 7:13-22.

Cooper PR (1992) Delayed traumatic intracerebral hemorrhage. Neurosurg Clin N Am 3:659-665.

Cormio M, Citerio G (2007) Continuous low dose diclofenac sodium infusion to control fever in neurosurgical critical care. Neurocrit Care 6:82-89.

Coronado VG, Thomas KE, Sattin RW, Johnson RL (2005) The CDC traumatic brain injury surveillance system: characteristics of persons aged 65 years and older hospitalized with a TBI. J Head Trauma Rehabil 20:215-228.

Cross J, Trent R (2003) Public Health and Aging: Nonfatal Fall-Related Traumatic Brain Injury Among Older Adults --- California, 1996--1999. Mortality and Morbidity Weekly Report 52:278-280.

Denny-Brown D, Russell WR (1941) Traumatic shock in experimental cerebral concussion. Proceedings of the Physiological Society Journal of Physiology 99:6-7.

Dikmen S, Machamer J, Temkin N, McLean A (1990) Neuropsychological recovery in patients with moderate to severe head injury: 2 year follow-up. J Clin Exp Neuropsychol 12:507-519.

Dixon CE, Clifton GL, Lighthall JW, Yaghmai AA, Hayes RL (1991) A controlled cortical impact model of traumatic brain injury in the rat. J Neurosci Methods 39:253-262.

Emsley HC, Smith CJ, Georgiou RF, Vail A, Hopkins SJ, Rothwell NJ, Tyrrell PJ (2005) A randomised phase II study of interleukin-1 receptor antagonist in acute stroke patients. J Neurol Neurosurg Psychiatry 76:1366-1372.

European Study Group (1994) A multicenter trial of the efficacy of nimodipine on outcome after severe head injury J Neurosurg 80:797-804.

Finnie J (2001) Animal models of traumatic brain injury: a review. Aust Vet J 79:628-633.

Floyd RA, Hensley K (2002) Oxidative stress in brain aging. Implications for therapeutics of neurodegenerative diseases. Neurobiol Aging 23:795-807.

Fox GB, Fan L, Levasseur RA, Faden AI (1998) Sustained sensory/motor and cognitive deficits with neuronal apoptosis following controlled cortical impact brain injury in the mouse. J Neurotrauma 15:599-614.

Franceschi C, Bonafe M, Valensin S, Olivieri F, De Luca M, Ottaviani E, De Benedictis G (2000) Inflamm-aging. An evolutionary perspective on immunosenescence. Ann N Y Acad Sci 908:244-254.

Gaetz M (2004) The neurophysiology of brain injury. Clin Neurophysiol 115:4-18.

Gennarelli TA (1994) Animate models of human head injury. J Neurotrauma 11:357-368.

Gentleman SM, Roberts GW, Gennarelli TA, Maxwell WL, Adams JH, Kerr S, Graham DI (1995) Axonal injury: a universal consequence of fatal closed head injury? Acta Neuropathol (Berl) 89:537-543.

Gomez CR, Boehmer ED, Kovacs EJ (2005) The aging innate immune system. Curr Opin Immunol.

Graham DI, Adams JH (1971) Ischaemic brain damage in fatal head injuries. Lancet 1:265-266.

Graham DI, McIntosh TK, Maxwell WL, Nicoll JA (2000) Recent advances in neurotrauma. J Neuropathol Exp Neurol 59:641-651.

Guha A (2004) Management of traumatic brain injury: some current evidence and applications. Postgrad Med J 80:650-653.

Hall ED, Sullivan PG, Gibson TR, Pavel KM, Thompson BM, Scheff SW (2005) Spatial and temporal characteristics of neurodegeneration after controlled cortical impact in mice: more than a focal brain injury. J Neurotrauma 22:252-265.

Hannay HJ, Feldman Z, Phan P, Keyani A, Panwar N, Goodman JC, Robertson CS (1999) Validation of a controlled cortical impact model of head injury in mice. J Neurotrauma 16:1103-1114.

Hendrick R (1999) Image Contrast and Noise. In: Magnetic Resonance Imaging, 3rd Edition (Stark D, Bradley W, eds). St. Louis: Mosby.

Hof PR (1997) Morphology and neurochemical characteristics of the vulnerable neurons in brain aging and Alzheimer's disease. Eur Neurol 37:71-81.

Holmin S, Soderlund J, Biberfeld P, Mathiesen T (1998) Intracerebral inflammation after human brain contusion. Neurosurgery 42:291-298; discussion 298-299.

Holmin S, Schalling M, Hojeberg B, Nordqvist AC, Skeftruna AK, Mathiesen T (1997) Delayed cytokine expression in rat brain following experimental contusion. J Neurosurg 86:493-504.

Hukkelhoven CW, Steyerberg EW, Rampen AJ, Farace E, Habbema JD, Marshall LF, Murray GD, Maas AI (2003) Patient age and outcome following severe traumatic brain injury: an analysis of 5600 patients. J Neurosurg 99:666-673.

King AI, Ruan JS, Zhou C, Hardy WN, Khalil TB (1995) Recent advances in biomechanics of brain injury research: a review. J Neurotrauma 12:651-658.

Kochanek PM, Marion DW, Zhang W, Schiding JK, White M, Palmer AM, Clark RS, O'Malley ME, Styren SD, Ho C, et al. (1995) Severe controlled cortical impact in rats: assessment of cerebral edema, blood flow, and contusion volume. J Neurotrauma 12:1015-1025.

Kraus JF, Black MA, Hessol N, Ley P, Rokaw W, Sullivan C, Bowers S, Knowlton S, Marshall L (1984) The incidence of acute brain injury and serious impairment in a defined population. Am J Epidemiol 119:186-201.

Laurer HL, McIntosh TK (1999) Experimental models of brain trauma. Curr Opin Neurol 12:715-721.

Lavie G, Teichner A, Shohami E, Ovadia H, Leker RR (2001) Long term cerebroprotective effects of dexanabinol in a model of focal cerebral ischemia. Brain Res 901:195-201.

Lenzlinger PM, Morganti-Kossmann MC, Laurer HL, McIntosh TK (2001a) The duality of the inflammatory response to traumatic brain injury. Mol Neurobiol 24:169-181.

Lenzlinger PM, Hans VH, Joller-Jemelka HI, Trentz O, Morganti-Kossmann MC, Kossmann T (2001b) Markers for cell-mediated immune response are elevated in cerebrospinal fluid and serum after severe traumatic brain injury in humans. J Neurotrauma 18:479-489.

Leone M, Visintini P, Alliez JR, Albanese J (2006) [What sedation for prevention and treatment secondary brain insult?]. Ann Fr Anesth Reanim 25:852-857.

Lighthall JW (1988) Controlled cortical impact: a new experimental brain injury model. J Neurotrauma 5:1-15.

Marshall LF, Maas AI, Marshall SB, Bricolo A, Fearnside M, Iannotti F, Klauber MR, Lagarrigue J, Lobato R, Persson L, Pickard JD, Piek J, Servadei F, Wellis GN, Morris GF, Means ED, Musch B (1998) A multicenter trial on the efficacy of using tirilazad mesylate in cases of head injury. J Neurosurg 89:519-525.

Mattson MP, Chan SL, Duan W (2002a) Modification of brain aging and neurodegenerative disorders by genes, diet, and behavior. Physiol Rev 82:637-672.

Mattson MP, Duan W, Chan SL, Cheng A, Haughey N, Gary DS, Guo Z, Lee J, Furukawa K (2002b) Neuroprotective and neurorestorative signal transduction mechanisms in brain aging: modification by genes, diet and behavior. Neurobiol Aging 23:695-705.

Maxwell WL, Povlishock JT, Graham DL (1997) A mechanistic analysis of nondisruptive axonal injury: a review. J Neurotrauma 14:419-440.

McIntosh TK, Smith DH, Garde E (1996) Therapeutic approaches for the prevention of secondary brain injury. Eur J Anaesthesiol 13:291-309.

McIntosh TK, Juhler M, Wieloch T (1998a) Novel pharmacologic strategies in the treatment of experimental traumatic brain injury: 1998. J Neurotrauma 15:731-769.

McIntosh TK, Saatman KE, Raghupathi R, Graham DI, Smith DH, Lee VM, Trojanowski JQ (1998b) The Dorothy Russell Memorial Lecture. The molecular and cellular sequelae of experimental traumatic brain injury: pathogenetic mechanisms. Neuropathol Appl Neurobiol 24:251-267.

McKinley BA, Parmley CL, Tonneson AS (1999) Standardized management of intracranial pressure: a preliminary clinical trial. J Trauma 46:271-279.

McLean A, Anderson R (1997) Biomechanics of Closed Head Injury. In: Head Injury (Reilly P, Bullock R, eds). London: Chapman.

Mendelow A, Crawford P (1997) Primary and Secondary Brain Injury. In: Head Injury (Reilly P, Bullock R, eds). London: Chapman.

Menzel M, Doppenberg EM, Zauner A, Soukup J, Reinert MM, Bullock R (1999) Increased inspired oxygen concentration as a factor in improved brain tissue oxygenation and tissue lactate levels after severe human head injury. J Neurosurg 91:1-10.

Narayan RK, Michel ME, Ansell B, Baethmann A, Biegon A, Bracken MB, Bullock MR, Choi SC, Clifton GL, Contant CF, Coplin WM, Dietrich WD, Ghajar J, Grady SM, Grossman RG, Hall ED, Heetderks W, Hovda DA, Jallo J, Katz RL, Knoller N, Kochanek PM, Maas AI, Majde J, Marion DW, Marmarou A, Marshall LF, McIntosh TK, Miller E, Mohberg N, Muizelaar JP, Pitts LH, Quinn P, Riesenfeld G, Robertson CS, Strauss KI, Teasdale G, Temkin N, Tuma R, Wade C, Walker MD, Weinrich M, Whyte J, Wilberger J, Young

AB, Yurkewicz L (2002) Clinical trials in head injury. J Neurotrauma 19:503-557.

Newcomb JK, Kampfl A, Posmantur RM, Zhao X, Pike BR, Liu SJ, Clifton GL, Hayes RL (1997) Immunohistochemical study of calpain-mediated breakdown products to alpha-spectrin following controlled cortical impact injury in the rat. J Neurotrauma 14:369-383.

Okonkwo DO, Povlishock JT (1999) An intrathecal bolus of cyclosporin A before injury preserves mitochondrial integrity and attenuates axonal disruption in traumatic brain injury. J Cereb Blood Flow Metab 19:443-451.

Ommaya AK (1963) Head injuries: aspects and problems. Med Ann Dist Columbia 32:18-22.

Pennings JL, Bachulis BL, Simons CT, Slazinski T (1993) Survival after severe brain injury in the aged. Arch Surg 128:787-793; discussion 793-784.

Perry VH, Anthony DC, Bolton SJ, Brown HC (1997) The blood-brain barrier and the inflammatory response. Mol Med Today 3:335-341.

Pettus EH, Christman CW, Giebel ML, Povlishock JT (1994) Traumatically induced altered membrane permeability: its relationship to traumatically induced reactive axonal change. J Neurotrauma 11:507-522.

Roberts I (2001) The CRASH trial: the first large-scale, randomised, controlled trial in head injury. Crit Care 5:292-293.

Roberts I, Yates D, Sandercock P, Farrell B, Wasserberg J, Lomas G, Cottingham R, Svoboda P, Brayley N, Mazairac G, Laloe V, Munoz-Sanchez A, Arango M, Hartzenberg B, Khamis H, Yutthakasemsunt S, Komolafe E, Olldashi F, Yadav Y, Murillo-Cabezas F, Shakur H, Edwards P (2004) Effect of intravenous corticosteroids on death within 14 days in 10008 adults with clinically significant head injury (MRC CRASH trial): randomised placebo-controlled trial. Lancet 364:1321-1328.

Rockswold SB, Rockswold GL, Defillo A (2007) Hyperbaric oxygen in traumatic brain injury. Neurol Res 29:162-172.

Sandhir R, Puri V, Klein RM, Berman NE (2004) Differential expression of cytokines and chemokines during secondary neuron death following brain injury in old and young mice. Neurosci Lett 369:28-32.

Satz P, Forney DL, Zaucha K, Asarnow RR, Light R, McCleary C, Levin H, Kelly D, Bergsneider M, Hovda D, Martin N, Namerow N, Becker D (1998) Depression, cognition, and functional correlates of recovery outcome after traumatic brain injury. Brain Inj 12:537-553.

Schmidt OI, Heyde CE, Ertel W, Stahel PF (2005) Closed head injury--an inflammatory disease? Brain Res Brain Res Rev 48:388-399.

Sherer M, Madison CF, Hannay HJ (2000) A review of outcome after moderate and severe closed head injury with an introduction to life care planning. J Head Trauma Rehabil 15:767-782.

Shirakuni T, Nagashima T, Tamaki N, Matsumoto S (1985) Magnetic resonance imaging of experimental brain edema in cats. Neurosurgery 17:557-563.

Smith DH, Soares HD, Pierce JS, Perlman KG, Saatman KE, Meaney DF, Dixon CE, McIntosh TK (1995) A model of parasagittal controlled cortical impact in the mouse: cognitive and histopathologic effects. J Neurotrauma 12:169-178.

Spetzler RF, Zabramski JM, Kaufman B, Yeung HN (1983) Acute NMR changes during MCA occlusion: a preliminary study in primates. Stroke 14:185-191.

Thomas WE (1992) Brain macrophages: evaluation of microglia and their functions. Brain Res Brain Res Rev 17:61-74.

Thurman D, Guerrero J (1999) Trends in hospitalization associated with traumatic brain injury. Jama 282:954-957.

Thurman DJ, Alverson C, Dunn KA, Guerrero J, Sniezek JE (1999) Traumatic brain injury in the United States: A public health perspective. J Head Trauma Rehabil 14:602-615.

Tobias JD (2005) Sedation and analgesia in the pediatric intensive care unit. Pediatr Ann 34:636-645.

Tolias CM, Bullock MR (2004) Critical appraisal of neuroprotection trials in head injury: what have we learned? NeuroRx 1:71-79.

Tyagi R, Donaldson K, Loftus CM, Jallo J (2007) Hypertonic saline: a clinical review. Neurosurg Rev 30:277-290.

Unterberg AW, Stroop R, Thomale UW, Kiening KL, Pauser S, Vollmann W (1997) Characterisation of brain edema following "controlled cortical impact injury" in rats. Acta Neurochir Suppl 70:106-108.

Verweij BH, Muizelaar JP, Vinas FC, Peterson PL, Xiong Y, Lee CP (2000) Improvement in mitochondrial dysfunction as a new surrogate efficiency measure for preclinical trials: dose-response and time-window profiles for administration of the calcium channel blocker Ziconotide in experimental brain injury. J Neurosurg 93:829-834.

Vitkovic L, Bockaert J, Jacque C (2000) "Inflammatory" cytokines: neuromodulators in normal brain? J Neurochem 74:457-471.

Wilson CJ, Finch CE, Cohen HJ (2002) Cytokines and cognition--the case for a head-to-toe inflammatory paradigm. J Am Geriatr Soc 50:2041-2056.

Wood M, Wehrli F (1999) Principles of Magnetic Resonance Imaging. In: Magnetic Resonance Imaging, 3rd Edition (Stark D, Bradley W, eds). St. Louis: Mosby.

Xiong Y, Gu Q, Peterson PL, Muizelaar JP, Lee CP (1997) Mitochondrial dysfunction and calcium perturbation induced by traumatic brain injury. J Neurotrauma 14:23-34.

Young W (1992) Role of calcium in central nervous system injuries. J Neurotrauma 9 Suppl 1:S9-25.

Zhou Z, Daugherty WP, Sun D, Levasseur JE, Altememi N, Hamm RJ, Rockswold GL, Bullock MR (2007) Protection of mitochondrial function and improvement in cognitive recovery in rats treated with hyperbaric oxygen following lateral fluid-percussion injury. J Neurosurg 106:687-694.

II. – RESEARCH OBJECTIVES

Specific Aim #1: To compare initial contusion volume, edema volume and time course, and development of the lesion cavity from controlled cortical impact in aged versus adult mice.

Preliminary results from MR imaging indicated that while ultimate lesion cavity volumes are similar for aged versus adult subjects, there may be differences in the lesion development following the injury. Specifically, we noted in several experiments an increased spatial extent of edema in the area surrounding the contused tissue (peri-contusion) when comparing T2-weighted MRI images taken at 24 hours post injury in aged versus adult animals. A greater number of subjects will need to be processed to assess if the edema difference is statistically significant. In addition to edema measurements, we will measure the contusion volume to compare fully aged versus adult subjects.

Hypothesis: There is more damage from TBI, in the aged compared to the adult animals, as evidenced by increased edema extent, and loss of tissue.

Specific Aim #2: To compare neurodegeneration after controlled cortical impact in aged versus adult mice.

Other studies with CCI in rodents have already shown that in addition to neuron degeneration and loss of tissue at the contusion site, there is significant, presumably "secondary", damage in more distant brain areas, especially in the thalamus and in the dentate gyrus, CA1, and CA3 fields of the hippocampus. The hippocampus is of

particular interest in this study since there is evidence that hippocampal neurons are more susceptible to damage in aged brains. Our preliminary results with Fluoro-Jade and amino-cupric staining techniques showed their ability to identify neurodegeneration and death at the contusion site, in the hippocampus, and in the thalamus. We will also use immunohistochemistry with antibodies to glial fibrillary acidic protein (GFAP) and intergrated calcium binding adaptor-1 (Iba1) to measure the inflammatory response at the injury site and in more distant locations.

Hypothesis: Neurodegeneration following TBI, at the injury site and in the hippocampus and thalamus, is greater in the aged animals, and this increased loss is accompanied by an increased glial activation.

Specific Aim #3: To compare behavioral deficits and deficit recovery patterns after controlled cortical impact in aged versus adult mice.

It is important to include behavioral assessments in order to measure TBI outcomes, for outcomes are of central importance in enabling the translation of results and knowledge gained in animal studies back to the human condition. Several specific behavioral tests have been chosen for their appropriateness and reliability for measurement of sensorimotor deficits resulting from focal injuries to the mouse sensorimotor cortex. We will assess sensorimotor function with Rotarod, the spontaneous forelimb (SFL) (or cylinder) task, and the gridwalk task. Our initial experiments indicate that each of these tests is sensitive enough to detect deficits from

moderately severe CCI injuries in mice. Preliminary Rotarod results suggest that aged animals have greater lasting deficits when compared with adult animals.

Hypothesis: Sensorimotor deficits from TBI are greater in the aged compared to the adult animals, and are correlated with the degree of tissue and neuron damage.

III – A MOUSE MODEL OF SENSORIMOTOR CONTROLLED CORTICAL IMPACT: CHARACTERIZATION USING LONGITUDINAL MAGNETIC RESONANCE IMAGING, BEHAVIORAL ASSESSMENTS AND HISTOLOGY

Abstract

The present study establishes a new mouse model for traumatic brain injury (TBI), using an electromechanically-driven linear motor impactor device to deliver a lateral controlled cortical impact (CCI) injury to the sensorimotor cortex. Lesion cavity size was measured, and inter-animal consistency demonstrated, at 14 days post injury. Qualitative information regarding damage progression over time was obtained by scanning with high field magnetic resonance imaging (MRI) at five time points following injury. Functional impairment and recovery were measured with the Rotarod, gridwalk and cylinder tests, and lesion cavity volume was measured post mortem with thionin-stained tissue sections. The study establishes the reliability of a linear-motor based device for producing repeatable damage in a CCI model, demonstrates the power of longitudinal MRI in studying damage evolution, and confirms that a simple battery of functional tests record sensorimotor impairment and recovery.

Introduction

Every year, traumatic brain injury (TBI) affects over 1.5 million people, claims over 50,000 lives, and imposes costs that exceed 50 billion dollars in the United States alone. Despite the burden of TBI, few treatment options exist, in part because of limited clinically relevant animal models.

Models to study TBI have been developed in several different animal species. Controlled cortical impact (CCI), as a model for focal contusions in the ferret, was first described by Lighthall in 1988, (Lighthall, 1988). CCI was subsequently adapted for other species, including the rat (Dixon et al., 1991) and the mouse (Smith et al., 1995; Fox et al., 1998; Hannay et al., 1999). In the last ten years, mouse models have gained popularity, primarily due to their economy and the ability to use various knockout and targeted overexpression strategies to isolate the role of specific genes and their products in TBI damage and repair mechanisms. Mouse CCI models have been demonstrated to produce contusions that are histopathologically similar to contusion injuries in human TBI patients (Cernak, 2005; Morales et al., 2005). While originally thought to produce focal lesions only, emerging evidence suggests that damage from mouse CCI can extend well beyond the site of the contused tissue (Hall et al., 2005).

Most mouse CCI research has used a "parasagittal cortex" injury location (Smith et al., 1995; Fox et al., 1998; Hannay et al., 1999). This location has been shown to yield pathology in brain areas at, around, and below the strike location, producing deficits in cognitive function, and in some cases, deficits in sensorimotor and visual function. There are two significant challenges with this location: difficulty in discerning primary from secondary damage in the hippocampus, and the scarcity of simple, reliable tests for cognitive performance that are not confounded by sensorimotor or visual impairments. We propose the use of a "sensorimotor cortex" injury location that offers an increased possibility of resolving primary from secondary damage by sparing most of the hippocampal and thalamic structures from direct damage from the initial strike. Furthermore, the sensorimotor injury lends itself to the use of a simple group of behavioral tests to assess the functional consequences of the cortical damage.

Many mouse CCI experiments have used a pneumatically actuated impactor, which has shown good reliability, although posing mechanical challenges in terms of the stroke overshoot, rebound control, and adjustment of contusion time. Electromechanical devices, especially those designed and implemented for high-throughput precision manufacturing uses, have recently been adapted for spinal cord injury models (Narayana et al., 2004; Bilgen, 2005). We now describe the use of an electromechanical injury apparatus adapted for use in mouse brain CCI. This device offers a real-time feedback control system to regulate stroke velocity, depth and time.

We have characterized the injury using repeated magnetic resonance imaging (MRI) and behavioral testing as well as traditional histological techniques. The non-invasive nature of MRI provides an opportunity to assess the evolution of damage after CCI injury and provides physiological data concurrent with behavioral assessment.

Our results indicate that a consistent, reliable injury can be achieved with the electromechanical device applied to a sensorimotor cortex location, that lesion cavity volume measurements from MRI are well correlated with measurements made by traditional histological techniques, and that the impact produces lasting sensorimotor deficits.

With this model and characterization method, we seek to extend and add to the value of existing mouse CCI research, by using an electromechanical injury device, by applying the CCI injury to the sensorimotor cortex, by using longitudinal high field MRI, and by assessing sensorimotor impairment and recovery using a simple battery of three behavioral tests.

Materials and Methods

Animals

Adult male C57BL/6 mice (28-30g, 20-25 weeks old) were housed with a 12-hour light-dark cycle, with *ad libitum* access to food and water. All animal procedures were approved by the University of Kansas Medical Center Institutional Animal Care

and Use Committee. A total of 16 mice were used for this study. Eight animals received CCI injury and eight animals received a sham injury.

CCI Impactor

This device was assembled from commercially available components, as described previously (Narayana et al., 2004; Bilgen, 2005). Briefly, the equipment included a linear motor device (the impactor), power supply and microprocessor controller (Linmot, Zurich, Switzerland), a Plexiglas table, and stand for the linear motor device made with an adjustable manipulator (Kopf, Tujunga, CA) that allowed precise positioning of the impactor. A polished stainless steel tip, which strikes the dura during CCI, was fitted to the end of the impactor slider. The size and shape of the tip, the velocity of the strike, and the contact depth and time, could be varied to achieve contusions of different sizes and severities. In this study, we used a 3.0mm diameter flat face tip with a slightly rounded edge, a 1.5m/s strike velocity, a 1.0mm strike depth, and an 85ms contact time.

Surgical Procedures

Following anesthesia with isoflurane (induction: 2.5%, maintenance: 1.0%), animals were stabilized in a Cunningham stereotaxic frame (Stoelting, Wood Dale, IN), and placed on a heated pad, which maintained core body temperature at 37+/- 1 °C. The scalp and epicranial aponeurosis were retracted, and a 3.5mm diameter circular craniotomy was performed with a burr drill, lateral (right side) to the mid-sagittal

suture, with the center at the following coordinates: AP = 0, ML = +2.0 from bregma. The burr and surface of the skull were cooled with periodic application of room temperature saline. Care was taken to avoid the blood vessels coursing along the superior sagittal sinus, and any bleeding from the skull was controlled with bone wax. Once the dural surface was exposed, the position of the impactor and tip was carefully adjusted to be centered within the craniotomy, and angled so the face of the impactor tip was tangential to the dural surface (see Figure 1). The impactor tip was slowly lowered in 0.05mm increments until the tip just contacted the dura (by visual inspection). The cortical impact was initiated through the device graphical user interface of the impactor control software. Firstly, there was a retraction of the tip of 20mm, and then a downward strike of 21mm (20mm retraction plus the 1.0mm programmed injury depth. Given that the injury center was 2.0mm lateral to bregma, the tip contact area included motor (M1, M2) and sensory (S1FL, S1HL) cortical areas. After the impact, the scalp was sutured closed, anesthesia was discontinued, and animal temperature was maintained at 37°C until recovery of locomotion. Sham animals (n=8) received the craniotomy but no impact from the CCI device.

MRI Scanning

Following induction of anesthesia with 2.5% isoflurane, the animals were positioned in a small plastic cradle attached to a Plexiglas sled. The breathing/anesthesia mask and surface coil were attached and then the sled introduced to the magnet. Animals were monitored for core body temperature and respiration rate throughout the MRI

experiments with an MRI-compatible monitoring system (SA Instruments, Stony Brook, NY). Warm humidified air was circulated in the magnet bore to maintain animal temperature at 37 +/1°C, and anesthesia was adjusted, between 1.0 and 1.5% isoflurane, to maintain breathing at a minimum of 20 respirations per minute.

Animals were scanned with a 9.4T Varian INOVA horizontal MRI scanner (Varian Inc., Palo Alto, CA) using a 400mT/m gradient coil set and a 31cm room temperature bore. Given the small size of mouse brains, approximately 10mm x 16mm x 6mm, and our desire for high resolution, high contrast images, surface coils were used. In particular, we used an inductively coupled surface coil, similar to that described previously (Bilgen, 2004), and a simple rectangular detection loop. The inductively coupled coil provided increased signal-to-noise ration and a limited/focused field of view, enabling high spatial resolution.

Scout images were acquired with a gradient echo multislice (GEMS) sequence to ensure precise placement of the brain at the magnet isocenter. Spin-echo multislice (SEMS) images were then acquired, in each of the three planes (TR/TE = 2500/45ms for T2-weighting, data matrix size = 128x128, slice thickness = 1mm, fields of view = 16mm x 10mm (anatomically coronal slices), 20mm x 10mm (sagittal), and 16mm x 20mm (axial), 4 averages per acquisition). The total scan time, including set-up and positioning, was about 90 minutes per animal. For longitudinal data acquisition, we scanned each mouse at 5 time points: at 24 hours, 48 hours, 96 hours, 7 days, and 14

days post injury. The scans at time points 1, 2, 4, and 5 were done immediately following the behavioral assessments. Images were evaluated using the Varian VnmrJ software tools and also by importing the images into NIH ImageJ, version 1.34S.

Injury location measurements for each animal were made from the anatomically horizontal T2-weighted image corresponding to the brain tissue at 0.5 to 1.0mm below the cortical surface, obtained at 24 hours post injury. On this image, two lines were drawn, the first along the sagittal midline and the second, perpendicular to the sagittal midline, just touching the rostral extreme of the olfactory bulbs. A circle that best fit the injury zone, as denoted by image hyperintensity, was then placed on the image, and the center of this circle was considered the injury location. The perpendicular distances from the center of the circle to the two drawn lines were measured using the VnmrJ software tools and these two measurements were the injury location coordinates.

Lesion cavity volume measurements were made from the anatomically coronal T2-weighted images, obtained at 14 days post injury, using the image analysis tools of the MRI scanning system. The closed polygon selection tool was used to delineate the cavity on each slice, with the dorsal aspect of the cavity estimated from a mirror image of the contour of the uninjured hemisphere, and the area function provided the area measurement for each image. The product of area and slice thickness provided

the cavity volume for each 1mm thick slice. Measurements were made on successive coronal slices where a cavity was apparent – typically three to five images – and then the volumes were summed to yield the total cavity volume.

Behavioral Tests

Rotarod

The Rotarod has been extensively used in mouse models of TBI, and its potential for high sensitivity to sensorimotor deficits has been demonstrated (Hamm et al., 1994). Rotarod training and measurement were performed using a four-lane Rotarod apparatus (Accuscan, Mentor, OH). Each day for five days prior to injury, animals were trained on the Rotarod at two different speeds (12 and 18 rpm) in the acceleration paradigm and at one speed (8 rpm) in the constant velocity paradigm. Mice were tested using three trials at each speed in each training or measurement session, with a minimum of 120 seconds of rest between trials. We have found this training sufficient to establish a reliable pre-injury baseline performance for each animal. Rotarod speeds were chosen to be sufficiently challenging during training to avoid ceiling effects, but to allow injured animals to complete the task. After surgery, we measured each animal's performance at five time points: 24, 48, 72 hours, and 7 and 14 days. Post injury scores were normalized using pre-injury means to control for variability in pre-injury performance.

Gridwalk

The gridwalk apparatus was fabricated as described by Baskin (Baskin et al., 2003), using a 1.1cm wire grid of 20cm x 35cm. Animals were allowed to walk on this grid for five minutes, during which their total actual walking time was measured (in real time by stopwatch or afterwards by review of videotape), and the numbers of foot faults for each foot were counted. Foot faults were defined as an instance where the animal attempted to place weight on a foot, which then passed completely through the plane of the wire grid. We observed that after surgery, animals in both age groups tended to walk less, especially at the earlier post injury time points. Since the animals were free to move about the grid, or to remain still and engage in grooming or other stationary behaviors, foot fault data were normalized to actual walking time to account for differences in the degree of locomotion seen in different trials. This was achieved by dividing the total counted foot faults by the total time spent walking to obtain a measure of foot faults per minute of walking. Two measurements were taken pre-injury to establish each animal's baseline performance, and to allow the animals to become familiar with the apparatus. Post injury measurements were taken beginning at 48 hours post injury and thereafter at the same time points as those for the Rotarod. Walking trials were repeated until at least 90 seconds of walking was observed for each animal at each time point.

Cylinder

The cylinder or spontaneous forelimb test (Schallert and Tillerson, 2000) modified for mouse (Baskin et al., 2003), involves the use of a 10cm diameter transparent cylinder.

Each animal was placed in the cylinder, and its spontaneous activity to rear up on its hind limbs and explore the vertical surface with its forelimbs was observed. Animals used either both forelimbs or a single forelimb for an exploration. The number of both, right only, or left only explorations was counted in a five-minute recording interval. Two pre-injury measurements were taken to control for limb preference. The laterality score (Schallert et al., 2000) was computed as follows:

(# of right only - # of left only) / (# of right only + # of left only + # of both)

Post injury, measurements were taken at the same time points as for the gridwalk. Animals showed a tendency, in the measurements at 48 hours post injury, to explore the cylinder less frequently and to spend a larger proportion of time engaged in grooming activities. Our approach was to perform additional five minute trials until at least 20 rearing observations were made.

Histology

After the fourteen day post injury behavioral and imaging studies, animals were anesthetized and perfused transcardially with 50 ml of phosphate buffered saline, followed by 100 ml of 4% buffered formaldehyde, delivered via a 23-gauge needle connected to a perfusion pump. The brains were removed, post-fixed in 4% buffered formaldehyde for 12 hours, then transferred to 30% sucrose for cryoprotection before blocking in a coronal mouse brain matrix (Zymed, Pittsburgh, PA), and freezing in 15 x 15mm cryomolds. Frozen coronal sections were cut at 20µm thickness on a Leica CM1850 cryostat (Leica Microsystems, Bannockburn, IL) and stained with 1%

thionin, cleared and coverslipped. Sections were visualized with a Nikon inverted-stage microscope at 20x magnification and digital images were captured with a SPOT microscope camera (Diagnostic Instruments, Sterling Heights, MI)

From these histological images, we measured frank tissue loss, i.e. the size of the cavity, with ImageJ software. On each image, the cavity was outlined with the polygon selection tool by visual inspection, with the dorsal aspect of the lesion estimated from the mirror image of the contour of the uninjured hemisphere. A pixel count was obtained with the histogram function in ImageJ. For each animal, the cavity area was measured in 5 to 7 sections, spaced approximately 0.5mm apart, and the total cavity volume was calculated using the formula $A_1 (0.5X_1) + A_2(0.5X_1+0.5X_2)+ A_{n-1}(0.5X_{n-1}+0.5X_n) +A_n(0.5X_n)$ where A_n is the area of the cavity for section (n) and X_n is the distance between sections (n) and (n-1) (Dash et al., 2004).

Statistical Analysis

For the analysis of behavioral data and comparisons between the injured and sham groups, we used the Wilcoxon Signed Rank test, a non-parametric test appropriate for small sized groups where the data distributions are not assumed to be Gaussian. For the comparison of MRI-obtained and histology-obtained lesion cavity volume data, we calculated the Spearman correlation coefficient. All statistical analyses were performed using GraphPad Instat software (GraphPad, San Diego, CA).

Results

MRI: Injury Presentation

Figure 2 shows example T2-weighted spin-echo images from an injured animal at 14 days in the coronal, sagittal and axial planes. These show a strong signal hyperintensity, corresponding to the fluid-filled cavity, where cortical and subcortical tissue has been lost. They also show a well-defined border between the hyperintense and normal-appearing areas, suggesting that by this time the cavity size and shape is stable. The lateral ventricle on the ispilateral side is expanded. There is loss of white matter in the corpus callosum, the ipsilateral cingulum, and the medial portion of the external capsule. The longitudinal cerebral fissure was deflected, towards the injured side, as seen in the anatomically axial images.

Evolution of Injury with Time

Figure 3 shows a time series of 1mm thick anatomically coronal T2-weighted spin-echo images from the same animal, showing the evolution of the injury and the development of the cavity over time. At the first scanning time point – 24 hours – there is typically signal hyperintensity at and around the injury site – and we interpret this as acute edema. By 48 hours, this hyperintensity is diminished, suggesting that the acute edema is resolving. At 7 days, there is typically an area of signal hyperintensity at the center of the injury location, surrounded by a “ring” or “zone” of

signal hypointensity. We interpret the central hyperintensity as an area where tissue has been lost and replaced by fluid, and we consider the "ring" as dying tissue (necrotic or apoptotic). At 14 days, there is a continued central hyperintensity and as well as marked hyperintensity in the "ring" region, suggestive of completed tissue loss and replacement by fluid. Also, at 14 days, the border between the cavity and the surrounding normal appearing tissue has become much more distinct than at earlier time points.

Injury Location

MR images were used to generate data on injury location, and to quantify lesion cavity size for comparison with data obtained from histological specimens. Injury location data were derived from anatomically axial MRI images. Figure 4 shows the data on injury location, from T2-weighted axial images at 24 hours post injury. The compact grouping of points on this graph (average distance from the mean location: 0.48mm, min: 0.02mm, max: 0.80mm) demonstrates that the injury location is consistent. Note that the grouping of the points reflects variations due to actual injury location, measurement error, and animal-to-animal differences in brain size.

Behavior

Rotarod results are shown in Figure 5. Post injury mean scores were expressed as a percent of pre-injury score, and error bars indicate standard error of the means. The greatest deficit, for acceleration to 18rpm over 90 seconds, occurred at 48 hours post

injury, when injured animals were at 42% and sham animals were at 119% of pre-injury performance, a statistically significant difference ($p=0.002$, 2-tailed Wilcoxon Sign Rank test). For the injured animals, there was gradual recovery to 72% by 7 days, and 88% of pre-injury performance by 14 days. The results for acceleration to 12rpm, and for constant velocity trials at 12rpm, showed lesser initial deficits, and greater variability, reflecting that these speeds present less challenge to the mice, before and after injury.

Gridwalk test results, for the left forelimb, are shown in Figure 6. Deficits in the gridwalk test were greatest at 72 hours post injury, reaching a mean of 6.3 footfaults per minute of walking. By 7 days, footfaults occurred at a rate of 4.49 per minute, and by 14 days, the footfaults occurred at a rate of 2.98 per minute. Although some animals did make footfaults with the right (i.e. ipsilateral to the injury) forelimb, especially at the first measurement point at 48 hours post injury, these faults had ceased by 7 days (data not shown).

An analysis of the raw (non-normalized) footfault data reveals similar results to those shown in Figure 6. In preinjury training, only 1 of the 16 animals made more than 2 left front foot faults during observation. At 72 hours post injury and at later time points, only one sham animal made greater than 2 left front footfaults at one time point (7 days), whereas all 8 injured animals made greater than 2 left front footfaults at every time point. Thus, at 72 hours and later, sham behavior was comparable to

pre-injury, while injured animals showed marked deficits. Thus analyzing the data with a non-parametric strategy reveals essentially identical results.

Spontaneous forelimb (cylinder) task results are shown in Figure 7. In this task, the mean laterality score of the injured group, which measures preference for the forelimb unaffected by (ipsilateral to) the injury, peaked at 0.25 at 7 days post injury, and was statistically significant compared to the sham group ($p=0.031$). On this task, normal uninjured performance, for an animal with no preference for right or left forelimb, is at or near zero. Our sham and injured animal groups both showed a slight pre-injury preference for the right side.

End-Point Histology and Lesion Cavity Volume

Thionin-stained coronal tissue sections, from brains harvested at 14 days after injury, were used for evaluation of gross pathology and for lesion cavity volume measurement. Examples of thionin-stained sections are shown in Figure 8. Observations of pathology made via light microscopy were qualitatively consistent with MRI findings. At 14 days, there was gross loss of cortical gray matter and subcortical white matter at the injury epicenter, with thinning of the cortical mantle at the margins of the impact zone. The lateral ventricle was expanded on the injured side, and the tissue was deflected at the midline. No obvious hippocampal damage is observed in sections caudal to the impact zone.

The MRI-derived and histology-derived lesion cavity volumes are highly correlated (ρ=0.88, p=0.004) as shown in Figure 9. Cavity volumes measured from MRI consistently exceed those measured by histology, by approximately 25%, consistent with other published rodent studies (Kochanek et al., 1995). Figure 9 also shows the data for lesion cavity reproducibility. Measured from MRI images, the mean cavity size was 6.99 mm^3 (S.E.M.=0.48), and measured from coronal tissue sections (histology), the mean cavity size was 5.31 mm^3 (S.E.M.=0.35).

Discussion

We have characterized a mouse model of lateral sensorimotor CCI, using a linear motor injury device. We used a simple set of behavioral tests sensitive to deficits up to 14 days following injury. Measurements of contusion size using MRI and histology were well correlated and demonstrated a consistent injury size. High field MRI confirmed injury location, and showed acute edema formation and resolution.

The imaging results show some interesting detail of the damage and its evolution. The anatomically axial images demonstrate the value – high resolution, high signal-to-noise ratio – of using a small surface coil for mouse brain imaging. The main tradeoff of this arrangement – a reduction in signal with increasing distance from the coil – is also evident in these images. Given the interest in imaging the lesion and the cortex, the tradeoff is acceptable. The anatomically axial images also show how the brain tissue tends to bulge at the site of the craniotomy, a result of our surgical methods

where the skull flap is not replaced after injury. Previous research has shown that replacement of the skull flap after parasagittal CCI can result in greater effective injury severities (Zweckberger et al., 2003). We chose not to replace the skull flap to avoid the complication of causing additional (and potentially variable) damage at surgery time from bringing the sharp piece of bone in contact with the bulging tissue.

Similar to other mouse CCI models, we observed gross loss of cortical and subcortical tissue under the impactor tip contact zone. As expected given the sensorimotor injury location we observed significant deficits in sensorimotor function. For the cylinder test, deficits were significant at 7 days post injury, and for the gridwalk test, animals showed a deficit that persisted at 14 days post injury.

This injury model, based on linear motor device, provides precise injuries, excellent repeatability, real-time strike control, and feedback. It is interesting to compare our results with other models of mouse CCI, particularly in terms of injury severity. We found that reduced strike speed and/or depth resulted in smaller observed lesions on MRI and lesser observed behavioral deficits. Conversely, increased depth caused mortality (unpublished data). It should be noted that the control parameters for this device are different from the parameters used in other devices. Our strike velocity (1.5 m/s), is less than that reported in other studies using pneumatically-actuated impactors (4.0 – 6.0 m/s) (Smith et al., 1995; Fox et al., 1998; Hannay et al., 1999; Hall et al., 2005). One possible explanation is that the linear motor device, via its

feedback/servo controller system, maintains tip velocity for the duration of the strike, therefore delivering more energy than a device where the tip begins to decelerate at the instant of impact.

From a behavioral perspective, our gridwalk results are consistent with those of Baskin (Baskin et al., 2003), which showed significant deficits lasting to 4 weeks in a mouse CCI model with a injury lateral to bregma, i.e., in a similar location to ours. However, our cylinder task results, with scores improving after one week post injury, are somewhat in contrast to the results of Baskin, where animals showed a worsening in score from 1 to 4 weeks post injury. It is possible that our injury was slightly less severe than that of Baskin. Unfortunately, there are no published reports of Rotarod scores after sensorimotor CCI in the mouse. In a study of parasagittal CCI in the mouse, Wang found, using a rotarod at 35 rpm – a more challenging speed than ours - that wildtype animals showed their greatest deficit at 24 hours post injury, with recovery to near 50% of pre-injury value by 7 days (Shi et al., 2003). Our Rotarod results show a similar profile, albeit with a shallower initial deficit, perhaps reflecting a less severe injury in our study.

In the context of studies of TBI with animal models, and in particular with genetically modified animals, mouse CCI models have already been shown to be of tremendous value (Longhi et al., 2001). A great majority of these CCI studies have employed the parasagittal injury location, there are very few reports of sensorimotor mouse CCI.

Indeed, rigorous characterizations of the sensorimotor injury and its time course have not been published. We believe that our results are a meaningful step in this direction.

This model is well-suited to the study of mechanisms of tissue damage and repair after TBI. Further, the model's ability to capture longitudinal same-animal information on damage evolution might make it particularly useful in experiments using transgenically modified animals to investigate damage mechanisms or to evaluate potential therapeutic interventions at the pre-clinical stage. With a high correlation between MR and tissue-measured cavity volume, our results illustrate the promise of longitudinal high-field MRI scanning as an important and appropriate technique for mouse CCI studies *in vivo*.

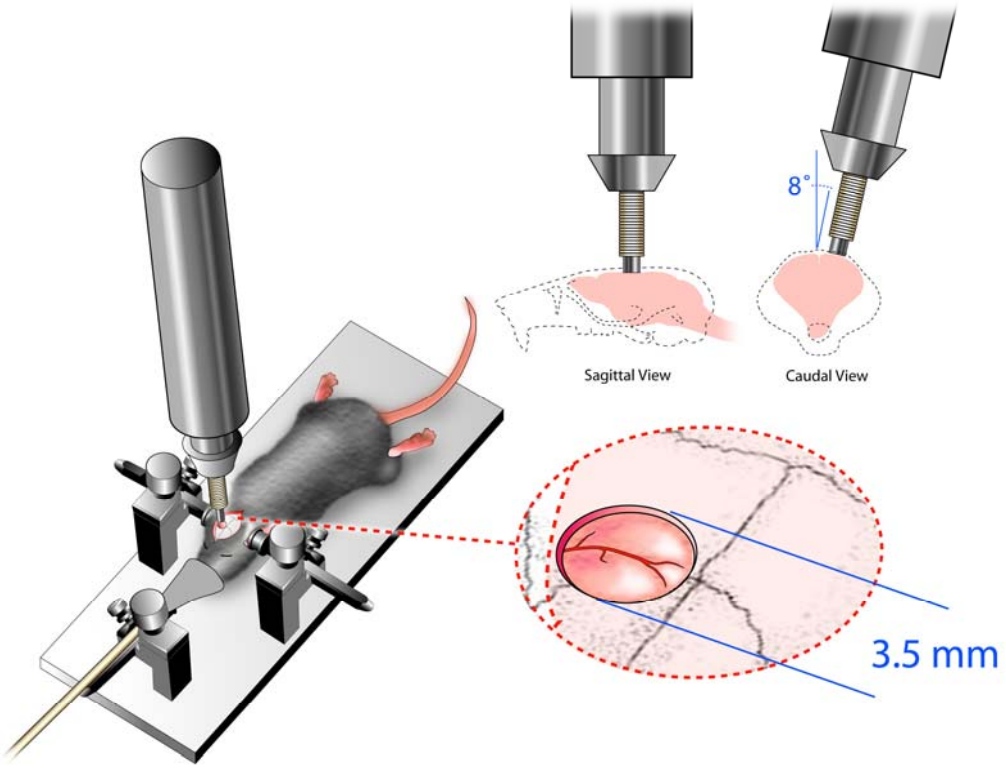

Figure 1: Drawing of the mouse CCI injury apparatus showing the impactor and part of its mounting system, the craniotomy location, and the orientation of the impactor tip to ensure perpendicularity to the exposed dura and to the surface of the brain.

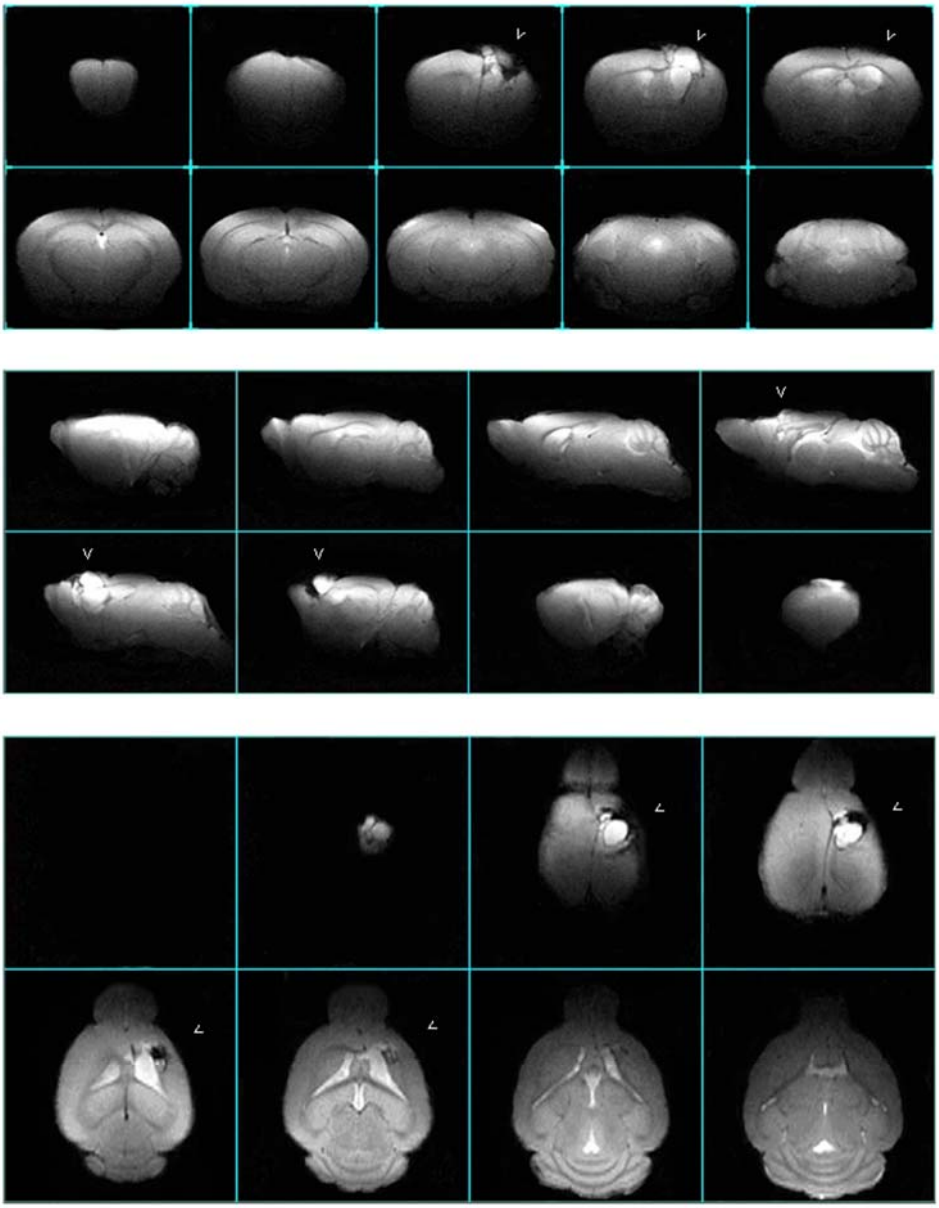

Figure 2: T2-weighted MR images of an injured animal, in the anatomically coronal (top), sagittal (middle) and horizontal (bottom) planes, scanned 14 days after injury. At this time point, the strong signal hyperintensity indicates that a lesion cavity has formed. Arrows denote the cavity. Contiguous slices, TR=2500ms, TE=45ms. Images segmented to show brain only.

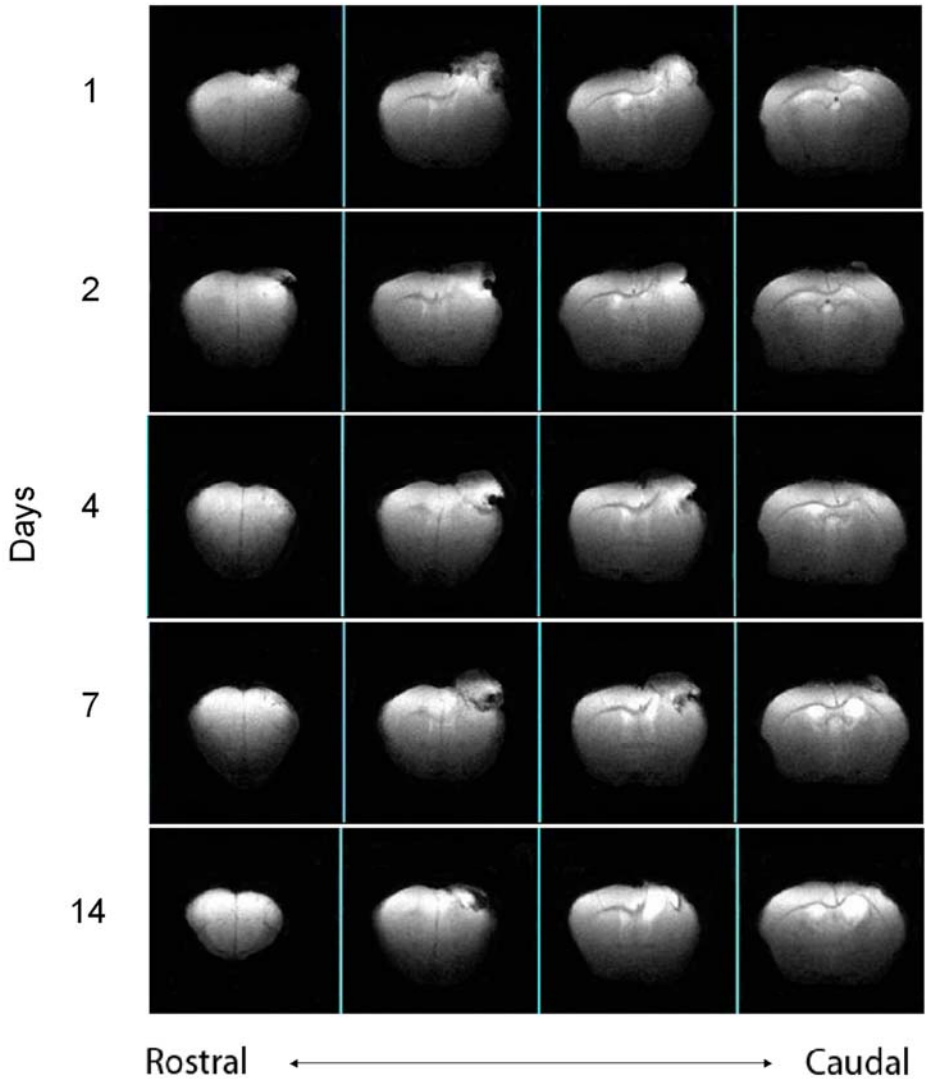

Figure 3: Series of T2-weighted MR images the same injured animal, scanned in the anatomically coronal plane, at 1, 2, 4, 7 and 14 days after injury. Contiguous 1mm slices, TR=2500ms, TE=45ms, field of view: 16mm x10mm. Images segmented to show brain only. This time course shows an early signal hyperintensity, corresponding to acute edema, and a later hyperintensity, consistent with the development of a lesion cavity. At 14 days, there is a well-defined border between the cavity and the adjacent normal-appearing tissue.

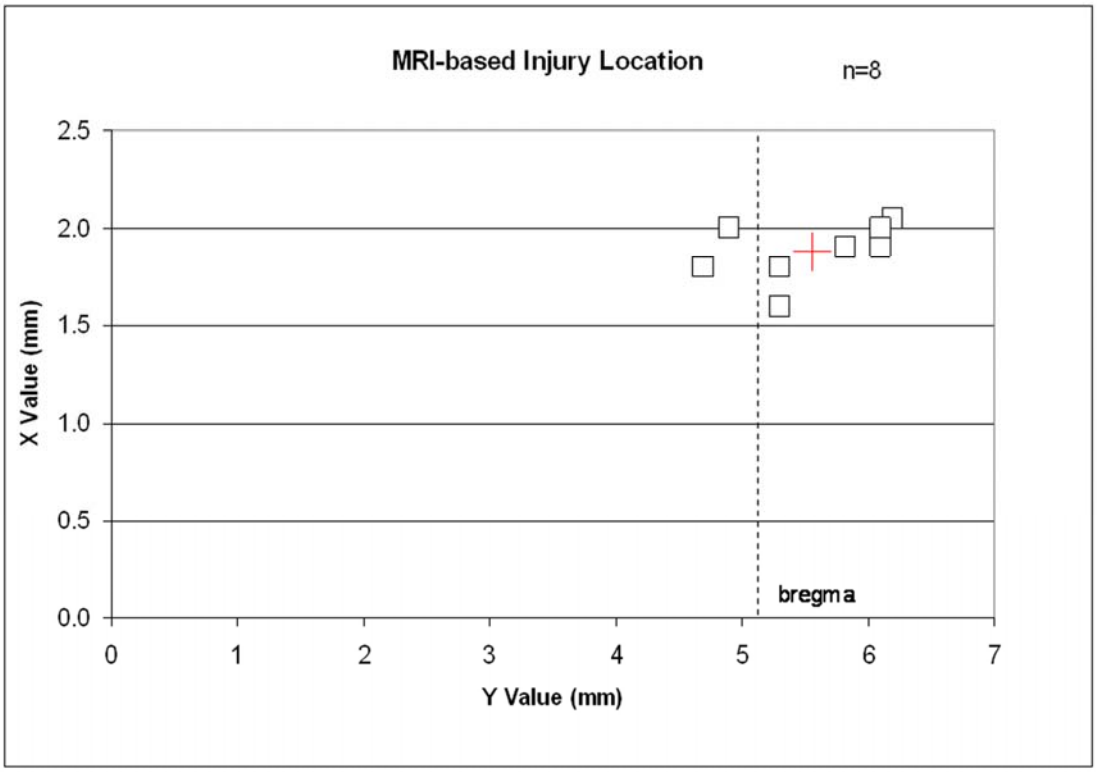

Figure 4: Injury location data obtained from T2-weighted anatomically horizontal images, indicating reliable placement of injury and repeatable technique for MRI-based location verification. Squares indicate individual measurements from eight animals, cross indicates mean location.

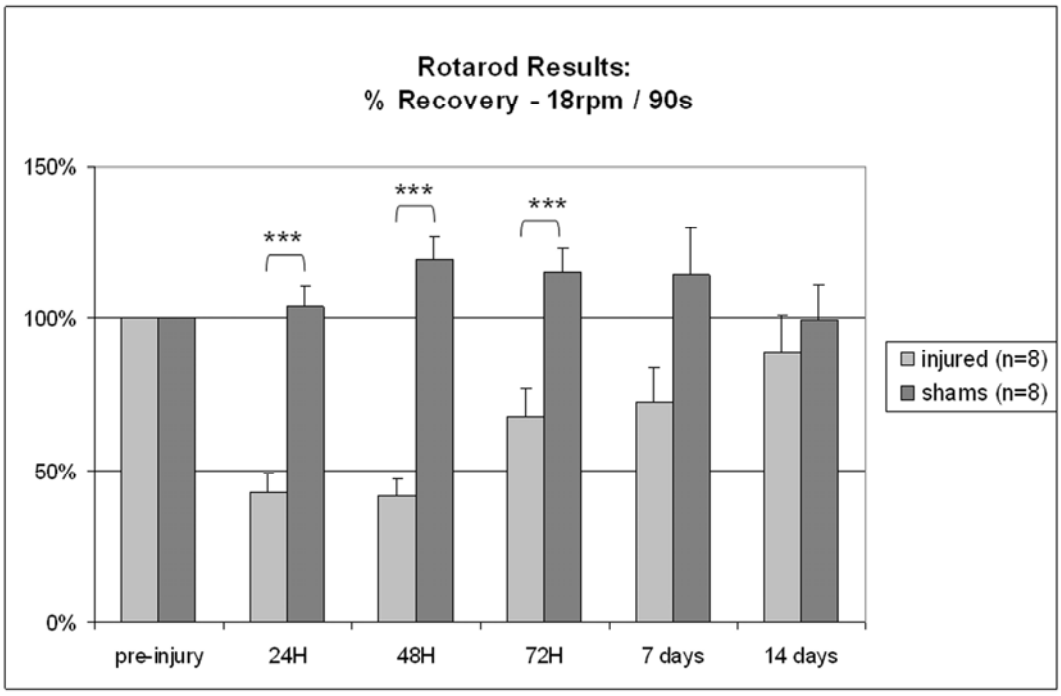

Figure 5: Rotarod latency impairment and recovery data, eight animals with injury compared to eight sham animals, showing that for the injured animals, the greatest deficit was at 24 and 48 hours, with recovery to 88% of pre-injury value by 14 days. Significant differences between injury and sham scores were seen at 24, 48 and 72 hours post injury. ***:$p<0.001$.

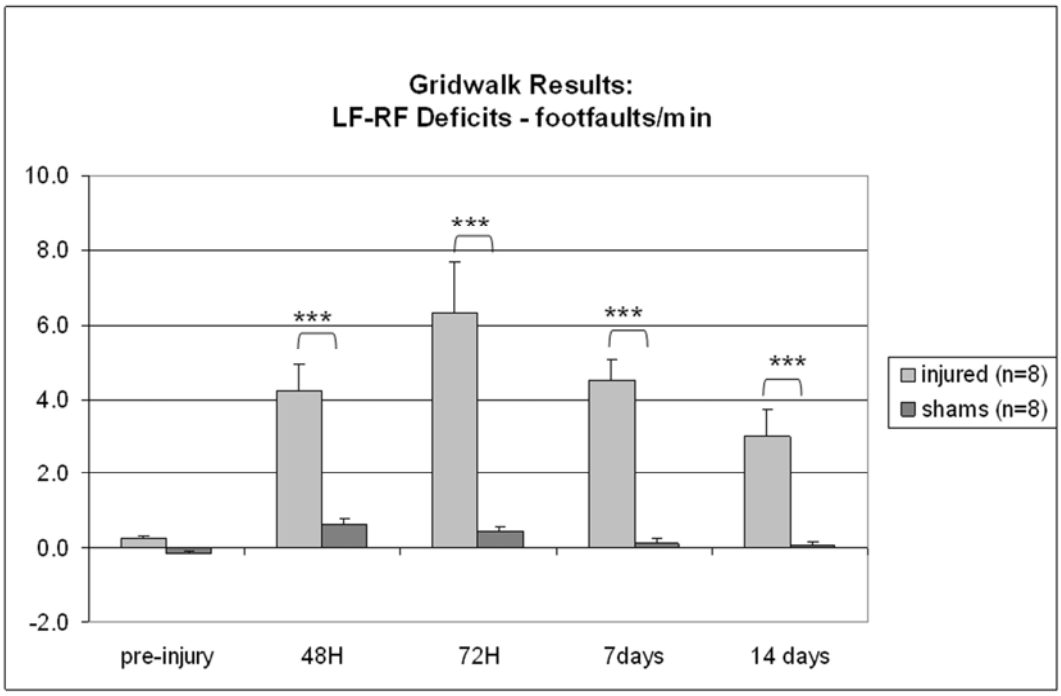

Figure 6: Gridwalk impairment and recovery data, presented as left forelimb minus right forelimb footfaults per minutes of walking, showing a peak value in the injured animals of 6.3 at 72 hours, with modest recovery to 3.0 at 14 days., Significant differences between injury and sham scores were seen at all post injury time points. ***:p<0.001.

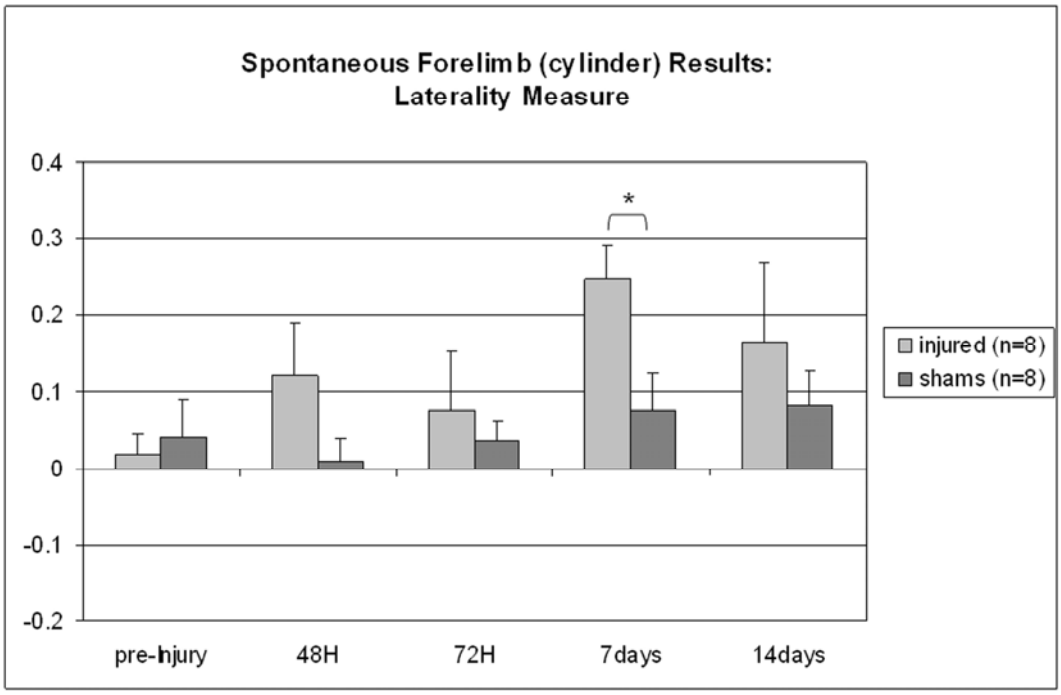

Figure 7: Spontaneous forelimb (cylinder) task impairment and recovery data, showing peak forelimb laterality score at 7 days, with reduction to 66% of peak at 14 days. Significant differences between injured and sham scores were seen at 7 days post injury *:$p<0.05$.

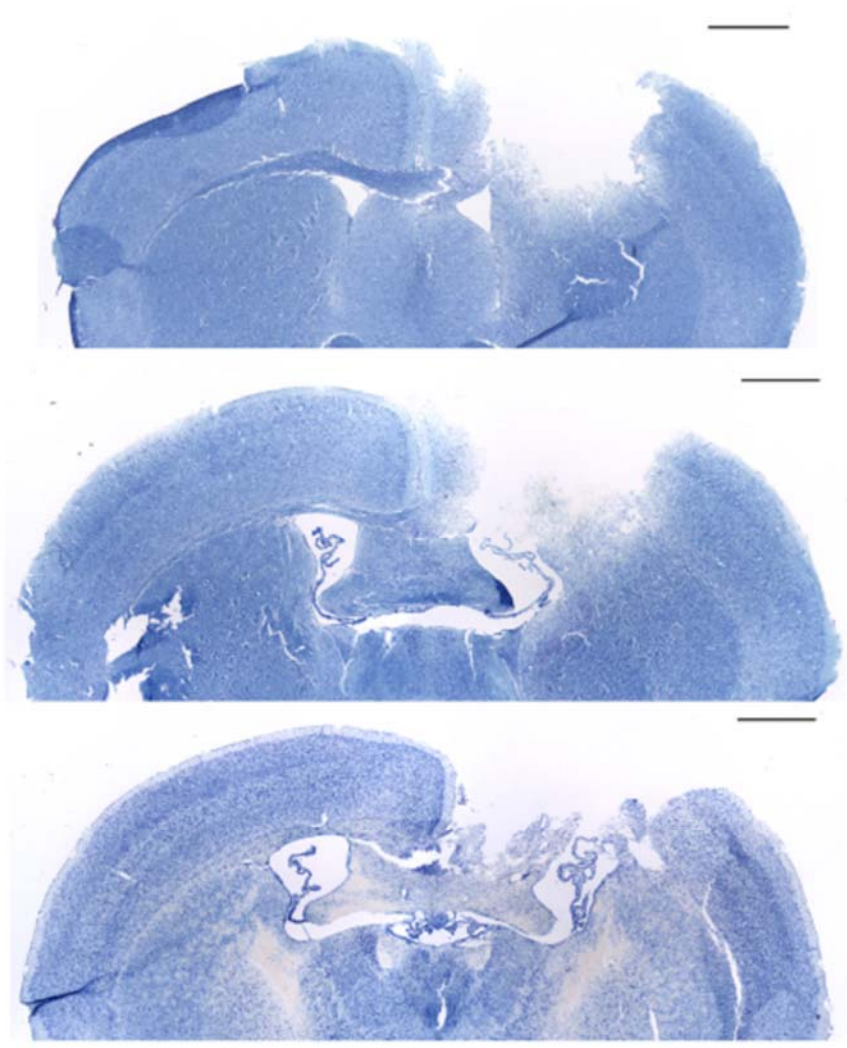

Figure 8: Examples of thionin-stained coronal sections near the injury epicenter. These sections are examples from three different injured animals, at the following AP coordinates with respect to bregma (top to bottom): +0.5, -0.2, -0.5. Scale bars: 1mm.

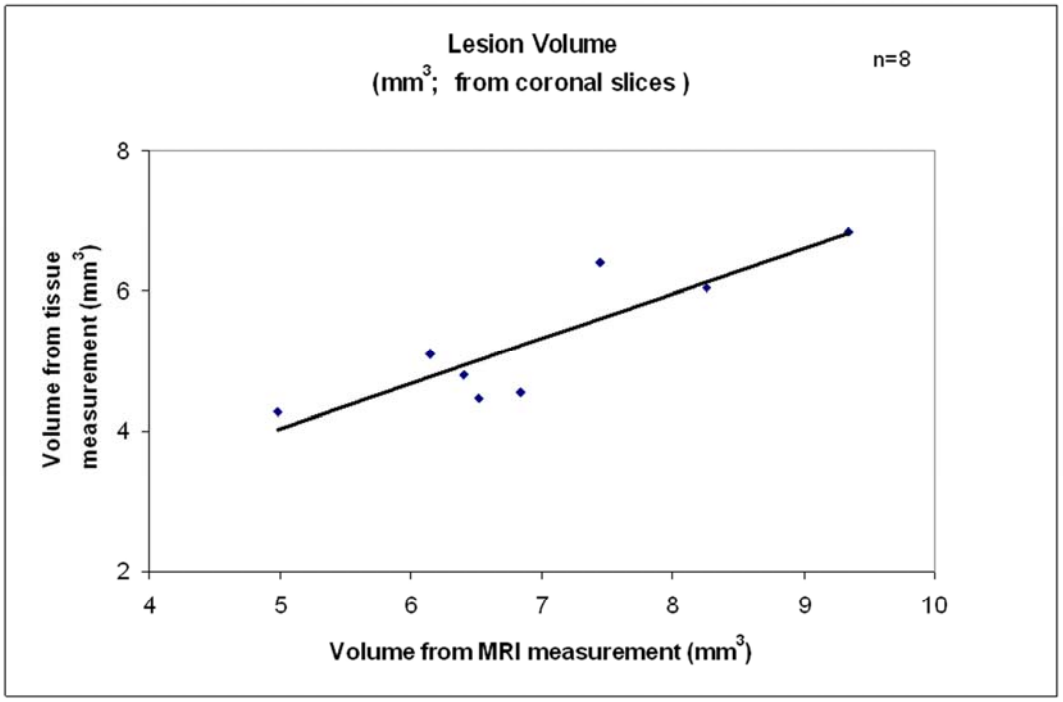

Figure 9: Correlation of lesion cavity volume measurements taken from thionin-stained coronal tissue sections with measurements taken from T2-weighted MR images at 14 days.

References

Baskin YK, Dietrich WD, Green EJ (2003) Two effective behavioral tasks for evaluating sensorimotor dysfunction following traumatic brain injury in mice. J Neurosci Methods 129:87-93.

Bilgen M (2004) Simple, low-cost multipurpose RF coil for MR microscopy at 9.4 T. Magn Reson Med 52:937-940.

Bilgen M (2005) A new device for experimental modeling of central nervous system injuries. Neurorehabil Neural Repair 19:219-226.

Cernak I (2005) Animal models of head trauma. NeuroRx 2:410-422.

Dash PK, Moore AN, Moody MR, Treadwell R, Felix JL, Clifton GL (2004) Post-trauma administration of caffeine plus ethanol reduces contusion volume and improves working memory in rats. J Neurotrauma 21:1573-1583.

Dixon CE, Clifton GL, Lighthall JW, Yaghmai AA, Hayes RL (1991) A controlled cortical impact model of traumatic brain injury in the rat. J Neurosci Methods 39:253-262.

Fox GB, Fan L, Levasseur RA, Faden AI (1998) Sustained sensory/motor and cognitive deficits with neuronal apoptosis following controlled cortical impact brain injury in the mouse. J Neurotrauma 15:599-614.

Hall ED, Sullivan PG, Gibson TR, Pavel KM, Thompson BM, Scheff SW (2005) Spatial and temporal characteristics of neurodegeneration after controlled cortical impact in mice: more than a focal brain injury. J Neurotrauma 22:252-265.

Hamm RJ, Pike BR, O'Dell DM, Lyeth BG, Jenkins LW (1994) The rotarod test: an evaluation of its effectiveness in assessing motor deficits following traumatic brain injury. J Neurotrauma 11:187-196.

Hannay HJ, Feldman Z, Phan P, Keyani A, Panwar N, Goodman JC, Robertson CS (1999) Validation of a controlled cortical impact model of head injury in mice. J Neurotrauma 16:1103-1114.

Kochanek PM, Marion DW, Zhang W, Schiding JK, White M, Palmer AM, Clark RS, O'Malley ME, Styren SD, Ho C, et al. (1995) Severe controlled cortical impact in rats: assessment of cerebral edema, blood flow, and contusion volume. J Neurotrauma 12:1015-1025.

Lighthall JW (1988) Controlled cortical impact: a new experimental brain injury model. J Neurotrauma 5:1-15.

Longhi L, Saatman KE, Raghupathi R, Laurer HL, Lenzlinger PM, Riess P, Neugebauer E, Trojanowski JQ, Lee VMY, Grady MS, Graham DI, McIntosh TK (2001) A Review and Rationale for the Use of Genetically Engineered Animals in the Study of Traumatic Brain Injury. J Cereb Blood Flow Metab 21:1241-1258.

Morales DM, Marklund N, Lebold D, Thompson HJ, Pitkanen A, Maxwell WL, Longhi L, Laurer H, Maegele M, Neugebauer E, Graham DI, Stocchetti N, McIntosh TK (2005) Experimental models of traumatic brain injury: do we really need to build a better mousetrap? Neuroscience 136:971-989.

Narayana PA, Grill RJ, Chacko T, Vang R (2004) Endogenous recovery of injured spinal cord: longitudinal in vivo magnetic resonance imaging. J Neurosci Res 78:749-759.

Schallert T, Tillerson JL (2000) Intervention strategies for degeneration of dopamine neurons in parkinsonism: optimizing behavioral assessment of outcome. In: Innovative models of CNS diseases: from molecule to therapy (Emerich DF, ed). New Jersey: Humana Press.

Schallert T, Fleming SM, Leasure JL, Tillerson JL, Bland ST (2000) CNS plasticity and assessment of forelimb sensorimotor outcome in unilateral rat models of stroke, cortical ablation, parkinsonism and spinal cord injury. Neuropharmacology 39:777-787.

Shi WD, Wang KB, Qin QS (2003) [Trauma brain injury and apoptosis]. Fa Yi Xue Za Zhi 19:54-56.

Smith DH, Soares HD, Pierce JS, Perlman KG, Saatman KE, Meaney DF, Dixon CE, McIntosh TK (1995) A model of parasagittal controlled cortical impact in the mouse: cognitive and histopathologic effects. J Neurotrauma 12:169-178.

Zweckberger K, Stoffel M, Baethmann A, Plesnila N (2003) Effect of decompression craniotomy on increase of contusion volume and functional outcome after controlled cortical impact in mice. J Neurotrauma 20:1307-1314.

IV – DETRIMENTAL EFFECTS OF AGING ON OUTCOME FROM TRAUMATIC BRAIN INJURY – A BEHAVIORAL, MAGNETIC RESONANCE IMAGING AND HISTOLOGICAL STUDY IN MICE

Abstract

Considerable evidence indicates that outcomes from TBI are worse in the elderly, but there has been little preclinical research to explore potential mechanisms. In this study, we examined the age-related effects on outcome in a mouse model of controlled cortical impact (CCI) injury. We compared the responses of adult (5-6 months old) and aged (21-24 months old) male mice following a moderate lateral CCI injury to the sensorimotor cortex. Sensorimotor function was evaluated with the rotarod, gridwalk and spontaneous forelimb behavioral tests. Acute edema was assessed from hyperintensity on T2-weighted magnetic resonance images. Blood-brain barrier opening was measured using anti-mouse IgG immunohistochemistry. Neurodegeneration was assessed by amino-cupric silver staining, and lesion cavity volumes were measured from histological images. Indicators of injury were generally worse in the aged than the adult mice. Acute edema, measured at 24 and 48 hours post-injury, resolved more slowly in the aged mice ($p<0.01$). Rotarod recovery ($p<0.05$) and gridwalk deficits ($p<0.01$) were significantly worse in aged mice. There was greater ($p<0.01$ at 3 days) and more prolonged post-acute opening of the blood-brain barrier in the aged mice. Neurodegeneration was greater in the aged mice ($p<0.01$ at 3 days). In contrast, lesion cavity volumes, measured at 3 days post-injury, were not different between injured groups. These results suggest that following moderate controlled cortical impact injury, the aged brain is more vulnerable than the adult brain to neurodegeneration, resulting in greater loss of function. Tissue loss at the impact site does not explain the increased functional deficits seen in the aged

animals. Prolonged acute edema, increased opening of the blood-brain barrier and increased neurodegeneration found in the aged animals implicate secondary processes in age-related differences in outcome.

Introduction

Traumatic brain injury (TBI) is a leading cause of death and disability in the United States. Despite the public health burden of TBI, few treatment options exist, in part because of the limited attention devoted to research aimed at understanding and modulating the damage and repair processes that occur after TBI. Even less research is aimed at TBI in the elderly.

The elderly population is particularly vulnerable to TBI. U.S. TBI Incidence data from 1999 show that starting at age 65, TBI incidence rates double for every additional 10 years of age (Coronado et al., 2005). Subsequent data show that rates of hospitalization and mortality after TBI are greater in individuals aged 65 and older than in any other age category (Rutland-Brown et al., 2006). As the size of the aged population continues to grow, from 35 million in 2000 to an estimated 71.5 million in 2030 in the United States (He et al., 2005), the burden represented by TBI in the elderly is expected to increase.

There is also an increasing body of published reports of clinically worse outcomes - including increased morbidity and mortality - in elderly TBI victims (Galbraith, 1987; Pennings et al., 1993). In particular, hospital stays of elderly patients who experience a moderate or severe TBI are longer (Leblanc et al., 2006), and their functional capability at hospital discharge is also worse (Susman et al., 2002; Mosenthal et al.,

2004; Thompson et al., 2006). In the long term, recovery is poorer in elderly survivors of TBI (Livingston et al., 2005; Testa et al., 2005; Frankel et al., 2006; Rapoport et al., 2006) than in younger patients.

Despite these findings in human patients, research on the mechanisms of worsened outcomes in elderly TBI is particularly scant. One rodent study, using a fluid percussion injury model, demonstrated poorer neurological response and increased motor and cognitive deficits in aged (20 months old) compared to young adult (3 months old) rats (Hamm et al., 1991; Hamm et al., 1992b). Another, showed hippocampal expression of aging-associated genes, p21 and BDNF, was increased and genes associated with repair and regeneration were decreased (Shimamura et al., 2004). Older (19-20 months old) rats were found to have significantly lower hippocampal increases of antioxidant ascorbate than younger (5-6 weeks old) in a closed head injury model (Moor et al., 2006). Transient increases in immunoreactivity to synuclein proteins measured in the brains of aged (24 months old) mice subjected to TBI indicated a link between TBI and Parkinson's disease (Uryu et al., 2003). The inflammatory response during retrograde neuronal degeneration, a type of secondary neuron death, was studied using a cortical aspiration injury model with young (4 months old) and aged (24 months old) mice, and thalamic expression of pro-inflammatory molecules TNF-alpha, IL-1beta, MCP-1, RANTES and iNOS was found to be greater in the aged mice (Sandhir et al., 2004).

Several questions about age-related differences in cell death, degeneration and functional compromise following TBI remain to be answered. Differential vulnerabilities in specific areas of the aged brain have yet to be elucidated. Of critical importance, the ability of rodent models of TBI to recapitulate what is seen at the cellular, tissue and functional levels in elderly human TBI patients has not been well explored. Finally, opportunities to uniquely tailor intervention strategies to the aged brain remain to be identified.

Inspired by the original works in the rat (Dixon et al., 1991; Kochanek et al., 1995) and the mouse (Smith et al., 1995; Fox et al., 1998; Hannay et al., 1999), we have recently adapted and characterized a mouse model of sensorimotor controlled cortical impact (CCI) for the study of TBI (Onyszchuk et al., 2007). Our model features an injury location lateral to bregma, over sensorimotor cortex, whereas the previous models were designed to injure at a more caudal "parasagittal" location. We used high field strength magnetic resonance imaging to provide *in vivo* images of the same animal as damage evolved over time, and we used a group of simple behavioral tests to assess the functional consequences of the brain injury. Our initial studies showed that a consistent, reliable injury could be achieved with the electromechanical device applied to a sensorimotor cortex location, that lesion cavity measurements from MRI were well correlated with measurements made by traditional histological techniques, and that the impact produced lasting sensorimotor deficits.

We now report the results of a series of experiments designed to probe age-related differences in damage mechanisms and outcome after TBI. In these experiments, adult (5-6 months old) and aged (21-24 months old) mice were injured using our mouse CCI model and outcomes measured with behavior, MRI, and histology.

Materials and Methods

Animals

Adult male C57BL/6 mice (28-32g, 5-6 months old), and aged male C57BL/6 mice (28-32g, 21-24 months old), were housed with a 12-hour light-dark cycle, with *ad libitum* access to food and water. These animals were obtained from the National Institute on Aging colonies, where they were barrier raised, monitored for genetic purity, and screened for bacterial and viral pathogens according to the NIA guidelines. All animal procedures were approved by the University of Kansas Medical Center Institutional Animal Care and Use Committee. A total of 110 animals were used for this study; 22 were used to gather MRI T2 data (10 injured adult, 12 injured aged); 38 were used to gather behavioral data (8 injured adult, 13 injured aged, 8 sham adult and 9 sham aged). Different animals were used for the MRI and behavioral assessments to avoid inter-facility animal transportation and potential influences of MRI scanning and anesthesia on behavioral assessment. Fifty animals were used to provide histological data at 4 different time points (22 injured adult, 22 injured aged, 3 sham adult and 3 sham aged).

Surgical Procedures

Following anesthesia with isoflurane (induction: 2.5%, maintenance: 1.0%), animals were stabilized in a Cunningham stereotaxic frame (Stoelting, Wood Dale, IN), and placed on a heated pad, which maintained core body temperature at 37±1 °C. The scalp and epicranial aponeurosis were retracted, and a 3.5mm diameter circular craniotomy was performed with a burr drill, lateral (right side) to the mid-sagittal suture, with the center at the following coordinates: AP=0, ML=+2.0 from bregma. The burr and surface of the skull were cooled with periodic application of room temperature saline. Care was taken to avoid the blood vessels coursing along the superior sagittal sinus, and any bleeding from the skull was controlled with bone wax. Once the dural surface was exposed, the position of the impactor and tip was carefully adjusted to be centered within the craniotomy, and angled at eight degrees so that the face of the impactor tip was tangential to the dural surface. The impactor tip was slowly lowered in 0.05mm increments until the tip just contacted the dura (by visual inspection under surgical microscope at 25x magnification). The cortical impact was initiated through the device graphical user interface. Given that the injury center was 2.0mm lateral to bregma, the tip contact area included motor (M1, M2) and sensory (S1FL, S1HL) cortical areas (Franklin and Paxinos, 1997). After the impact, the scalp was closed with 6-0 silk suture, anesthesia was discontinued, and the animal temperature was maintained at 37°C until recovery of locomotion. Sham animals received the craniotomy but no impact from the CCI device.

CCI Impactor

This device was assembled from commercially available components, as described previously (Narayana et al., 2004; Bilgen, 2005; Onyszchuk et al., 2007). Briefly, the equipment included a linear motor device (the impactor) with a stainless steel tip, power supply and microprocessor controller (Linmot, Zurich, Switzerland), a Plexiglas table, and a stand for the linear motor device made with an adjustable manipulator (Kopf, Tujunga, CA) that allowed precise positioning of the impactor. In this study, we used a 3.0mm diameter tip with a flat face and a slightly rounded edge, a strike velocity of 1.5m/s, and a 1.0mm strike depth, and a contact time of 85ms. This parameter set was considered to provide a "moderate" CCI injury. A preliminary study of adult and aged animal injuries (not part of this study, n=4 adult, n=4 aged), using the same parameters except for a greater strike depth of 1.5mm, yielded a 50% mortality rate in the aged animals and a 25% mortality rate in the adult animals. Accordingly, to ensure adequate numbers of animals surviving injury to allow assessment of neurodegeneration and behavioral recovery, we reduced the strike depth to 1.0 mm.

MRI Scanning

Animals were scanned with a 9.4T Varian INOVA horizontal MRI scanner with a 31cm room temperature bore (Varian Inc., Palo Alto, CA) using a 400mT/m gradient coil set. Animals were monitored for core body temperature and respiration rate

throughout with an MRI-compatible monitoring system (SA Instruments, Stony Brook, NY). Warm, humidified air was circulated in the magnet bore to maintain animal temperature at 37±1°C, and anesthesia was adjusted to maintain breathing at a minimum of 20 respirations per minute. Given the small size of mouse brains, approximately 10mm x 16mm x 6mm, and our desire for high resolution, we used an inductively coupled surface coil, similar to that described previously (Onyszchuk et al., 2007) and a simple rectangular detection loop. The inductively coupled coil provided a limited field of view, but enabled high spatial resolution.

Following induction of anesthesia with 2.5% isoflurane, the animals were positioned in a small plastic cradle attached to a Plexiglas sled. The breathing/anesthesia mask and surface coil were attached and the sled introduced to the magnet. Scout images were acquired with a gradient echo multislice (GEMS) sequence to ensure precise placement of the brain at the magnet isocenter. Spin-echo multislice (SEMS) images were then acquired, in two planes (TR/TE = 2500/45ms for T2-weighting, data matrix size = 128x128, slice thickness = 0.5mm, fields of view = 16mm x 10mm (anatomically coronal slices), and 14mm x 18mm (anatomically horizontal slices), four averages per acquisition). The total scan time, including set-up and positioning, was about 70 minutes per animal. Mice in the T2 measurement groups were scanned at 24 and 48 hours post-injury. Two adult, and two aged of these animals were scanned at 28 days to gather qualitative information at that time point.

Signal hyperintensity measurements were made from anatomically horizontal T2-weighted images, obtained at 24 and 48 hours post-injury. We interpreted the signal hyperintensity at and around the site of cortical impact as edema resulting from the injury (Brant-Zawadzki et al., 1984; Bartkowski et al., 1985; Schwarcz et al., 2001; Schuhmann et al., 2002). Hyperintensities were measured from MR images using a thresholding technique in NIH ImageJ (v1.37). Following segmentation to remove non-brain areas, a threshold was established by calculating the average of the mean pixel intensity within the pseudo-lesion and the mean pixel intensity within the corresponding contralateral region in each image. Using a masking step, a modified image containing only hyperintense pixels with their original intensity values was created. The histogram of this modified image was stored and used for pixels counts and for calculation of the total hyperintensity signal. The hyperintense tissue volume was calculated by multiplying the total hyperintense pixel count for each brain by the tissue volume corresponding to one pixel. The total hyperintensity signal was calculated according to:

$$\sum a_n * (n - t), \text{ for } t < n \leq 255$$

where t is the threshold value, a_n is the number of pixels of intensity = n. Ratios of 48 hour to 24 hour values were then calculated, for each animal, for hyperintense tissue volume and for summed hyperintensity signal. Same-animal ratios provided a simple metric for characterizing edema clearance and for comparing the clearance between

the injured adult and the injured aged groups. Measurements were done by a person blinded to experimental group and time point.

Behavioral Tests

Rotarod

The Rotarod test was used to measure sensorimotor performance, as it has been previously shown to be effective in rodent TBI experiments (Hamm et al., 1994; Fujimoto et al., 2004). Rotarod training and measurement were performed using a four-lane Rotarod apparatus (Accuscan, Mentor, OH). Each day for six days prior to injury, animals were trained on the Rotarod at two different speeds (18 and 30rpm) in the acceleration paradigm and at one speed (12rpm) in the constant velocity paradigm. Animals were tested using three trials at each speed in each training or measurement session, with a minimum of 120 seconds of rest between trials. We found this training sufficient to establish a reliable pre-injury baseline performance for each animal. Rotarod speeds were chosen to be sufficiently challenging during training to avoid ceiling effects, thus they were high enough that an animal could not walk for more than three minutes. Speeds were chosen to avoid floor effects following injury, thus they were low enough that the animals were able to walk for some time before falling off the device. After surgery, we measured each animal's performance at five time points: 24, 48, 72 hours, and seven and 14 days. Post-injury scores were normalized using pre-injury means to control for variability in pre-injury performance.

Gridwalk

The gridwalk test has been shown to be effective in measuring sensorimotor deficits after TBI in the mouse (Baskin et al., 2003). It is of particular value in unilateral injury models since it allows measurement of individual limbs. This test was performed as previously described (Onyszchuk et al., 2007). Animals were allowed to walk on a 11cm grid for five minutes, during which their total walking time was measured and the numbers of foot faults for each foot were counted. Foot faults were defined as an instance where the animal attempted to place weight on a foot, which then passed completely through the plane of the wire grid. We observed that after surgery, animals in both age groups tended to walk less, especially at the earlier post-injury time points. Foot fault data were normalized to account for differences in the degree of locomotion seen in different trials. This was achieved by dividing the total counted foot faults by the total time spent walking to obtain a measure of foot faults per minute of walking. Two measurements were taken pre-injury to establish each animal's baseline performance and to allow the animals to become familiar with the apparatus. Post-injury measurements were taken beginning at 48 hours post-injury and thereafter at the same time points as those for the Rotarod.

Cylinder

The cylinder test, also well-suited to a unilateral injury, has been shown to be effective in measuring forelimb sensorimotor deficits in TBI and other mouse brain

injury models (Baskin et al., 2003; Li et al., 2004). This test was performed as previously described (Onyszchuk et al., 2007). Animals were placed in a 10cm diameter glass cylinder and were observed during their spontaneous movements where they reared onto their hindlimbs, raised their bodies towards a vertical position, and explored the vertical cylinder surface with their forelimbs. The numbers of explorations using both left and right, right only, or left only forelimbs were counted in each of two five-minute observation sessions on each post-injury assessment day. Two pre-injury measurements were taken to control for limb preference. The laterality score (Schallert et al., 2000) was computed as follows:

(# of right only - # of left only) / (# of right only + # of left only + # of both)

Post-injury, measurements were taken at the same time points as for the gridwalk.

Histology

Tissue Preparation

For the histological assessments, our primary interest was to measure differences between the injured groups at 72 hours post-injury. At this time post-injury, we expected that primary damage processes would be well-advanced, and that secondary damage processes would likely be underway and at their early stages (Muessel et al., 2002). In order to have sufficient power to detect smaller differences between groups, we set our sample size for this time point at 10 for the injured adult and injured aged animals. Small groups (n=4) of additional samples were added to the experiments to allow, as a secondary interest, the evaluation of staining trends over time.

Accordingly, at 24 hours (n=4 adult, n=4 aged), 48 hours (n=4 adult, n=4 aged), 72 hours (n=10 adult, n=10 aged), and 7 days (n=4 adult, n=4 aged) post-injury, animals were anesthetized and perfused transcardially with 50 ml of phosphate buffered saline, followed by 100 ml of 4% buffered formaldehyde, delivered via a 23-gauge needle connected to a perfusion pump. Six shams, three adult and three aged, were also processed. The brains were removed, post-fixed in 4% buffered formaldehyde for 12 hours, then cryoprotected and embedded in 5 x 5 arrays in gelatin blocks using the Multibrain^{TM} process (Neuroscience Associates, Knoxville, TN). Frozen sections were cut at 35µm thickness, with each tissue sheet containing 1 coronal section from each of the 25 brains. Sheets were stored in an ethylene glycol solution at -80°C prior to immunostaining.

Blood-Brain Barrier

Blood-brain barrier opening was assessed using mouse IgG immunostaining. Extravasation of mouse IgG (molecular weight 150 kDa) into the brain parenchyma, as a measure of blood brain barrier breakdown, has been well documented in other mouse brain injury studies (Smith et al., 1995; Benkovic et al., 2006; Saatman et al., 2006). Tissue sheets were rinsed in 1X PBS, and then incubated for two hours with 1:1000 diluted biotinylated anti-mouse IgG secondary antibody BA-2001 (Vector Labs, Burlingame, CA). Detection of staining was accomplished with Vectastain Elite ABC amplification (Vector Labs, Burlingame, CA) and visualization was done using a nickel-diaminobenzidine chromogen.

Sections were visualized with a Nikon inverted-stage microscope at 20x magnification and digital images were captured with a SPOT microscope camera (Diagnostic Instruments, Sterling Heights, MI). The same white balance and exposure settings were used to capture all images. From these histological images, we measured anti-IgG staining, in each hemisphere with the NIH ImageJ software, using a thresholding technique. The threshold was set at a level just above that which would have counted background and non-specific staining of the gelatin mountant medium in the tissue sheets. Brain pixels in each hemisphere were also counted, allowing the ratio of stained/total brain tissue to be calculated, for both hemispheres in each coronal brain section. Measurements were done by a person blinded to experimental group and time point.

Amino-Cupric Silver Staining

Amino-cupric silver staining was used to assess the extent of neurodegeneration. This technique has been demonstrated to have excellent sensitivity and selectivity for the identification of degeneration of neurons, including their cell bodies, processes and synapses (Switzer, 2000). Tissue sheets were stained with amino-cupric silver and counter-stained with Neutral Red. Sections were visualized with a Nikon inverted-stage

microscope at 20x magnification and digital images were captured with a SPOT microscope camera (Diagnostic Instruments, Sterling Heights, MI). Four slightly-

overlapping digital images were acquired for each coronal section, and these images were merged to yield a single high resolution image of the entire coronal section. The silver staining was measured using densitometric thresholding, in a manner similar to that in previously reported mouse CCI work (Hall et al., 2005). Measurements were made in each hemisphere, for each brain, in 12 sections spaced 0.42mm apart, by a person blinded to experimental group and time point.

Lesion Cavity

At 72 hours post-injury, there was loss of tissue at the impact site. Measurements of frank tissue loss were made from the images of the amino-cupric silver / neutral red stained 72 hour post-injury tissues.

On each image, the cavity was outlined with the polygon selection tool by visual inspection, with the dorsal aspect of the lesion shaped as a mirror image to the contour of the uninjured hemisphere. A pixel count was obtained with the histogram function in ImageJ. For each animal, the cavity area was measured in five to eight sections spaced approximately 0.42mm apart, and the total cavity volume was calculated using the formula $A_1 (0.5X_1) + A_2(0.5X_1+0.5X_2)+ A_{n-1}(0.5X_{n-1}+0.5X_n) +A_n(0.5X_n)$ where A_n is the area of the cavity for section (n) and X_n is the distance between sections (n) and (n-1) (Dash et al., 2004).

Statistical Analysis

For the analysis of MRI and histological data and comparisons between the adult and aged groups, we used the two-tailed t-test for data with normal distributions, and the Mann-Whitney U-test for data with non-normal distributions. Normality was assessed with Kolmogorov-Smirnov (KS) test. For analysis of the behavioral data and comparisons between the adult and aged groups, we used the repeated measures ANOVA test. All statistical analyses were performed using GraphPad Prism4software (GraphPad, San Diego, CA).

Results

Magnetic Resonance Imaging

Early Acute T2 Hyperintensity

Figure 1 shows example 0.5mm thick anatomically-axial T2-weighted spin-echo images taken at 24 and 48 hours post-injury from injured adult and aged animals. At 24h, there was signal hyperintensity at, and around, the injury site that we interpret as acute edema. By 48h, this hyperintensity was diminished, indicating that the acute edema had begun to resolve. Comparing the images from the adult and aged animals, an increased collapse of the lateral ventricle on the ipsilateral side of the aged brain was clearly visible.

Figure 2 shows the results for T2 hyperintensity measurements, with the data presented as ratios of 48h to 24h values for each animal. The T2 hyperintense tissue volume ratio was greater in the injured aged animals than the injured adults (102% vs.

74%; t-test, $p<0.01$) indicating persistent edema. The total T2 hyperintensity signal ratio was also greater in the injured aged (108%) than in injured adult animals (91%) a difference approaching significance (t-test, $p=0.08$).

Injury Presentation at 28 Days

Figures 3 and 4 show example T2-weighted spin-echo images from injured adult aged animals, respectively, at 28 days post-injury, in the coronal and horizontal planes. These show a strong signal hyperintensity, corresponding to a fluid-filled lesion cavity, where cortical and subcortical tissue had been lost. They also show a well-defined border between the hyperintense and normal-appearing areas, suggesting that by this time the lesion cavity size and shape was stable. The lateral ventricle on the ipsilateral side was expanded (see arrows in panels v and w of Figures 3 and 4). There was loss of white matter in the corpus callosum, and in the ipsilateral cingulum and medial portion of the external capsule. The longitudinal cerebral fissure was shifted towards the injured side, as seen in the horizontal images (see arrowheads in panels t and u of Figures 3 and 4). In regions adjacent the fluid-filled cavity, thinning of cortical grey matter was observed in the coronal images (see asterisks in panels f, g and m of Figures 3 and 4). In several of the coronal images, the rostral thalamus on the ipsilateral side demonstrated a signal hypointensity (see large arrows in panels h and I of Figure 3 and panels g and h of Figure 4).

Behavior

Rotarod

Rotarod results are shown in Figure 5. Post-injury mean scores were expressed as a percent of pre-injury score, and error bars indicate standard error of the means. A repeated measures ANOVA of rotarod performance of the injured adult and injured aged groups revealed significant effects of age ($F(1,72)=6.57$, $p<0.05$) and time ($F(4,72)=16.1$, $p<0.001$), as well as an interaction ($F(4,72)=2.9$, $p<0.05$). For acceleration to 18rpm over 90 seconds, injured adult animals performed at about 40% of their pre-injury level at 24 and 48 hours, after which there was gradual improvement. By 14 days, the injured adult animals had improved to 88% of pre-injury. The aged animals were slower to recover, showing little improvement by 72 hours, although by 14 days their performance improved to 56% of their pre-injury level. A single comparison of injured adult and injured aged scores at 14 days post-injury revealed that aged animals performed worse than adult animals (t-test, $p<0.05$), demonstrating poorer recovery from injury.

Gridwalk

Gridwalk test results, for the left forelimb minus right forelimb, are shown in Figure 6. Deficits in the gridwalk test were found for both injured groups compared with shams. These deficits were greatest at the early time points (48 and 72 hours post-injury), for both adult and aged animal groups, after which both groups showed gradual recovery. A repeated measures ANOVA of gridwalk performance revealed

significant effects of age ($F(1,54)=3.62$, $p<0.01$) and time ($F(3,54)=4.81$, $p<0.01$), as well as an interaction ($F(3,54)=2.9$, $p<0.05$). At the 14 day time point, deficits in the injured aged group were 80% greater than those in the injured adult group, a statistically significant difference (t-test, $p<0.05$), demonstrating worse outcome or poorer recovery after injury.

Spontaneous Forelimb Task

Spontaneous forelimb task results are shown in Figure 7. The laterality data for each animal are corrected by subtraction of the pre-injury score. Deficits were found for both the adult and injured aged groups, compared to shams. Deficits for the adult group were greatest at 7 days, while deficits in the aged group were greatest at 72 hours. The deficits in the aged animals were greater than in the adult animals at every time point. A repeated measures ANOVA of spontaneous forelimb performance revealed a nearly significant effect of age ($F(1,54)=3.62$, $p=0.09$) and a significant effect of time ($F(4,54)=4.81$, $p<0.01$). At the 7 and 14 day time points, the deficits in the injured aged animals were 46% and 52% greater than those in the injured adult group, suggesting worse outcome or poorer recovery after injury.

Figures 5, 6 and 7 include previously reported behavioral results from adult animals (Onyszchuk et al., 2007), that are presented here for age comparisons.

Histology

Blood Brain Barrier

Representative images of anti-mouse IgG stained coronal sections, near the injury epicenter (bregma), and at two more caudal locations, near bregma -1.5 and bregma -2.5, are shown in Figure 8. Staining in the adult sham images was apparent at very low levels in the lateral septal nucleus (LSD), the septofimbrial (SFi) nucleus, the stratum radiatum (Rad) of the hippocampus, the molecular layers (LMol, Mol) of the hippocampus, the fimbria (fi) of the hippocampus, the oriens layer (Or) of the hippocampus and in the dorsal and lateral hypothalamic nuclei (ArcD, ArcL) (Franklin and Paxinos, 1997). Staining in the aged sham images was found at a low level in the cortex, and at an increased level compared to adult shams in all of the hippocampal structures above, especially in the oriens layer (Figure 8j).

Qualitative Assessment

The anti-IgG staining in the injured brains was diffuse, extending well beyond the site of impact. The staining appeared more intense and more widespread in the injured aged brains compared to the injured adult brains. The staining also extended deeper below the cortical surface in the injured aged brains compared to the injured adult brains (Figure 8d, h and l).

Quantitative Measurements

The results for measurement of blood-brain-barrier compromise via IgG immunostaining are shown in Figure 9. At 3 days post-injury, staining was significantly greater in the aged animals than the adults when examining absolute values (t-test , $p<0.01$), and when examining increases above background (t-test, $p<0.05$). At 7 days post-injury, staining was significantly greater in the aged animals when examining absolute values (t-test, $p<0.05$), and approached significance when examining increases above control values (t-test, $p=0.07$). Comparing 3 day and 7 day values, staining showed a diminishing trend (not significant) in the adult that was not observed in the aged brains, suggesting some recovery of blood-brain barrier integrity in the adult, but not in the aged brains.

Amino-cupric Silver Staining

Representative images of amino-cupric silver stained coronal sections, near the injury epicenter (bregma), and at two caudal locations, near bregma -1.3 and bregma -2.0, from animals sacrificed at 3 days post-injury, are shown in Figure 10. Sections from adult shams showed little staining, whereas the aged sham sections were lightly stained in the fornix, fimbria and in the periventricular areas (Figure 10b, f).

Qualitative Assessment - Near Injury Epicenter (Bregma)

The adult and aged sections near the injury epicenter were extensively stained in the ipsilateral cortex, corpus callosum and caudate-putamen. In the ipsilateral cortex, staining was greatest near the site of impact, in the primary somatosensory forelimb

(S1FL) and primary motor (M1) regions, but extended to additional cortical areas, including secondary motor (M2), cingulate (Cg1, Cg2), primary and secondary sensory (S1, S2), granular insular (GI), primary somatosensory barrel field (S1BF), primary somatosensory hindlimb (S1HL) and primary somatosensory dysgran zone (S1DZ) (Franklin and Paxinos, 1997). Staining in these areas was noted at all four post-injury time points examined (Figure 10c, d, g, and h).

In the cortex contralateral to the injury, staining was less extensive than ipsilateral cortex, with most staining in the S1FL and M1 areas. This light contralateral staining was visible in three (one adult, two aged) of the eight 48 hour samples, but was more intense and visible in 15 of 20 of the 3 day samples, and in eight of the eight 7 day samples. In the contralateral subcortical white matter, some light staining was observed in 24 and 48 hour samples, and much more substantial staining was observed in the 3 and 7 day samples. In the contralateral caudate-putamen, staining was not found at 24 and 48 hours post-injury, but was visible in samples from longer survival times.

Qualitative Assessment - Caudal to Injury (Bregma -1.5mm to Bregma -3.5mm)

The injured adult and injured aged sections at and just beyond the caudal extremity of the impact and just beyond were also extensively stained in the cortex and subcortical white matter, and to a lesser extent, in the hippocampus and thalamus. In the ipsilateral hippocampus, staining was observed in the dentate gyrus, as well as in the

CA1 and CA3 regions. A very low level of staining was observed in the contralateral dentate gyrus in a small number of sections (data not shown).

In the ipsilateral thalamus, some staining was noted at 48 hours and 72 hours, the greatest and most extensive staining was observed in the 7 day samples – where all eight samples were stained. Examples of thalamic staining in 7 day adult and aged samples are shown in Figure 11. In the 7 day samples, as seen in the figure, staining was extensive in the ventral posterolateral (VPL), ventral posteromedial (VPM), ventrolateral (VL), posterior (Po), central lateral (CL), paracentral (PC) and laterodorsal (LDVL, LDDM) thalamic areas (Franklin and Paxinos, 1997). In the contralateral thalamus, low levels of staining were observed in the VPL and VPM regions in the 3 and 7 day samples.

Caudal to the injury zone, at bregma -2.50 to bregma -2.90, moderate staining was observed in the 7 day samples in the ipsilateral cerebral peduncle (in seven of eight samples), ipsilateral cingulum (eight of eight), and ipsilateral substantia nigra (five of eight).

To summarize the qualitative observations, we observed extensive silver staining in the injured cortex, and in the ipsilateral corpus callosum and caudate-putamen. In the corresponding contralateral regions, staining was less intense, and delayed in onset. Hippocampal staining was observed in the ipsilateral dentate gyrus, CA1 and CA3

regions and at a low level in the contralateral dentate gyrus. Thalamic staining, of greatest intensity at 7 days, was observed in six dorsal thalamic nuclei, and was most prominent in VPL, VPM and VL regions. A low level of contralateral thalamic staining was also observed. A moderate level of staining was observed in grey and white matter areas as far as 2.9 mm caudal to the injury epicenter.

Quantitative Measurements

The results for measurement of neurodegeneration by amino-cupric silver staining are shown in Figure 12. Data presented are for the ipsilateral hemisphere only, and for ipsilateral hemisphere minus contralateral hemisphere to reduce the impact of non-specific staining that might be common to both hemispheres. At three days post-injury, staining in the aged animals was significantly greater than in the adult for the ipsilateral only (t-test, $p<0.01$), and for the ipsilateral minus contralateral (t-test, $p<0.01$).

Lesion Cavity

Measurements of lesion cavity volume, from histology images of brains at 3 days post-injury are shown in Figure 13. There was no significant difference between the measurements for the adult and aged animals.

Discussion

This study showed several significant differences in the response to sensorimotor CCI injury in the aged compared to the adult animals. The resolution of post-injury focal edema assessed by high-field MR imaging was slower in the aged compared to the adult brains. The degree of blood-brain-barrier opening assessed by anti-IgG staining was greater in the aged compared to the adult brains. The degree of neurodegeneration at 3 days post-injury assessed by amino-cupric silver staining was greater in the aged compared to the adult brains. The recovery from behavioral deficits was slower and less complete in the aged compared to adult animals.

Our data show that acute edema was prolonged in the aged brain compared to the adult following CCI injury. This finding is consistent with the results of other studies in different injury models. Edema was increased in aged rodents after a cortical freezing lesion (Unterberg et al., 1994), and after intracerebral hemorrhage (Gong et al., 2004). In the latter study, the authors suggest that erythrocyte fragility, iron toxicity, and upregulation of heat shock proteins HSP27 and HSP32 may have played roles in the observed increases in edema. In the context of damage mechanisms following TBI, edema has been described as having a "crucial impact on morbidity and mortality" (Unterberg et al., 2004). The phenomenon of increased edema in the aged brain compared to the adult after TBI, might be of clinical importance and might motivate more aggressive management of edema as part of an overall treatment strategy for elderly patients.

Behavioral measurements, demonstrating poorer recovery from sensorimotor deficits in the injured aged animals in the Rotarod, gridwalk, and spontaneous forelimb tests, were consistent with an earlier study of TBI in a rat model in which aged animals showed greater acute neurological and motor deficits (Hamm et al., 1991; Hamm et al., 1992a), and with a study of hemorrhage in which aged rats showed greater deficits and slower recovery in forelimb placing and cylinder tests (Gong et al., 2005). Taken together, our behavioral results across three tests, Rotarod, gridwalk and spontaneous forelimb indicate that both groups of injured animals performed worse than age-matched shams. Moreover, the deficits seen in the aged animals were greater and lasted longer than those seen in the adults, consistent with the greater functional impairments and cognitive deficits seen in elderly survivors of TBI (Rapoport et al., 2006; Thompson et al., 2006).

The anti-IgG staining at 3 and 7 days showed interesting age-related differences in magnitude and timing. The downward trend in staining in the injured adult animals but not in the injured aged animals suggests recovery of the blood-brain barrier in the younger animals over the time course of these experiments. The prolonged and greater opening of the blood-brain barrier in the aged animals may well have been an important contributing factor to the increased neurodegeneration in the aged brains. The potential detrimental effects of a more leaky blood-brain barrier after TBI have been described in many reviews, where a compromised or “hyperpermeable” blood-

brain barrier is considered a “hallmark” of TBI pathophysiology, leading to increased access of ions, water, proteins and free radicals to the brain parenchyma, loss of cerebral autoregulation, increased vasogenic edema, increased intracranial pressure, osmotic disruption, intraparenchymal hemorrhage, infiltration of pro-inflammatory mediators, systemic inflammation and neuroinflammation (Zink, 1996; Suo et al., 2004; Unterberg et al., 2004; Scholz et al., 2007).

Conversely, the more open blood-brain barrier in the injured aged brain – at least to molecules up to approximately 150 kDa size - may represent a clinically relevant opportunity. An extended opening of the aged blood-brain barrier after brain injury may provide an enhanced and extended window of opportunity for the delivery of therapeutic agents that do not traverse a normal, intact barrier. The failure of potentially neuroprotective compounds to penetrate the blood-brain barrier has been described as an important factor in the failure of these compounds in clinical trials (Bullock et al., 1999; Faden, 2001; Tolias and Bullock, 2004; Helmy et al., 2007). It is possible that the injured aged brain might allow beneficial compounds better penetration over an extended period to injured tissues, possibly yielding better efficacy in the injured aged brain compared to the adult.

Our data for amino-cupric silver staining showed that there was significantly greater neurodegeneration in the injured aged brains at 3 days post-injury, with a trend towards increased neurodegeneration at 7 days post-injury. The staining extended

well beyond the site of cortical impact in the injured hemisphere, to specific regions in the contralateral hemisphere, confirming results a recent study of CF-1 adult mice using a pneumatic CCI device and a more caudal injury location (Hall et al., 2005). In contrast to that study, our staining was less extensive in the hippocampus, reflecting our more rostral injury location. Staining of the dorsal thalamic nuclei, including VL, VPL, VM, CM and CL, was consistent with the cortical targets for these nuclei (Jones, 1985), and the observation of maximum staining in these areas at 7 days post-injury is consistent with retrograde neurodegeneration of thalamic neurons resulting from damage in the cortical target areas and loss of functional cortical connectivity. The observation of maximum staining at 7 days post-injury suggests that neurodegeneration in this model is delayed compared to thalamic neuron loss measured in the lateral geniculate nucleus after cortical ablation, where significant reduction in neuron population in wild type adult mice was noted at 3 days post-injury (Muessel et al., 2002). Taken with the increased acute edema measured from MRI, and increased blood-brain-barrier permeability assessed by anti-IgG staining, our neurodegeneration data provides strong evidence for increased damage in aged brains compared to adult brains following the same CCI injury.

Our edema, blood-brain barrier and neurodegeneration data suggest increased vulnerability of the aged brain to TBI that is also reflected in the behavioral testing results. This is consistent with the notion of "reduced cerebral reserve" in aged TBI patients that were first described over 20 years ago (Galbraith, 1987). Numerous

subsequent reports suggest that the principal cells of the brain – neurons, astrocytes, microglia, oligodendrocytes – are subject to increased oxidative, metabolic and ionic stress, have accumulated damage to proteins, DNA and mitochondria, and are subject to pro-inflammatory and pro-apoptotic conditions as they age (Beal, 1995; Morrison and Hof, 1997; Franceschi et al., 2000; Felzien et al., 2001; Benn and Woolf, 2004; Mattson and Magnus, 2006). All of these factors combined support a hypothesis that cells in the aged brain should have increased vulnerability – to loss of function and to death - following traumatic injury.

In contrast with the silver staining findings, our lesion cavity volume measurements at 3 days post-injury showed comparable results in the injured adult and injured aged groups. Certainly, measurement of lesion volume is not without limitations, including the possible effects of differing brain sizes, tissue shrinkage during processing, brain water content variation, and loss of brain tissue in remote regions. And, although the cavity measurements assessed tissue loss at the injury site, the silver staining assessed neurodegeneration over the entire brain hemisphere. Also, there is evidence from transgenic studies suggesting that gross tissue loss following TBI in the mouse is not well correlated with functional impairment (Tehranian et al., 2006), and that modest reduction in cavity volume after CCI does not necessarily reduce behavioral deficits (Raghupathi et al., 1998). Given that the amino-cupric silver stain is known to have a wide detection period - from before neuron death to well afterwards (Switzer, 2000) – our results at 3 days post-injury may reflect an

increased neurodegeneration in the aged group that has not yet culminated in neuron death and loss of tissue.

With results for the localized cavity measurements at one time point and the hemispheric silver measurements at four time points, we do not have a complete picture of overall neurodegeneration and tissue loss in this model. Nevertheless, the silver and cavity results taken together are consistent with the possibility that the aged brains are equally vulnerable to primary injury but more vulnerable to secondary injury than the adult. Equally, the results are consistent with the possibility that the aged brains are equally vulnerable to damage at the site of impact but more vulnerable to damage in remote brain regions than the adult.

These results suggest that the aged brain is more vulnerable than the adult brain to neurodegeneration and loss of function, following controlled cortical impact injury. Similar lesion cavity volumes in the injured groups indicate that acute loss of tissue at the injury site is not the cause of increased functional deficits in the aged injured animals. The prolonged acute edema, more widespread blood-brain barrier opening, and increased neurodegeneration seen in the aged animals suggest that secondary processes play a major role in the worsened outcome in the aged brain after TBI. Edema and blood-brain barrier compromise may represent opportune targets for treatment strategies aimed at improving outcomes in elderly TBI patients.

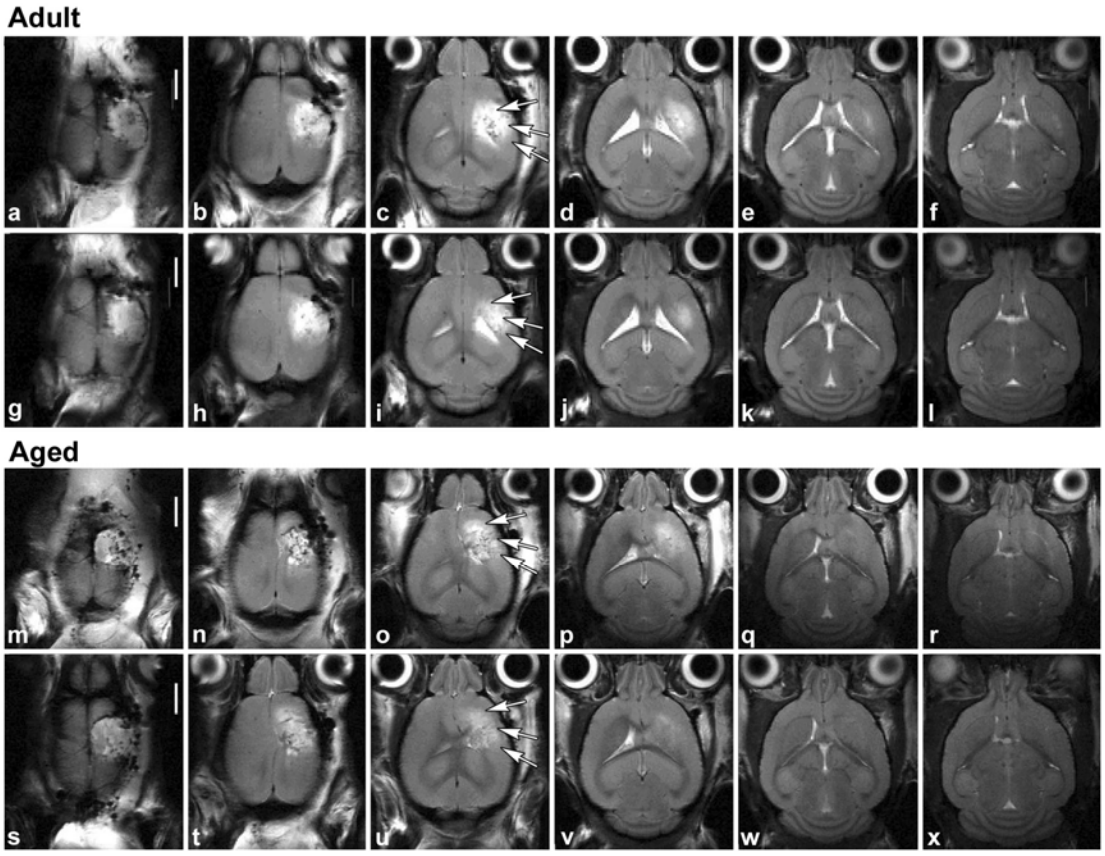

Figure IV-1: T2-weighted MR images of an injured adult animal, acquired at 24 hours and 48 hours post-injury (top 2 rows), and of an injured aged animal, acquired at 24 hours and 48 hours post-injury (bottom 2 rows). Contiguous anatomically horizontal slices, slice thickness =0.5mm. TR=2500ms, TE=45ms, field of view: 18mm x 14mm. Scale bar 2mm. Arrows in panels c, i, o and u highlight hyperintense tissue. Collapsed lateral ventricle in the hemisphere ipsilateral to the injury is indicative of brain swelling.

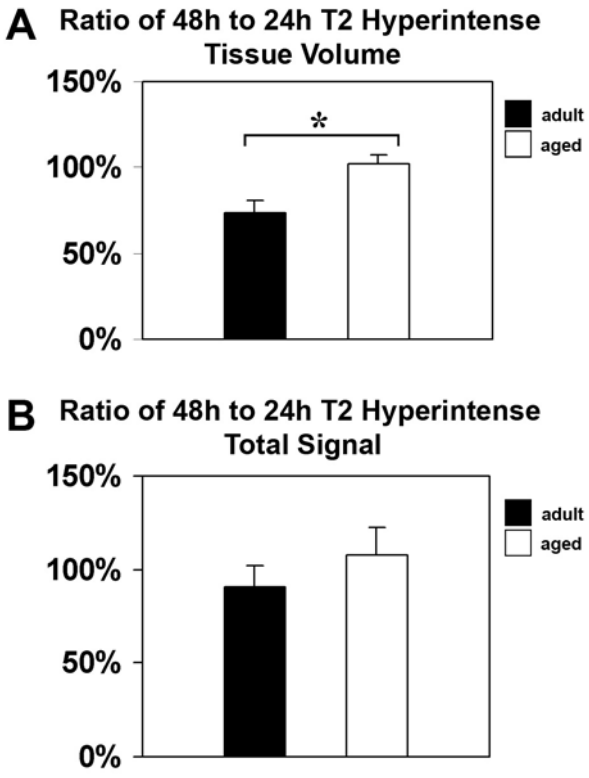

Figure IV-2: Ratios of same animal 48 hour to 24 hour T2 hyperintense tissue volumes (A) and T2 hyperintense total signals (B), showing slower resolution of hyperintense tissue in the aged brains ($p<0.01$), and slower decline in total hyperintense signal ($p=0.36$). n=8-9 per group. (indicates $p<0.01$).**

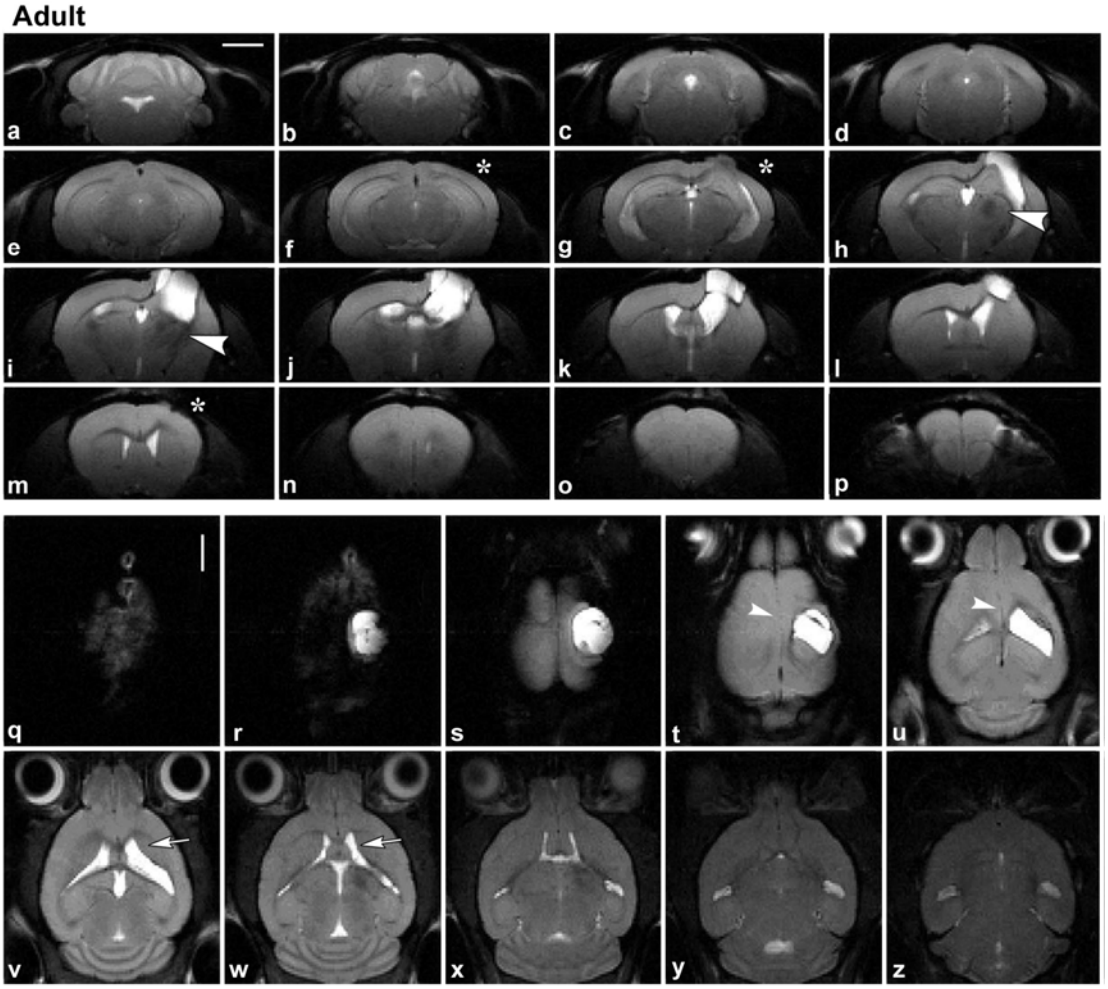

Figure IV-3: T2-weighted MR images of an injured adult animal, in the anatomically coronal (top), and horizontal (bottom) planes, acquired at 28 days after injury. Contiguous slices, slice thickness = 0.5mm. TR=2500ms, TE=45ms, field of view: 16mm x 10mm and 18mm x 14mm, respectively. Asterisks indicate thinning of the cortical mantle (f, g), large arrowheads point to areas of signal hypointensity (h, i), small arrowheads indicate midline shift (t, u), and arrows indicate expanded ispilateral ventricle (v, w), Scale bar 2mm.

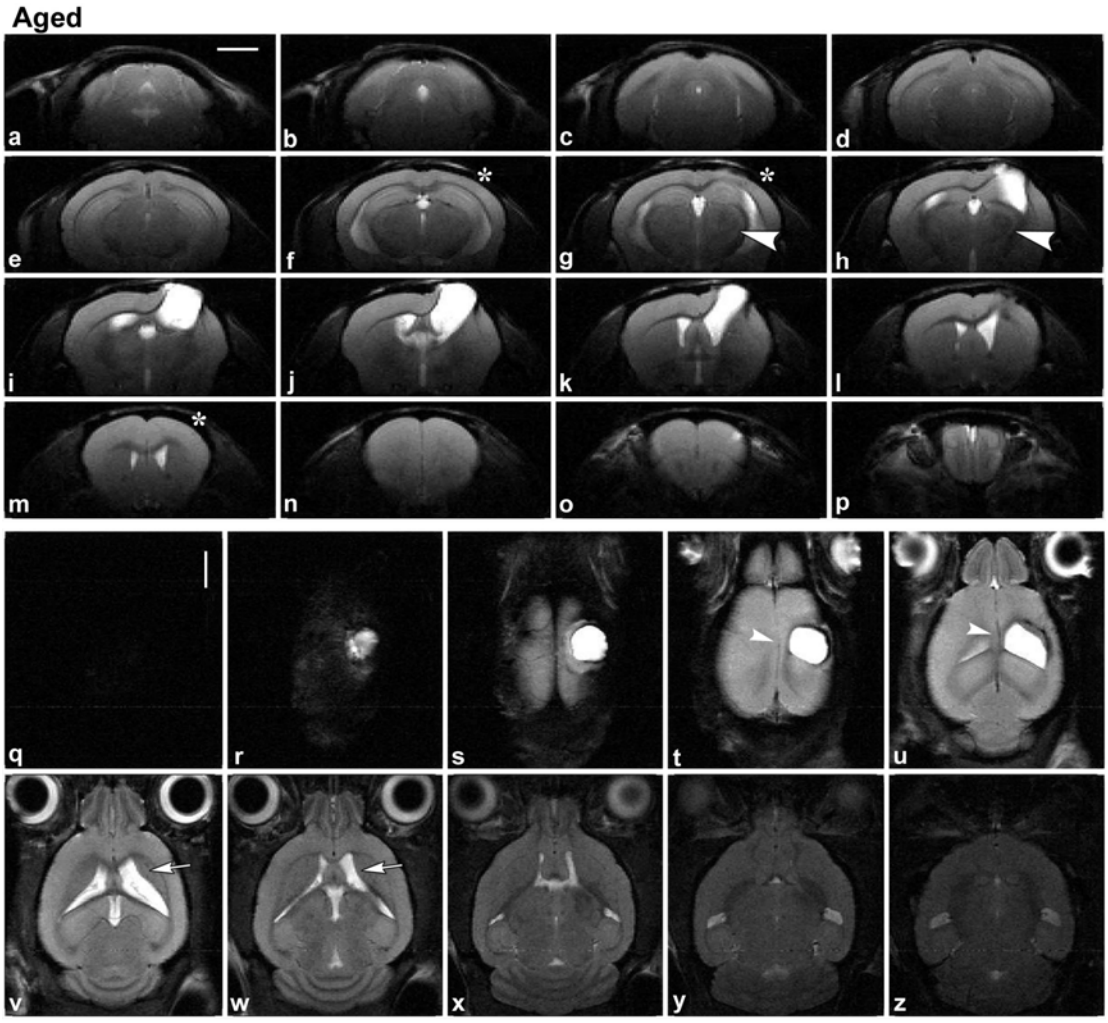

Figure IV-4: T2-weighted MR images of an injured aged animal, in the anatomically coronal (top), and horizontal (bottom) planes, acquired at 28 days after injury. Contiguous slices, slice thickness = 0.5mm. TR=2500ms, TE=45ms, field of view: 16mm x 10mm and 18mm x 14mm, respectively. Asterisks indicate thinning of the cortical mantle (f, g), large arrowheads point to areas of signal hypointensity (g, h), small arrowheads indicate midline shift (t, u), and arrows indicate expanded ispilateral ventricle (v, w), Scale bar 2mm.

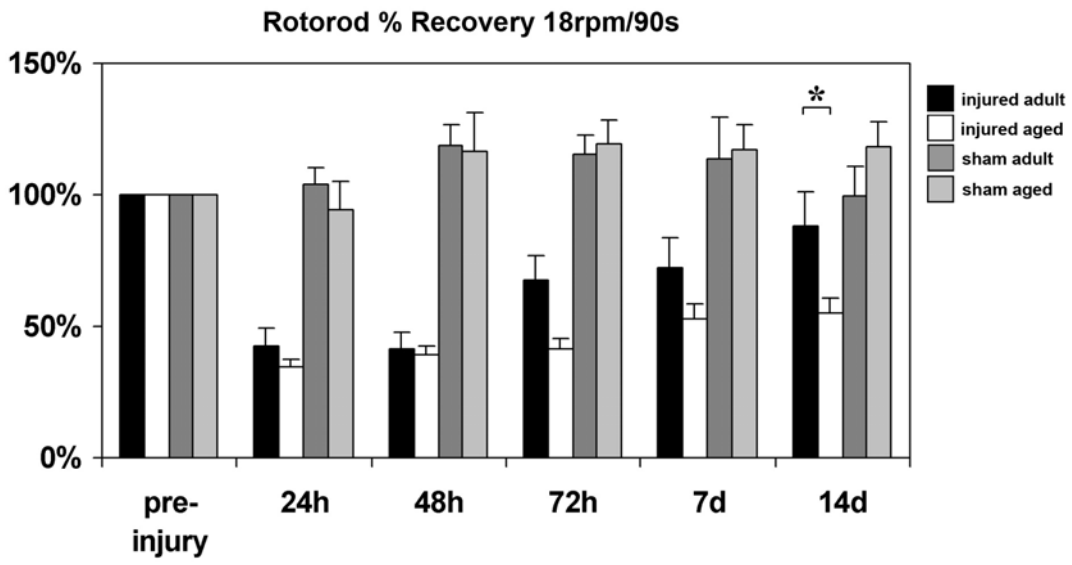

Figure IV-5: Results for Rotarod measurement of sensorimotor deficit and recovery. At 72 hours, injured adult animals have begun to recover, while injured aged animals have not. At 14 days post-injury, injured adult animals have recovered to 88% of pre-injury performance, while injured aged animals have recovered to only 56% of pre-injury performance. n=8-12 per group.

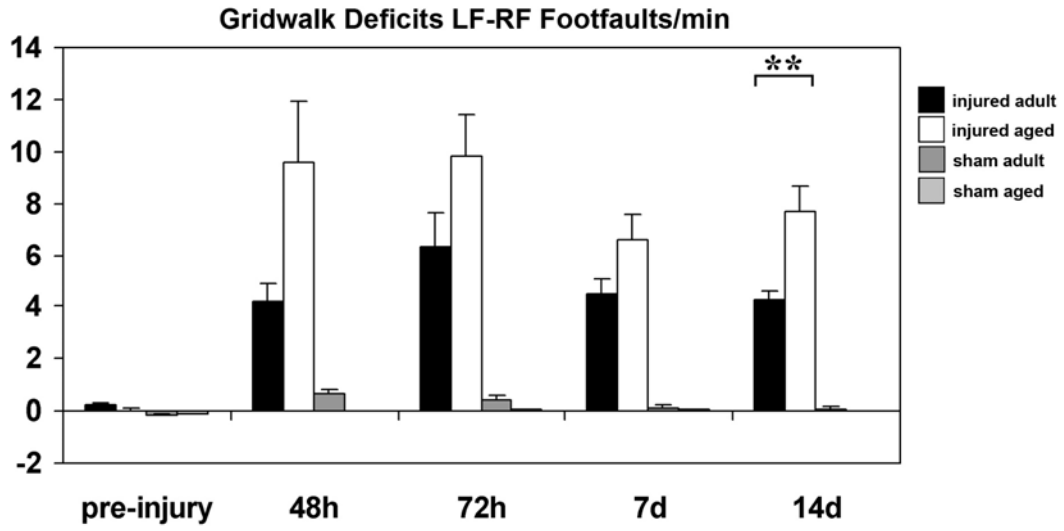

Figure IV-6: Results for Gridwalk measurement of sensorimotor impairment and recovery, presented as left forelimb minus right forelimb footfaults per minute of walking. Deficits are greater in the injured aged animals than the injured adult animals at all post-injury time points. n=8-12 per group.

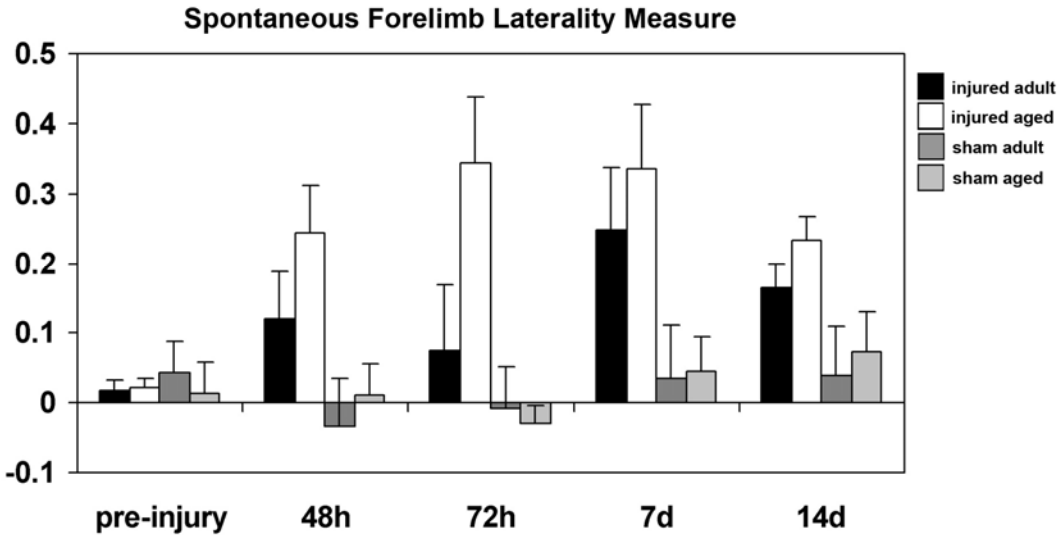

Figure IV-7: Results for spontaneous forelimb (cylinder) task impairment and recovery data, showing peak forelimb laterality scores at 72 hours (injured aged) and 7 days (injured adult), with some recovery by 14 days. Deficits are greater in the injured aged animals than the injured adult animals at all post-injury time points. n=8-12 per group.

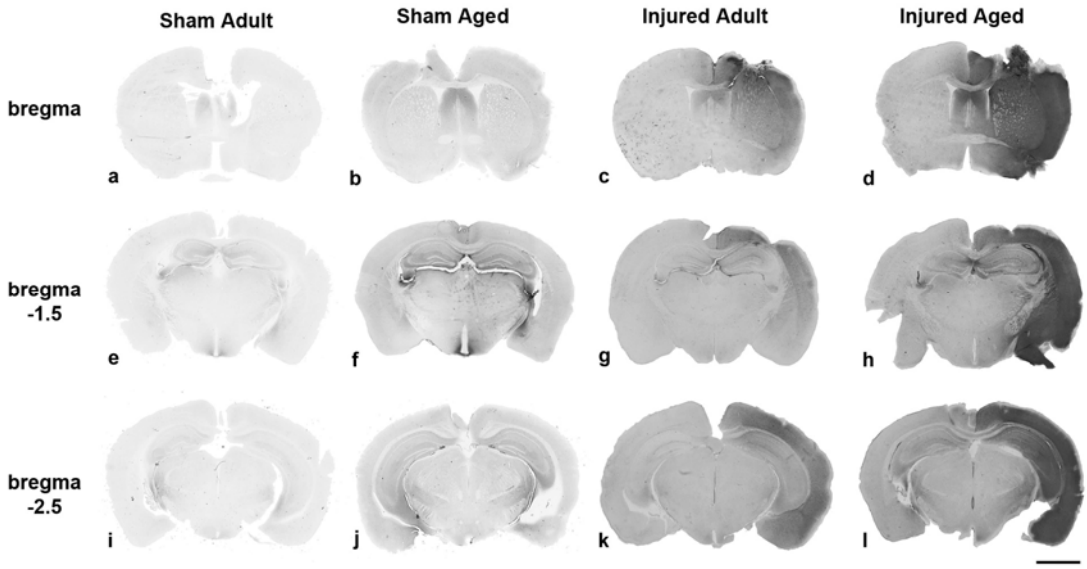

Figure IV-8: Representative images of anti-IgG stained coronal sections, of injured animals at 3 days post-injury. Brains from injured aged animals show considerably more disrupted blood-brain-barrier than those from adults. Scale bar 2mm.

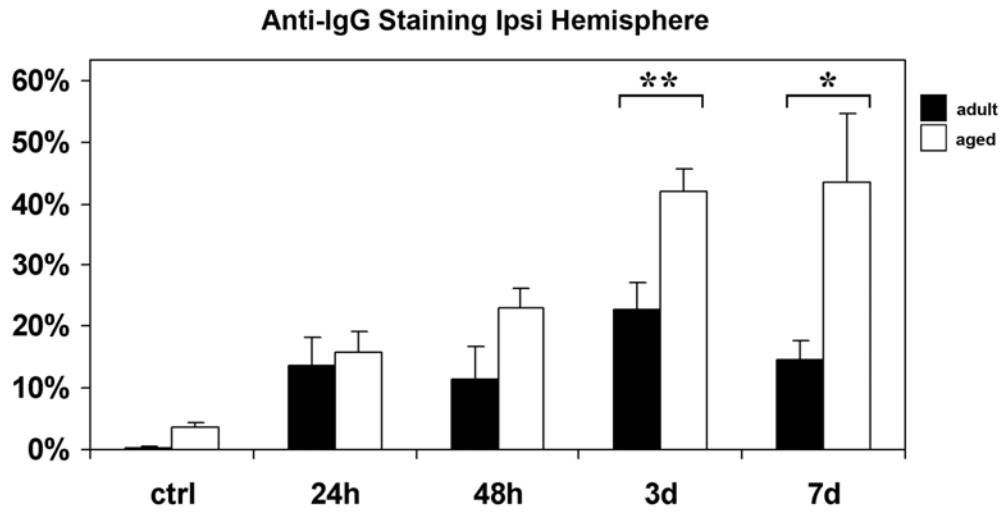

Figure IV-9: Measurements of anti-IgG staining in control and injured sections to assess blood-brain barrier compromise, showing statistically significant differences between injured adult and injured aged at 3 ($p<0.01$) and 7 days post-injury ($p<0.05$). Percent staining is calculated from the ration of stained pixels to total brain pixels in the hemisphere. Following injury, repair of the blood-brain barrier is slower or delayed in the injured aged brains. n=3, 4, 4, 10, and 4 per group, for control, 24h, 48h, 3d and 7d groups respectively. (indicates $p<0.01$, * indicates $p<0.05$).**

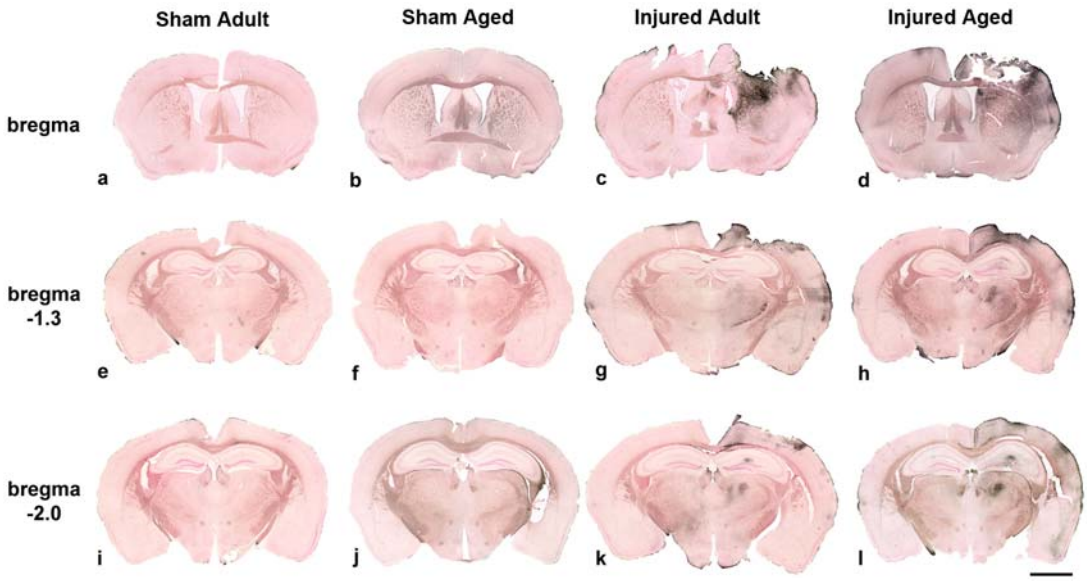

Figure IV-10: Representative images of amino-cupric silver stained coronal sections, of injured animals at 3 days post-injury. Injured aged animals show considerably more neurodegeneration than injured adult animals. Scale bar 2mm.

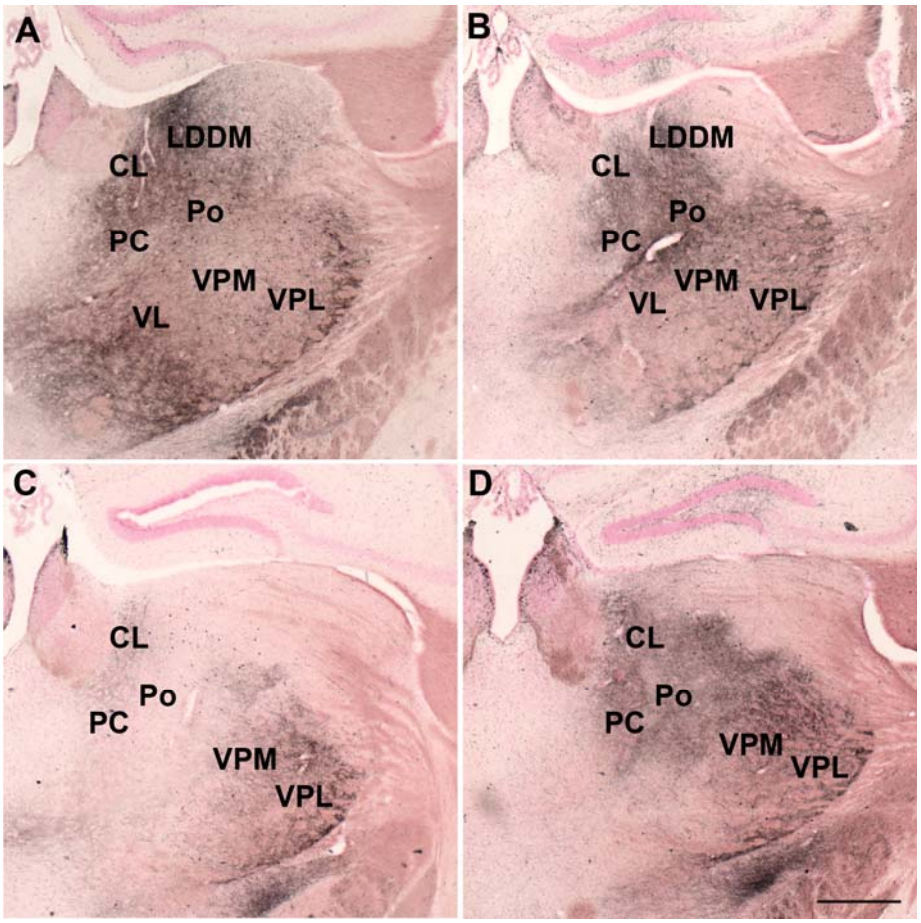

Figure IV-11: Example images of amino-cupric silver staining in the thalamus (coronal sections) of one injured adult animal (panels A and C) and one injured aged animal (panels B and D) at 7 days post-injury. Panela A and C at bregma -1.4, panels B and D at bregma -1.8. Panels A, B and D show some light staining in the dentate gyrus. Scale bar 0.5mm.

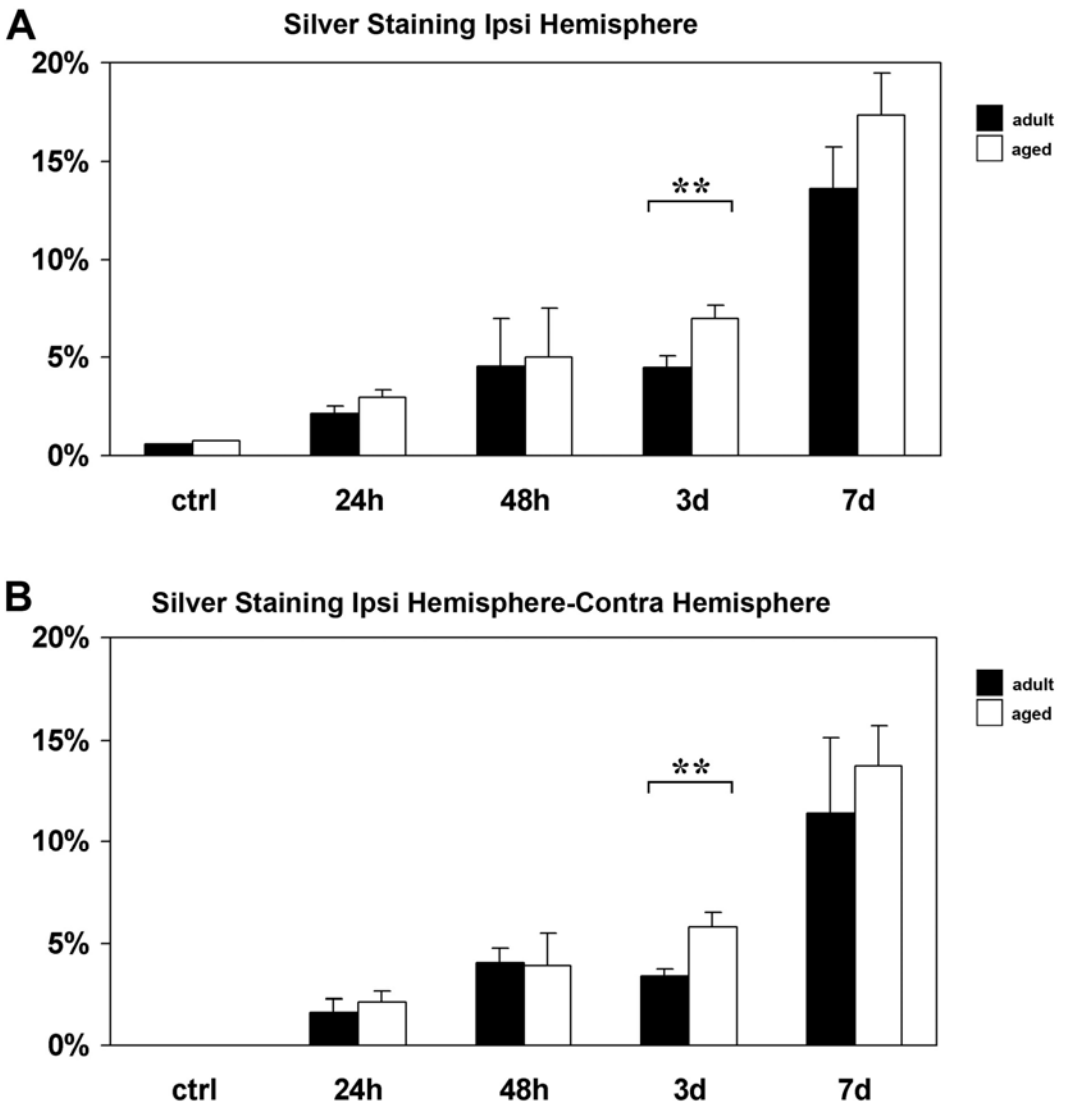

Figure IV-12: Measurements of amino-cupric silver staining in control and injured sections to assess neurodegeneration, ipsilateral hemisphere only (A), and ipsilateral minus contralateral (B). Ipsilateral-only staining in the aged brains was 73% greater than in the adult brains ($p<0.01$), and ipsilateral minus contralateral staining was 57% greater than in the adult brains ($p<0.01$). Percent staining is calculated from the ratio of stained pixels to total pixels. n=3, 4, 4, 10, and 4 per group, for control, 24h, 48h, 3d and 7d groups respectively. (indicates $p<0.01$).**

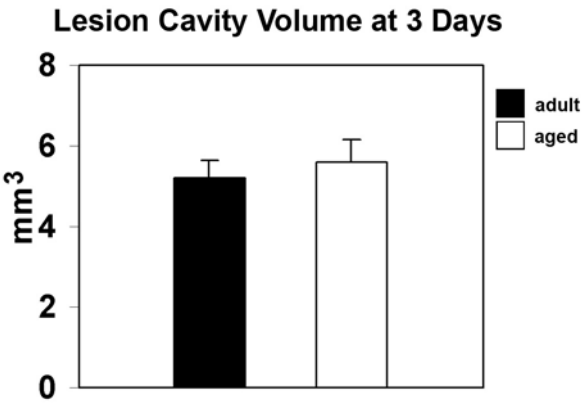

Figure IV-13: Lesion cavity volume at 3 days post-injury, measured from images of amino-cupric silver and neutral red stained coronal tissue sections, showing comparable cavity volumes at this time point. n=10 per group.

References

Bartkowski HM, Pitts LH, Nishimura M, Brant-Zawadzki M, Moseley M, Young G (1985) NMR imaging and spectroscopy of experimental brain edema. J Trauma 25:192-196.

Baskin YK, Dietrich WD, Green EJ (2003) Two effective behavioral tasks for evaluating sensorimotor dysfunction following traumatic brain injury in mice. J Neurosci Methods 129:87-93.

Beal MF (1995) Aging, energy, and oxidative stress in neurodegenerative diseases. Ann Neurol 38:357-366.

Benkovic SA, O'Callaghan JP, Miller DB (2006) Regional neuropathology following kainic acid intoxication in adult and aged C57BL/6J mice. Brain Res 1070:215-231.

Benn SC, Woolf CJ (2004) Adult neuron survival strategies--slamming on the brakes. Nat Rev Neurosci 5:686-700.

Bilgen M (2005) A new device for experimental modeling of central nervous system injuries. Neurorehabil Neural Repair 19:219-226.

Brant-Zawadzki M, Bartkowski HM, Ortendahl DA, Pitts LH, Hylton NM, Nishimura MC, Crooks LE (1984) NMR in experimental cerebral edema: value of T1 and T2 calculations. AJNR Am J Neuroradiol 5:125-129.

Bullock MR, Lyeth BG, Muizelaar JP (1999) Current status of neuroprotection trials for traumatic brain injury: lessons from animal models and clinical studies. Neurosurgery 45:207-217; discussion 217-220.

Coronado VG, Thomas KE, Sattin RW, Johnson RL (2005) The CDC traumatic brain injury surveillance system: characteristics of persons aged 65 years and older hospitalized with a TBI. J Head Trauma Rehabil 20:215-228.

Dash PK, Moore AN, Moody MR, Treadwell R, Felix JL, Clifton GL (2004) Post-trauma administration of caffeine plus ethanol reduces contusion volume and improves working memory in rats. J Neurotrauma 21:1573-1583.

Dixon CE, Clifton GL, Lighthall JW, Yaghmai AA, Hayes RL (1991) A controlled cortical impact model of traumatic brain injury in the rat. J Neurosci Methods 39:253-262.

Faden AI (2001) Neuroprotection and traumatic brain injury: the search continues. Arch Neurol 58:1553-1555.

Felzien LK, McDonald JT, Gleason SM, Berman NE, Klein RM (2001) Increased chemokine gene expression during aging in the murine brain. Brain Res 890:137-146.

Fox GB, Fan L, Levasseur RA, Faden AI (1998) Sustained sensory/motor and cognitive deficits with neuronal apoptosis following controlled cortical impact brain injury in the mouse. J Neurotrauma 15:599-614.

Franceschi C, Bonafe M, Valensin S, Olivieri F, De Luca M, Ottaviani E, De Benedictis G (2000) Inflamm-aging. An evolutionary perspective on immunosenescence. Ann N Y Acad Sci 908:244-254.

Frankel JE, Marwitz JH, Cifu DX, Kreutzer JS, Englander J, Rosenthal M (2006) A follow-up study of older adults with traumatic brain injury: taking into account decreasing length of stay. Arch Phys Med Rehabil 87:57-62.

Franklin KBJ, Paxinos G (1997) The Mouse Brain in Stereotaxic Coordinates: Academic Press.

Fujimoto ST, Longhi L, Saatman KE, Conte V, Stocchetti N, McIntosh TK (2004) Motor and cognitive function evaluation following experimental traumatic brain injury. Neurosci Biobehav Rev 28:365-378.

Galbraith S (1987) Head injuries in the elderly. Br Med J (Clin Res Ed) 294:325.

Gong Y, Hua Y, Keep RF, Hoff JT, Xi G (2004) Intracerebral hemorrhage: effects of aging on brain edema and neurological deficits. Stroke 35:2571-2575.

Gong Y, Xi GH, Keep RF, Hoff JT, Hua Y (2005) Aging enhances intracerebral hemorrhage-induced brain injury in rats. Acta Neurochir Suppl 95:425-427.

Hall ED, Sullivan PG, Gibson TR, Pavel KM, Thompson BM, Scheff SW (2005) Spatial and temporal characteristics of neurodegeneration after controlled

cortical impact in mice: more than a focal brain injury. J Neurotrauma 22:252-265.

Hamm RJ, Jenkins LW, Lyeth BG, White-Gbadebo DM, Hayes RL (1991) The effect of age on outcome following traumatic brain injury in rats. J Neurosurg 75:916-921.

Hamm RJ, White-Gbadebo DM, Lyeth BG, Jenkins LW, Hayes RL (1992a) The effect of age on motor and cognitive deficits after traumatic brain injury in rats. Neurosurgery 31:1072-1077; discussion 1078.

Hamm RJ, Pike BR, O'Dell DM, Lyeth BG, Jenkins LW (1994) The rotarod test: an evaluation of its effectiveness in assessing motor deficits following traumatic brain injury. J Neurotrauma 11:187-196.

Hamm RJ, Dixon CE, Gbadebo DM, Singha AK, Jenkins LW, Lyeth BG, Hayes RL (1992b) Cognitive deficits following traumatic brain injury produced by controlled cortical impact. J Neurotrauma 9:11-20.

Hannay HJ, Feldman Z, Phan P, Keyani A, Panwar N, Goodman JC, Robertson CS (1999) Validation of a controlled cortical impact model of head injury in mice. J Neurotrauma 16:1103-1114.

He W, Sengupta M, Velkoff V, DeBarros K (2005) 65+ in the United States. In: Current Population Reports, pp P23-209: US Census.

Helmy A, Carpenter KL, Hutchinson PJ (2007) Microdialysis in the human brain and its potential role in the development and clinical assessment of drugs. Curr Med Chem 14:1525-1537.

Jones EG (1985) The Thalamus. New York: Plenum Press.

Kochanek PM, Marion DW, Zhang W, Schiding JK, White M, Palmer AM, Clark RS, O'Malley ME, Styren SD, Ho C, et al. (1995) Severe controlled cortical impact in rats: assessment of cerebral edema, blood flow, and contusion volume. J Neurotrauma 12:1015-1025.

Leblanc N, Chen S, Swank PR, Levin H, Schachar R (2006) Impairment and recovery in inhibitory control after traumatic brain injury in children: effect of age at injury, injury severity and lesion location. Brain Cogn 60:208-209.

Li X, Blizzard KK, Zeng Z, DeVries AC, Hurn PD, McCullough LD (2004) Chronic behavioral testing after focal ischemia in the mouse: functional recovery and the effects of gender. Exp Neurol 187:94-104.

Livingston DH, Lavery RF, Mosenthal AC, Knudson MM, Lee S, Morabito D, Manley GT, Nathens A, Jurkovich G, Hoyt DB, Coimbra R (2005) Recovery at one year following isolated traumatic brain injury: a Western Trauma Association prospective multicenter trial. J Trauma 59:1298-1304; discussion 1304.

Mattson MP, Magnus T (2006) Ageing and neuronal vulnerability. Nat Rev Neurosci 7:278-294.

Moor E, Shohami E, Kanevsky E, Grigoriadis N, Symeonidou C, Kohen R (2006) Impairment of the ability of the injured aged brain in elevating urate and ascorbate. Exp Gerontol 41:303-311.

Morrison JH, Hof PR (1997) Life and death of neurons in the aging brain. Science 278:412-419.

Mosenthal AC, Livingston DH, Lavery RF, Knudson MM, Lee S, Morabito D, Manley GT, Nathens A, Jurkovich G, Hoyt DB, Coimbra R (2004) The effect of age on functional outcome in mild traumatic brain injury: 6-month report of a prospective multicenter trial. J Trauma 56:1042-1048.

Muessel MJ, Klein RM, Wilson AM, Berman NE (2002) Ablation of the chemokine monocyte chemoattractant protein-1 delays retrograde neuronal degeneration, attenuates microglial activation, and alters expression of cell death molecules. Brain Res Mol Brain Res 103:12-27.

Narayana PA, Grill RJ, Chacko T, Vang R (2004) Endogenous recovery of injured spinal cord: longitudinal in vivo magnetic resonance imaging. J Neurosci Res 78:749-759.

Onyszchuk G, Al-Hafez B, He YY, Bilgen M, Berman NE, Brooks WM (2007) A mouse model of sensorimotor controlled cortical impact: characterization using longitudinal magnetic resonance imaging, behavioral assessments and histology. J Neurosci Methods 160:187-196.

Pennings JL, Bachulis BL, Simons CT, Slazinski T (1993) Survival after severe brain injury in the aged. Arch Surg 128:787-793; discussion 793-784.

Raghupathi R, Fernandez SC, Murai H, Trusko SP, Scott RW, Nishioka WK, McIntosh TK (1998) BCL-2 overexpression attenuates cortical cell loss after traumatic brain injury in transgenic mice. J Cereb Blood Flow Metab 18:1259-1269.

Rapoport MJ, Herrmann N, Shammi P, Kiss A, Phillips A, Feinstein A (2006) Outcome after traumatic brain injury sustained in older adulthood: a one-year longitudinal study. Am J Geriatr Psychiatry 14:456-465.

Rutland-Brown W, Langlois JA, Thomas KE, Xi YL (2006) Incidence of traumatic brain injury in the United States, 2003. J Head Trauma Rehabil 21:544-548.

Saatman KE, Feeko KJ, Pape RL, Raghupathi R (2006) Differential behavioral and histopathological responses to graded cortical impact injury in mice. J Neurotrauma 23:1241-1253.

Sandhir R, Puri V, Klein RM, Berman NE (2004) Differential expression of cytokines and chemokines during secondary neuron death following brain injury in old and young mice. Neurosci Lett 369:28-32.

Schallert T, Fleming SM, Leasure JL, Tillerson JL, Bland ST (2000) CNS plasticity and assessment of forelimb sensorimotor outcome in unilateral rat models of stroke, cortical ablation, parkinsonism and spinal cord injury. Neuropharmacology 39:777-787.

Scholz M, Cinatl J, Schadel-Hopfner M, Windolf J (2007) Neutrophils and the blood-brain barrier dysfunction after trauma. Med Res Rev 27:401-416.

Schuhmann MU, Stiller D, Skardelly M, Mokktarzadeh M, Thomas S, Brinker T, Samii M (2002) Determination of contusion and oedema volume by MRI

corresponds to changes of brain water content following controlled cortical impact injury. Acta Neurochir Suppl 81:213-215.

Schwarcz A, Berente Z, Osz E, Doczi T (2001) In vivo water quantification in mouse brain at 9.4 Tesla in a vasogenic edema model. Magn Reson Med 46:1246-1249.

Shimamura M, Garcia JM, Prough DS, Hellmich HL (2004) Laser capture microdissection and analysis of amplified antisense RNA from distinct cell populations of the young and aged rat brain: effect of traumatic brain injury on hippocampal gene expression. Brain Res Mol Brain Res 122:47-61.

Smith DH, Soares HD, Pierce JS, Perlman KG, Saatman KE, Meaney DF, Dixon CE, McIntosh TK (1995) A model of parasagittal controlled cortical impact in the mouse: cognitive and histopathologic effects. J Neurotrauma 12:169-178.

Suo Z, Citron BA, Festoff BW (2004) Thrombin: a potential proinflammatory mediator in neurotrauma and neurodegenerative disorders. Curr Drug Targets Inflamm Allergy 3:105-114.

Susman M, DiRusso SM, Sullivan T, Risucci D, Nealon P, Cuff S, Haider A, Benzil D (2002) Traumatic brain injury in the elderly: increased mortality and worse functional outcome at discharge despite lower injury severity. J Trauma 53:219-223; discussion 223-214.

Switzer RC, 3rd (2000) Application of silver degeneration stains for neurotoxicity testing. Toxicol Pathol 28:70-83.

Tehranian R, Rose ME, Vagni V, Griffith RP, Wu S, Maits S, Zhang X, Clark RS, Dixon CE, Kochanek PM, Bernard O, Graham SH (2006) Transgenic mice that overexpress the anti-apoptotic Bcl-2 protein have improved histological outcome but unchanged behavioral outcome after traumatic brain injury. Brain Res 1101:126-135.

Testa JA, Malec JF, Moessner AM, Brown AW (2005) Outcome after traumatic brain injury: effects of aging on recovery. Arch Phys Med Rehabil 86:1815-1823.

Thompson HJ, McCormick WC, Kagan SH (2006) Traumatic brain injury in older adults: epidemiology, outcomes, and future implications. J Am Geriatr Soc 54:1590-1595.

Tolias CM, Bullock MR (2004) Critical appraisal of neuroprotection trials in head injury: what have we learned? NeuroRx 1:71-79.

Unterberg A, Schneider GH, Gottschalk J, Lanksch WR (1994) Development of traumatic brain edema in old versus young rats. Acta Neurochir Suppl (Wien) 60:431-433.

Unterberg AW, Stover J, Kress B, Kiening KL (2004) Edema and brain trauma. Neuroscience 129:1021-1029.

Uryu K, Giasson BI, Longhi L, Martinez D, Murray I, Conte V, Nakamura M, Saatman K, Talbot K, Horiguchi T, McIntosh T, Lee VM, Trojanowski JQ (2003) Age-dependent synuclein pathology following traumatic brain injury in mice. Exp Neurol 184:214-224.

Zink BJ (1996) Traumatic brain injury. Emerg Med Clin North Am 14:115-150.

V – AGED MICE DEMONSTRATE BLUNTED ASTROCYTOSIS AND AUGMENTED MICROGLIOSIS AFTER CONTROLLED CORTICAL IMPACT INJURY

Abstract

There is substantial evidence of worsened outcomes after TBI in the elderly, compared to younger adults, but little preclinical research has probed the potential effects of older age on the mechanisms of damage and repair in the injured brain. In this study, we examined the age-related effects on outcome in a mouse model of controlled cortical impact (CCI) injury using histological techniques. We compared the responses of adult (5-6 months old) and aged (21-24 months old) male mice following a moderate lateral CCI injury to the sensorimotor cortex. Regional neurodegeneration was assessed by amino-cupric silver staining, while regional astrocyte and microglial activation were examined with anti-GFAP and anti-Iba1 immunohistochemistry. Measurements were made in the cortex, hippocampus and thalamus of animals with survival times of 1, 2, 3 and 7 days post-injury. Neurodegeneration was significantly greater in the ipsilateral cortex of injured aged mice compared to the injured adult ($p<0.01$ at 3 days). In the hippocampus and thalamus, neurodegeneration trended higher in the aged mice compare to the adult in 13 of 16 measurements, and was significantly greater ($p<0.05$) in the aged mice in the contralateral hippocampus at 3 and 7 days. In contrast, astrocyte staining showed a blunted response in the ipsilateral hippocampus ($p<0.05$, at 3 days) and a blunted response trend in the ipsilateral thalamus of injured aged mice compared to the injured adult ($p=0.16$ at 3 days). Microglial staining in the cortex was similar between injured groups, however in the hippocampus and thalamus, staining increases above control values trended higher in the aged brains in 6 of 8

measurements. The results suggest a blunted astrocyte activation or reduced astrocyte survival and an upward trending microglial activation – in areas remote from the primary injury site - in the aged brains compared to the adult. These altered glial responses may drive aggravated secondary damage processes in the aged brain after TBI.

Introduction

Traumatic brain injury (TBI) in the elderly population is a devastating cause of death, disability and loss of functional independence. A growing number of reports describe increased morbidity and mortality, reduced functional capability, and poorer ultimate recovery in elderly TBI patients (Galbraith, 1987; Pennings et al., 1993; Susman et al., 2002; Mosenthal et al., 2004; Rapoport et al., 2006). As the population continues to age, we can expect the burden of TBI in the elderly to continue to increase.

Despite these findings in human patients, there has been little research on how increasing age might modulate the mechanisms of brain damage and repair following injury in the elderly. A small number of rodent studies using a fluid percussion injury model demonstrated poorer neurological response, increased motor and cognitive deficits, increased hippocampal expression of aging-associated genes and reduced hippocampal expression of repair and regeneration in aged rats following injury (Hamm et al., 1991; Hamm et al., 1992a; Shimamura et al., 2004). Synuclein protein immunoreactivity in aged mice subjected to TBI has been examined as a mechanistic link between TBI and Parkinson's disease (Uryu et al., 2003). We recently found that aged mice had poorer behavioral recovery, prolonged acute edema, increased and prolonged blood-brain barrier compromise, and greater neurodegeneration than adults following a controlled cortical impact (CCI) (Onyszchuk, et.al, 2007, accepted manuscript).

However, other mechanisms such as inflammation could contribute to a different response to injury in the aged compared to the adult brain. There is substantial evidence that under normal aging, the body and brain acquire a pro-inflammatory status (Franceschi et al., 2000; Floyd and Hensley, 2002; Gomez et al., 2005) and further evidence to implicates neuroinflammation in many central nervous system disorders (Floyd, 1999; Rosenberg, 2002; Koistinaho and Koistinaho, 2005; Tuppo and Arias, 2005; Weydt and Moller, 2005; Whitton, 2007). Finally, there have been extensive reports and reviews of the role of inflammation in the pathology of TBI (Faden, 1993; McIntosh et al., 1996; Morganti-Kossman et al., 1997; Gennarelli and Graham, 1998; McIntosh et al., 1998b; Lenzlinger et al., 2001a; Schmidt et al., 2005; Lucas et al., 2006). Thus, ample evidence exists to implicate neuroinflammation as a particularly important component in mechanisms of damage and repair following traumatic injury to the aged brain.

Glial cells have critical roles in the normal functioning of the central nervous system, and are also considered key mediators on the neuroinflammatory response (Streit et al., 2004; Pekny and Nilsson, 2005). Evidence from studies of tissues from TBI patients have shown that astrocytes and microglia are intimately involved in the brain's damage and repair processes (Castejon, 1998; Gentleman et al., 2004). Studies in cortical stab wounds (Kyrkanides et al., 2001), intracerebral hemorrhage (Gong et al., 2004) and pro-inflammatory cytokine injection (Deng et al., 2006) have probed

the glial response in aged animals following injury, but little has been done to examine gliosis in aged animals following TBI. Accordingly, we set out to examine the response of astrocytes and microglia to controlled cortical impact injury in aged mice. We now report the results of experiments designed to probe age-related differences in the glial response in the brain after TBI. In these experiments, adult (5-6 months old) and aged (21-24 months old) mice were injured, and outcomes measured using immunohistochemical techniques.

Materials and Methods

Animals

Adult male C57BL/6 mice (28-32g, 5-6 months old), and aged male C57BL/6 mice (28-32g, 21-24 months old), were housed with a 12-hour light-dark cycle, with *ad libitum* access to food and water. These animals were obtained from the National Institute on Aging colonies, where they were barrier raised, monitored for genetic purity, and screened for bacterial and viral pathogens according to the NIA guidelines. All animal procedures were approved by the University of Kansas Medical Center Institutional Animal Care and Use Committee. A total of 50 animals were used to provide histological data at 4 different time points. Adult (n=22) and aged (n=22) animals received moderate CCI injury to the sensorimotor cortex. Three adult and three aged mice served as controls.

CCI Impactor

Our injury device was assembled from commercially available components, as described previously (Narayana et al., 2004; Bilgen, 2005; Onyszchuk et al., 2007). Briefly, the equipment included a linear motor device (the impactor) with a stainless steel tip, power supply and microprocessor controller (Linmot, Zurich, Switzerland), a Plexiglas table, and a stand for the linear motor device made with an adjustable manipulator (Kopf, Tujunga, CA) that allowed precise positioning of the impactor. In this study, we used a 3.0mm diameter tip with a flat face and a slightly rounded edge, a strike velocity of 1.5m/s, a strike depth of 1.0mm, and a contact time of 85ms. This parameter set was selected to provide a "moderate" CCI injury, since as we have noted previously (Onyszchuk, et.al, 2007, submitted manuscript), a greater strike depth of 1.5mm, yielded mortality rates of 25% in the adult and 50% in the aged animals.

Surgical Procedures

We used previously reported procedures (Onyszchuk, et.al, 2007, submitted manuscript). Following anesthesia with isoflurane (induction: 2.5%, maintenance: 1.0%), animals were stabilized in a Cunningham stereotaxic frame (Stoelting, Wood Dale, IN), and placed on a heated pad, which maintained core body temperature at 37+/- 1 °C. The scalp and epicranial aponeurosis were retracted, and a 3.5mm diameter circular craniotomy was performed with a burr drill, lateral (right side) to the mid-sagittal suture, with the center at the following coordinates: AP = 0, ML = +2.0 from bregma. The burr and surface of the skull were cooled with periodic

application of room temperature saline. Care was taken to avoid the blood vessels coursing along the superior sagittal sinus, and any bleeding from the skull was controlled with bone wax. Once the dural surface was exposed, the position of the impactor and tip was carefully adjusted to be centered within the craniotomy, and angled so that the face of the impactor tip was tangential to the dural surface. The impactor tip was slowly lowered in 0.05mm increments until the tip just contacted the dura (by visual inspection under microscope). The cortical impact was initiated through the device graphical user interface. Given that the injury center was 2.0mm lateral to bregma, the tip contact area included motor (M1, M2) and sensory (S1FL, S1HL) cortical areas (Franklin and Paxinos, 1997). After the impact, the scalp was closed with 6-0 silk suture, anesthesia was discontinued, and the animal temperature was maintained at 37°C until recovery of locomotion. Control animals received anesthesia exposure but no craniotomy nor impact from the CCI device.

Tissue Preparation

Our principal interest was to make histological comparisons between the injured groups at 72 hours post-injury. It was expected that both primary and secondary damage processes would be active at this time. For sufficient power to detect small between-group differences, a sample size of 10 was selected for this time point. Additional smaller samples (n=4) were added at different times to allow the evaluation of histological trends over time. Therefore, at 24 (n=4 adult, n=4 aged), 48 (n=4 adult, n=4 aged), and 72 hours (n=10 adult, n=10 aged) and at 7 days (n=4 adult,

n=4 aged) post injury, injured animals were anesthetized and perfused transcardially with 50ml of phosphate buffered saline, followed by 100 ml of 4% buffered formaldehyde, delivered via a 23-gauge needle connected to a perfusion pump. Six sham controls, three adult and the aged, were also processed. The brains were removed, post-fixed in 4% buffered formaldehyde for 12 hours, then cryoprotected and embedded in 5 x 5 arrays in gelatin blocks using the Multibrain^{TM} process (Neuroscience Associates, Knoxville, TN). Frozen sections were cut at 35μm thickness, with each tissue sheet containing 1 coronal section from each of the 25 brains. Sheets were stored in an ethylene glycol solution at -80°C prior to immunostaining.

Regional Neurodegeneration

Amino-cupric silver staining was used to assess the extent of neurodegeneration. This technique has been demonstrated to have excellent sensitivity and selectivity for the identification of degeneration of neurons, including their cell bodies, processes and synapses (Switzer, 2000). Tissue sheets were stained with amino-cupric silver and counter-stained with Neutral Red. Sections were visualized with a Nikon inverted-stage microscope at 20x magnification and digital images were captured with a SPOT microscope camera (Diagnostic Instruments, Sterling Heights, MI). Four slightly-overlapping digital images were acquired for each coronal section, and then these images were merged to yield a single high resolution image of the entire coronal section.

The silver staining was measured using densitometric thresholding, in a manner similar to that reported previously (Hall et al., 2005). Specific brain regions were outlined and selected using the polygon selection tool in NIH ImageJ (v1.37). Measurements were made of the ipsilateral and contralateral dorsal cortex, for each brain, in 12 sections spaced 0.42mm apart. Measurements of the rostral hippocampus were made in 4 sections spaced 0.42mm apart, and measurements of the thalamus were made in 5 sections spaced 0.42mm apart. Measurements were done by a person blinded to experimental time point and group.

Astrocyte Staining

Tissue sheets were stained with anti-GFAP to detect astrocytes and to measure astrocyte activation. Briefly, tissue sheets were rinsed in 1X PBS, permeabilized with Triton X-100 (0.2%) in 10% , rinsed again, quenched for peroxidase activity using 0.6% $H_2O_{2,}$, rinsed again, incubated with 10% NGS blocking serum, and incubated overnight with 1:2000 rabbit anti-mouse GFAP (Chemicon AB-5804). Sheets were then rinsed again, and incubated for 2 hours with 1:500 biotinylated goat anti-rabbit (Vector Labs BA-1000). Detection of staining was accomplished with Vectastain Elite ABC amplification (Vector Labs, Burlingame, CA) and visualization was done using a diaminobenzidine chromogen.

Sections were visualized with a Nikon inverted-stage microscope at 100x magnification and digital images were captured with a SPOT microscope camera (Diagnostic Instruments, Sterling Heights, MI). From these histological images, we measured anti-GFAP staining, in each region of interest, using a thresholding technique in NIH ImageJ. Brain pixels in each region were also counted, allowing the ratio of stained/total brain tissue to be calculated for each measurement region. Measurements were done by a person blinded to experimental group and time point. This method measured the increased staining that resulted from increased abundance of intracellular GFAP in hypertrophic/thickened astrocytic processes. Although this is not a direct measure of astrocyte function, it has been shown to be a reasonable measure for astrocyte activation (Eng and Ghirnikar, 1994; Ridet et al., 1997).

Microglial Staining

Tissue sheets were stained with anti-Iba1 to detect microglia and to measure microglial. Briefly, tissue sheets were rinsed in 1X PBS, permeabilized with Triton X-100 (0.2%) in 10% , rinsed again, quenched for peroxidase activity using 0.6% H_2O_2,, rinsed again, incubated with 10% NGS blocking serum, and incubated overnight with 1:2000 rabbit anti-mouse Iba1 (Wako 019-19741). Sheets were then rinsed again, and incubated for 2 hours with 1:500 biotinylated goat anti-rabbit (Vector Labs BA-1000). Detection of staining was accomplished with Vectastain Elite ABC amplification (Vector Labs, Burlingame, CA) and visualization was done using a diaminobenzidine chromogen.

Sections were visualized with a Nikon inverted-stage microscope at 100x magnification and digital images were captured with a SPOT microscope camera (Diagnostic Instruments, Sterling Heights, MI). From these histological images, we measured anti-Iba1 staining, in each region of interest, using a thresholding technique in NIH ImageJ. Brain pixels in each region were also counted, allowing the ratio of stained/total brain tissue to be calculated for each measurement area. Measurements were done by a person blinded to experimental group and time point. This method measured the increased staining that resulted from increased abundance of intracellular Iba1 in hypertrophic/thickened microglial processes. Although this is not a direct measure of microglial function, it has been shown to be a reasonable measure for microglial activation (Ito et al., 1998; Ito et al., 2001)**.**

Statistical Analysis

For the analysis of histological data and comparisons between the adult and aged groups, we used the two-tailed t-test. In the anti-GFAP and anti-Iba1 data analysis, comparisons of absolute staining levels between the injured groups are supplemented with comparisons of increases in staining above control levels, to account for age-related differences in control levels. All statistical analyses were performed using GraphPad Prism4software (GraphPad, San Diego, CA).

Results

Regional Neurodegeneration

Representative images of amino-cupric silver stained coronal sections, near the injury epicenter (bregma), at bregma +1.5, and at bregma -1.5, from animals sacrificed at seven days post-injury, are shown in Figure 1. The adult control sections had very little staining, whereas the aged control sections were lightly stained in the fornix, fimbria and in the periventricular areas. In the adult and aged injured brains, there was extensive silver staining in the cortex and subcortical white matter immediately under and adjacent to the site of impact. Staining at seven days was also prominent in the ipsilateral caudate putamen, and in the ipsilateral dorsal thalamic nuclei. Moderate staining was observed in the ipsilateral hippocampus. Contralateral staining was noted in the cortex, subcortical white matter, and caudate putamen, and to a lesser extent, in the hippocampus and thalamus.

Measurements of amino-cupric silver staining in the ipsilateral and contralateral cortex of control and injured brains are shown in Figure 2. Staining was greater than age-matched controls at all timepoints. In the ipsilateral cortex, staining in the aged brains was significantly greater than in the adult at three days (t-test, $p<0.05$), and trended greater at seven days. In the contralateral cortex, staining was increased 3.2-fold in the adult and up 4.3-fold in the aged at seven days compared to three days. Moreover, staining in the aged brains trended higher than in the adult at seven days.

Measurements of amino-cupric silver staining in the ipsilateral and contralateral hippocampus and thalamus are shown in Figure 3. Staining was greater than age-matched sham controls at all timepoints. In the ipsilateral hippocampus, staining trended greater in the aged brains than in the adult at two and seven days post-injury, and in the contralateral hippocampus, staining trended greater in the aged brains at all measured time points. In the ipsilateral thalamus, at all time points post-injury, staining trended greater in the aged brains than in the adult. In the contralateral thalamus, staining trended greater in the aged brains than in the adult at all time points, and was significantly greater at three days (t-test $p<0.01$) and seven days (t-test, $p<0.05$). In the ipsilateral thalamus, staining was increased 2.5-fold in the adult and 2.4-fold in the aged at seven days compared to three days.

Astrocyte Staining

Representative images of anti-GFAP stained sections are shown in Figure 4. In general, aged control brains were more extensively stained in the hippocampus and thalamus than were adult controls. In the cortex, small numbers of stained astrocytes were visible in most aged control sections, whereas very few were seen in the adult controls.

Measurements of anti-GFAP staining in ipsilateral and contralateral cortex are shown in Figure 5. Staining in the injured brains was greater than age-matched sham controls

at all timepoints. In the ipsilateral cortex, staining in injured groups was similar, whereas in the contralateral cortex, staining trended greater in the aged brains compared to the adults. In the ipsilateral cortex, the sharpest increases in staining occurred at three days post-injury. In the contralateral cortex, staining levels declined, in injured adult and aged brains, after two days post-injury.

Measurements of anti-GFAP staining in ipsilateral and contralateral hippocampus and thalamus are shown in Figure 6. Staining in the injured adult hippocampus was greater than age-matched controls at all timepoints, whereas in the aged it was only elevated in the ipsilateral hippocampus at three days post-injury. In the ipsilateral hippocampus, at three days post-injury, the staining increase above control was significantly less in the aged brains compared to the adult (t-test, $p<0.05$). Hippocampal staining showed a diminishing trend from three to seven days post-injury in both injured groups.

In the ipsilateral and contralateral thalamus, no significant differences were noted comparing the two injured groups. Staining in the injured ipsilateral thalamus was greater than age-matched controls at both time points. In the ipsilateral thalamus, the staining increase above control at three days trended lower in the aged brains (t-test, $p=0.16$) compared to the adult. In the ipsilateral thalamus, staining values were increased 2.4-fold in the adult and 2.4-fold in the aged at seven days compared to three days.

Microglial Staining

Representative images of anti-Iba1 stained sections are shown in Figure 7. In general, adult and aged control brains were lightly stained, to similar degrees, in the cortex, hippocampus and thalamus.

Measurements of anti-Iba1 staining in ipsilateral and contralateral cortex are shown in Figure 8. Staining levels in the injured brains were greater than in age-matched controls at all timepoints. And, staining levels were equivalent between the injured aged and adult brains at all time points measured. In the ipsilateral cortex, staining increased 1.8-fold in the adult and 1.8-fold in the aged at seven days compared to three days.

Measurements of anti-Iba1 staining in the ipsilateral and contralateral hippocampus and thalamus are shown in Figure 9. Staining levels in the injured brains were greater than in the age-matched controls at all timepoints. Although no significant differences were noted between the two injured groups, staining values in the aged brains trended greater than those in the adult brains. In the hippocampus, staining in the adult brains showed a diminishing trend from three to seven days post-injury, whereas staining in the aged brains demonstrated a flat trend. In the thalamus, the increase in staining over control values trended greater in the injured aged brains than in the injured adult at at three (ipsilateral only) and seven days (ipsilateral and contralateral).

Discussion

This study showed several differences in the response to sensorimotor CCI injury in the aged compared to the adult animals. Neurodegeneration in the cortex, assessed by amino-cupric silver staining, trended greater in the aged compared to the adult brains in seven of eight measurements, and was significantly greater in the ipsilateral cortex at three days post injury. Similar results were obtained for the hippocampus and thalamus, with staining trending greater in the aged compared to the adult brains in 15 of the 16 measurements, and significantly greater in the contralateral thalamus. Anti-GFAP staining, to detect astrocyte morphology changes, was similar between injured groups in the cortex, and in the hippocampus and thalamus, there was a blunted response in the aged brains compared to the adult. Anti-Iba1 staining, to detect microglial morphology, was similar between injured groups in the cortex, trended higher in the aged brains in the hippocampus and ipsilateral thalamus, and was significantly increased in the contralateral thalamus in the aged brains compared to the adult.

The silver staining results for ipsilateral cortex are consistent with recently published results (Onyszchuk, et.al, 2007, accepted manuscript), where overall neurodegeneration in the ipsilateral hemisphere was found to be significantly greater in the aged brains compared to the adult at three days post-injury. Greater staining in the aged cortex may reflect an increased vulnerability of aged cortical neurons to

primary and/or secondary damage processes. It is interesting that, comparing the adult and aged groups, the staining values were remarkably similar at one and two days post-injury, and then diverged – greater in the aged – at three and seven days. This delayed divergence trend suggests that the aged-related increased vulnerability may be the result of differential age-related secondary damage rather than factors related to the primary impact.

It is also interesting that the neurodegeneration in contralateral cortex, contralateral hippocampus, and ipsilateral and contralateral thalamus was maximal at seven days post-injury, and most divergent between the injured groups at seven days post-injury. This further suggests that secondary processes may underlie the aged-related differences in neurodegeneration seen in these structures.

Anti-GFAP staining in the ipsilateral cortex increased markedly, in both injured groups, between the two day and three days post-injury time points. This astrocytic response preceded and may have contributed to the delayed neurodegeneration in this region that was indicated by the large increase in silver staining between three and seven days post-injury. In the ipsilateral hippocampus, while silver staining trends during the first three days post-injury were similar between age groups, we found less increase above control values in anti-GFAP staining in the aged compare to the adult brains, suggesting a weaker link between neurodegeneration and astrocyte-mediated inflammation in this structure during this time period. Examining the time courses of

adult and aged silver and anti-GFAP staining in the ipsilateral thalamus over the full seven days, we have a trend towards increased neurodegeneration in the aged brains, concurrent with a trend towards reduced increase in astrocyte staining above control levels. This suggests a weaker link between neurodegeneration and astrocyte-mediated inflammation in this structure, or it may reflect a reduction in astroctye-mediated neuroprotection in the aged thalamus.

Anti-Iba1 staining in the ipsilateral cortex increased markedly, in both injured groups, between the two day and three days post-injury time points. In a manner similar to the astrocytic response mentioned above, this microglial response preceded and may have contributed to the delayed neurodegeneration in the ipsilateral cortex that was indicated by the large increase in silver staining between three and seven days post-injury. There was also a marked increase in ipsilateral cortex anti-Iba1 staining at seven days post-injury. It is not clear whether this represents microglial activation resulting from ongoing neurodegeneration or if it reflects sustained neuroinflammation with the potential to cause additional damage at later times. In the hippocampus and thalamus, silver and anti-Iba1 staining followed similar trends over time. Microglial staining increases above control values trended greater in the aged brains in six of the eight measurements in the hippocampus and thalamus, in contrast to the blunted response observed in astrocyte in the aged brains. Also, for all measurements at seven days post-injury in the hippocampus and thalamus, staining increases above control values trended greater in the aged brains, hinting that ongoing

microglia-mediated neuroinflammation in these structures may be prolonged in the aged brains compared to the adult.

The few published studies of rodent TBI with aged animals do not include histological evaluations of the glial response. However, in cortical stab injury studies in rats, astrocyte mRNA production was increased in aged animals (Kyrkanides et al., 2001), and astrocyte labeling was increased in middle-aged cortex but not in the hippocampus (Topp et al., 1989). In published reports of MPTP neurotoxicity in aged mice (Sugama et al., 2003), and of retinal ischemia in aged rats (Kim et al., 2004), the response of microglia to injury was elevated in the older compared to the younger animals. Following focal cerebral ischemia in aged rats, an accelerated glial response has been described (Badan et al., 2003). In a study of intracerebral hemorrhage, senescence-accelerated prone mice demonstrated increased microglia/monocyte activation but no difference in anti-GFAP staining when compared to senescence-accelerated resistant mice (Lee et al., 2006).

Our anti-GFAP data contrast with these findings, in that we found no structure where the aged brains demonstrated a greater increase in staining above control levels than the adult. It is possible in our injury model, with extensive degeneration and loss of tissue that is not a feature of milder injuries, that the damage to and demise of astrocytes masks the increased activation of those astrocytes that remain viable. It is equally possible that there was more astrocyte death in the aged injured brains –

consistent with recent in-vitro data suggesting a reduced survival of aged astrocytes under conditions of oxidative stress (Lu et al., 2007). Finally, it is also possible that there was an age-related reduction in astrocyte proliferation and/or neuroprotection in the injured aged brains, consistent with reports of senescence-related changes in astrocyte function (Fotheringham et al., 2000; Popa-Wagner et al., 2007).

Our anti-Iba1 data for the hippocampus and thalamus are congruent with published reports of CNS injury in aged rodents, as we have measured greater increases in microglial activation in the aged brains. To properly evaluate whether the microglial response is prolonged in the aged brain, and whether there is aggravated subacute or chronic neuroinflammation beyond seven days post-injury, would required an expand series of time points and may make for an interesting follow-on study.

Of course, caution must be used when comparing previously published results of the glial response, in different injury models, with those in the present study. Not only may results differ due to model, brain region, species and age differences, but comparison of measurements of GFAP and Iba1 mRNA and protein levels with examinations and measurements of cell morphology via immunoreactivity to antibodies to GFAP and Iba1 can be problematic. There is evidence that GFAP mRNA increases with age, in rodent and in human brains (Nichols et al., 1993). It has also been shown that age-associated increases in basal GFAP protein levels are not associated with increased rates of transcription or DNA methylation (Laping et al.,

1994). And, there is evidence that the intensity of GFAP does not always correlate with GFAP content (Eng and Ghirnikar, 1994). Post-transcriptional regulation, message stability, protein turnover, phosphorylation and even cleavage of GFAP by caspases (Fujita et al., 1998) could cause mRNA and protein measurements to diverge from morphological assessments. Thus, there is considerable complexity in measuring and interpreting the glial response in aged brain injury, and clearly no single technique or measurement domain will provide the complete picture.

These results provide evidence for an altered neuroinflammatory response in the aged brain following cortical impact. In particular, we have observed a blunted astrocyte response in the aged brains, possibly indicating increased age-related astrocyte vulnerability. We have further observed a trend towards increased microglial activation in the aged brains, suggesting an intact microglia-mediated response to injury, and an upward trend in microglial staining in several brain structures at seven days post-injury, hinting at a possibly prolonged sub-acute microglial response. Taken together, our data suggest that efforts to promote astrocyte survival and functional integrity without over stimulating or prolonging the microglial response may be of particular interest in preclinical research aimed at developing treatment strategies for elderly TBI patients.

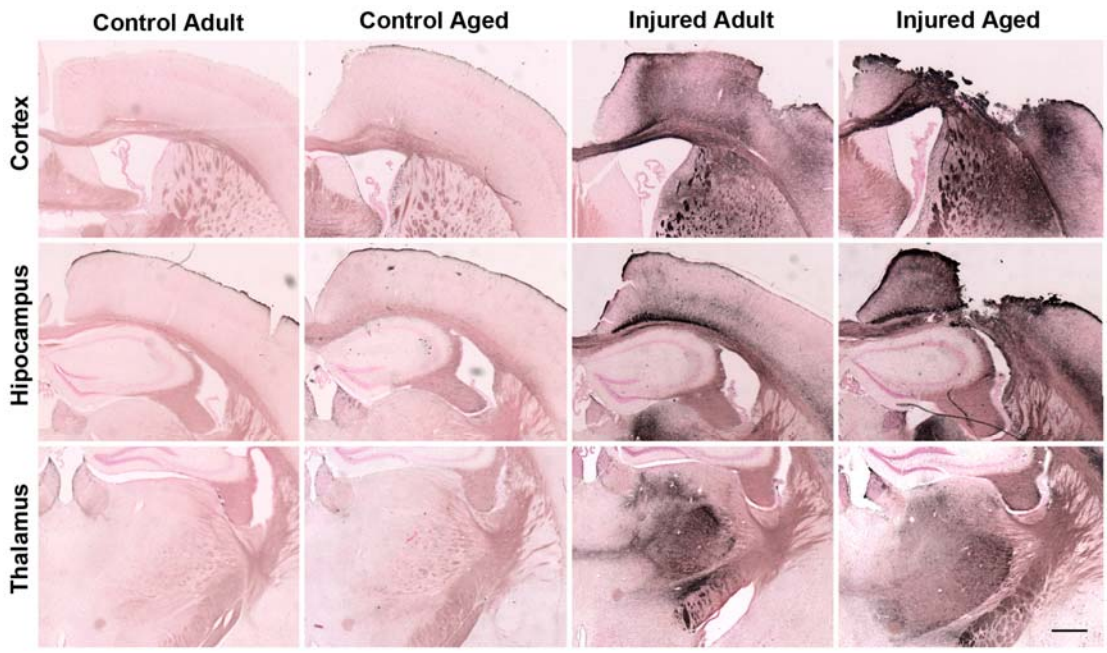

Figure 1: Representative images of amino-cupric silver stained coronal sections, with injured animals at 7 days post injury. Scale bar 0.5mm.

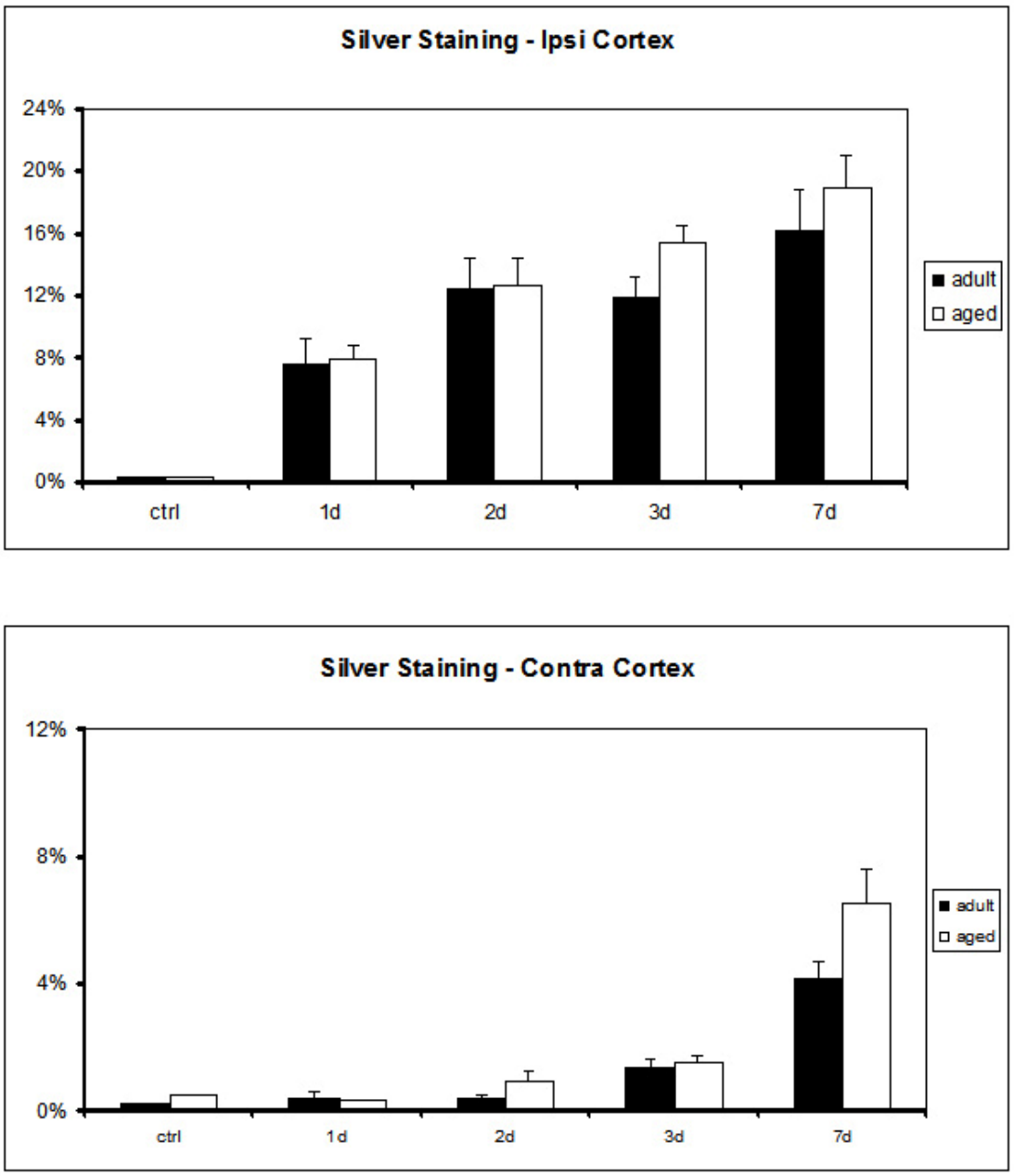

Figure 2: Measurements of silver staining in ipsilateral (A) and contralateral cortex (B). n=4 per group, except at 3 days n=10 per group.

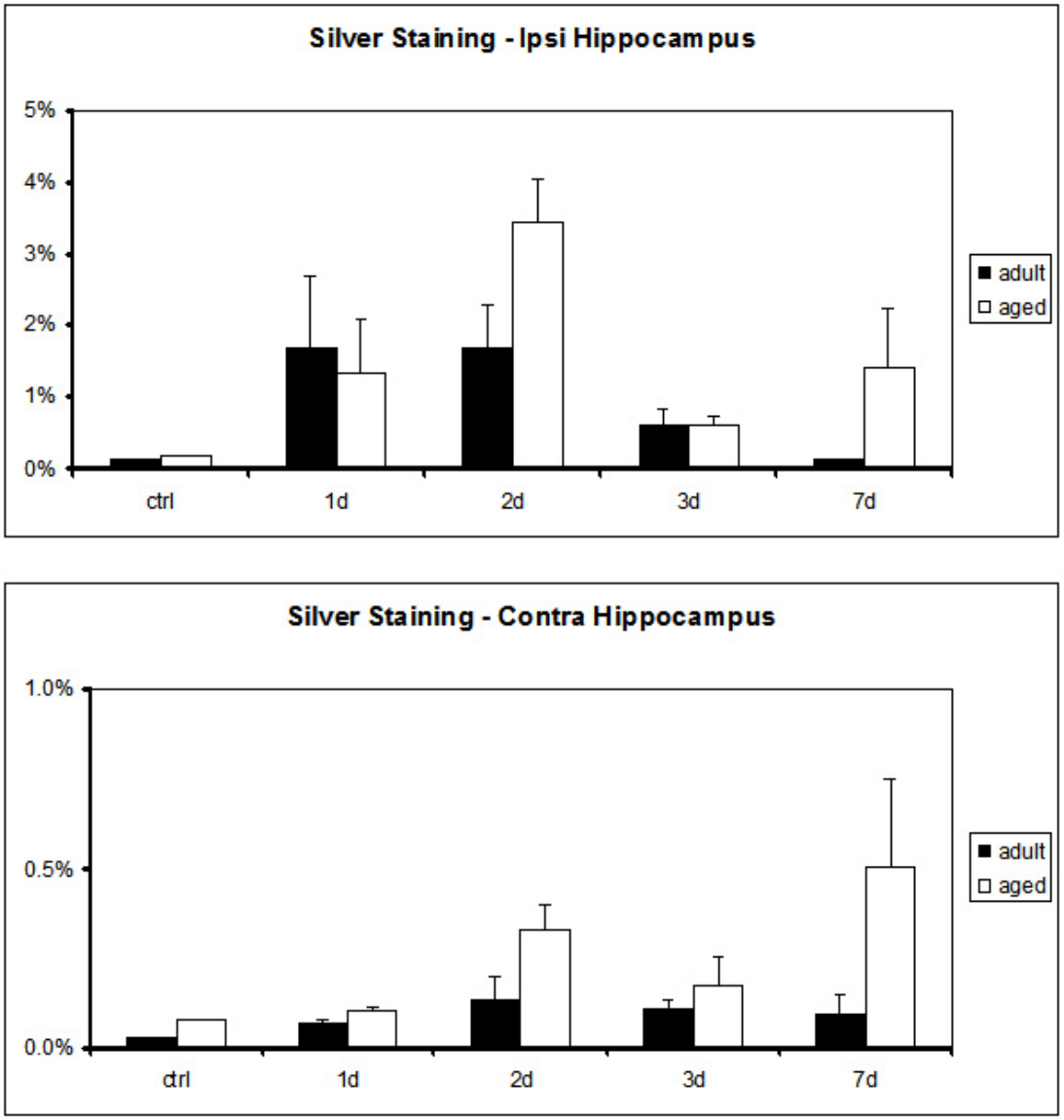

Figure 3A: Measurements of silver staining in ipsilateral and contralateral hippocampus. n=4 per group, except at 3 days n=6 per group.

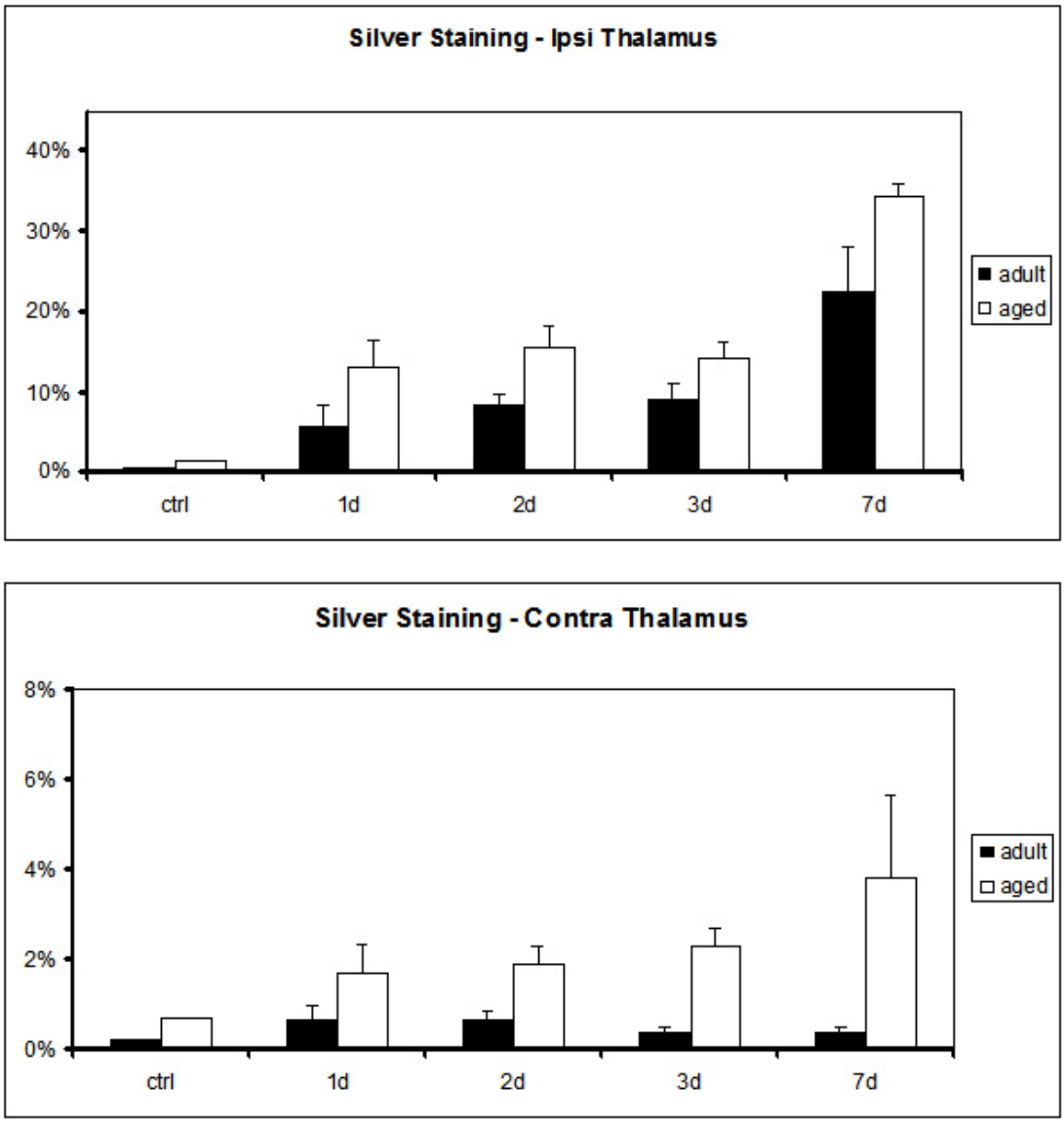

Figure 3B: Measurements of silver staining in ipsilateral and contralateral thalamus. n=4 per group, except at 3 days n=6 per group.

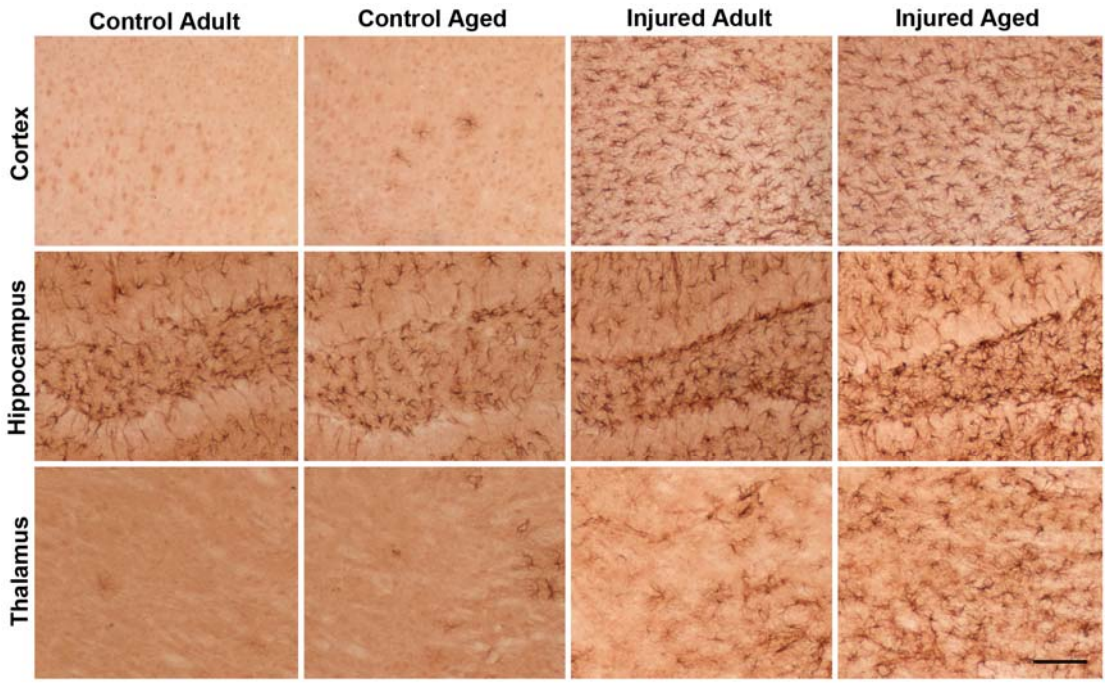

Figure 4: Representative images of anti-GFAP stained coronal sections, with injured animals at 7 days post injury. Images taken at 100x magnification. Scale bar 0.1mm.

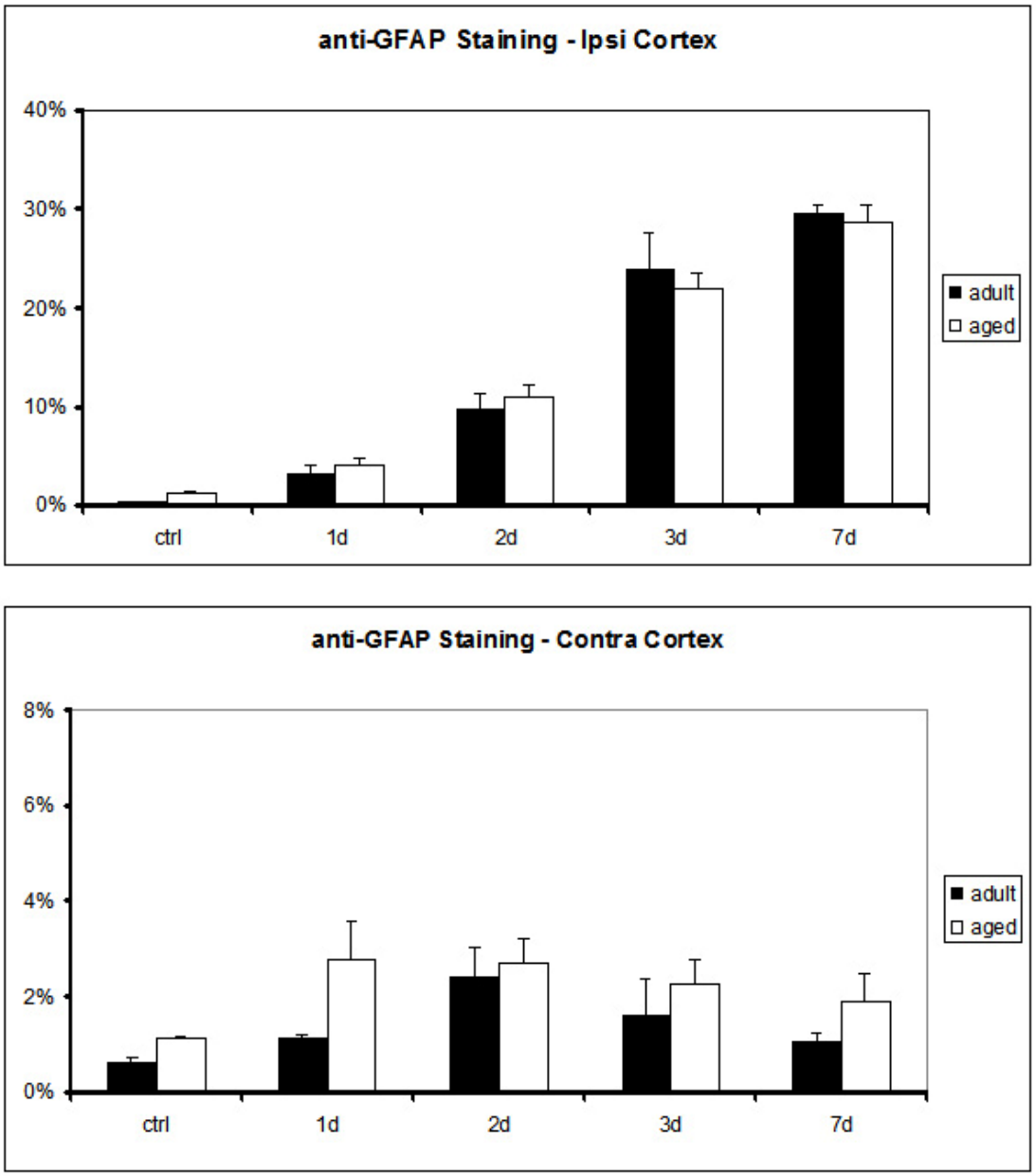

Figure 5: Measurements of anti-GFAP staining in ipsilateral (A) and contralateral cortex (B). n=4 per group, except at 3 days n=10 per group.

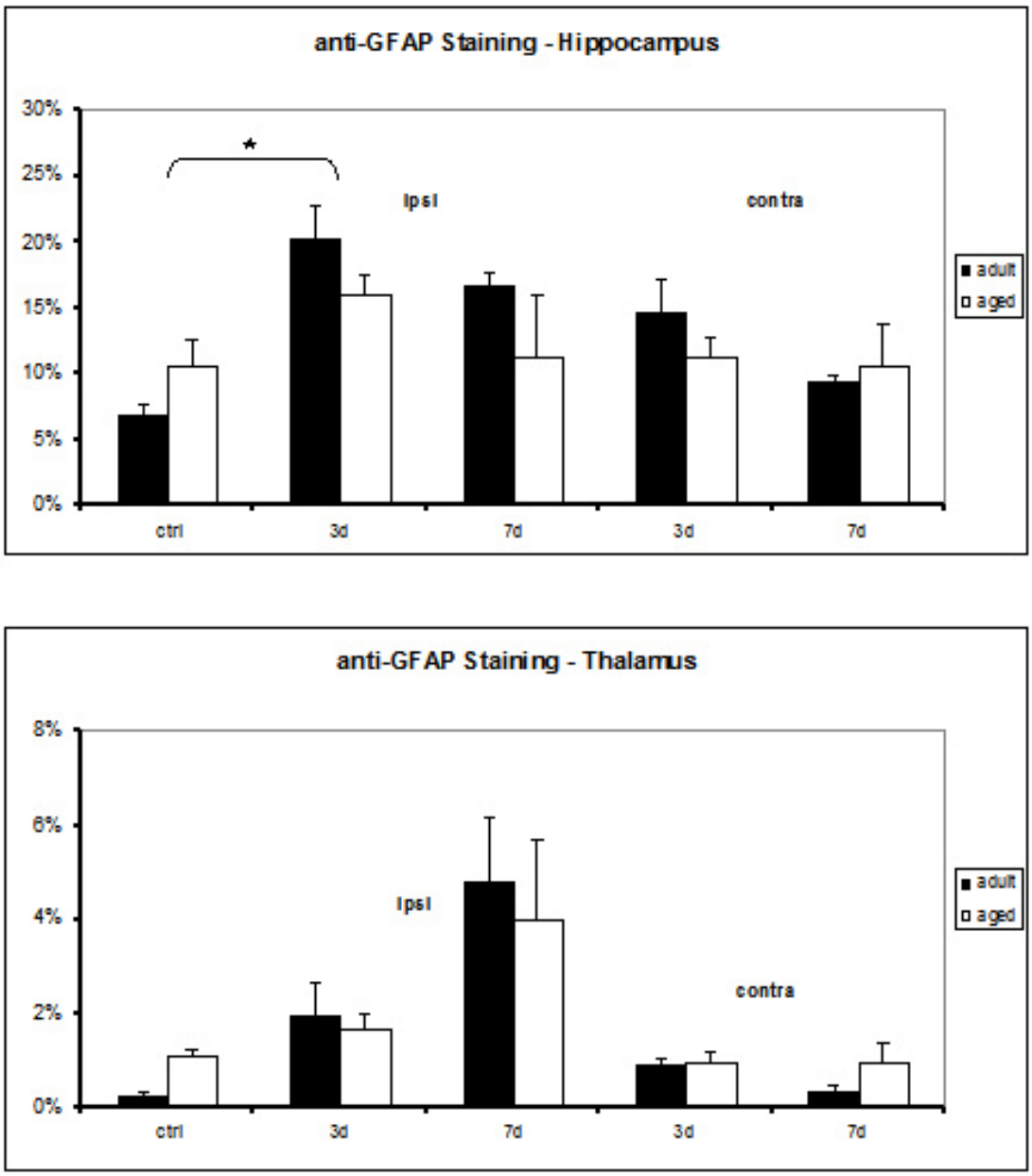

Figure 6: Measurements of anti-GFAP staining in ipsilateral and contralateral hippocampus (A) and thalamus (B). n=4 per group, except at 3 days n=6 per group.

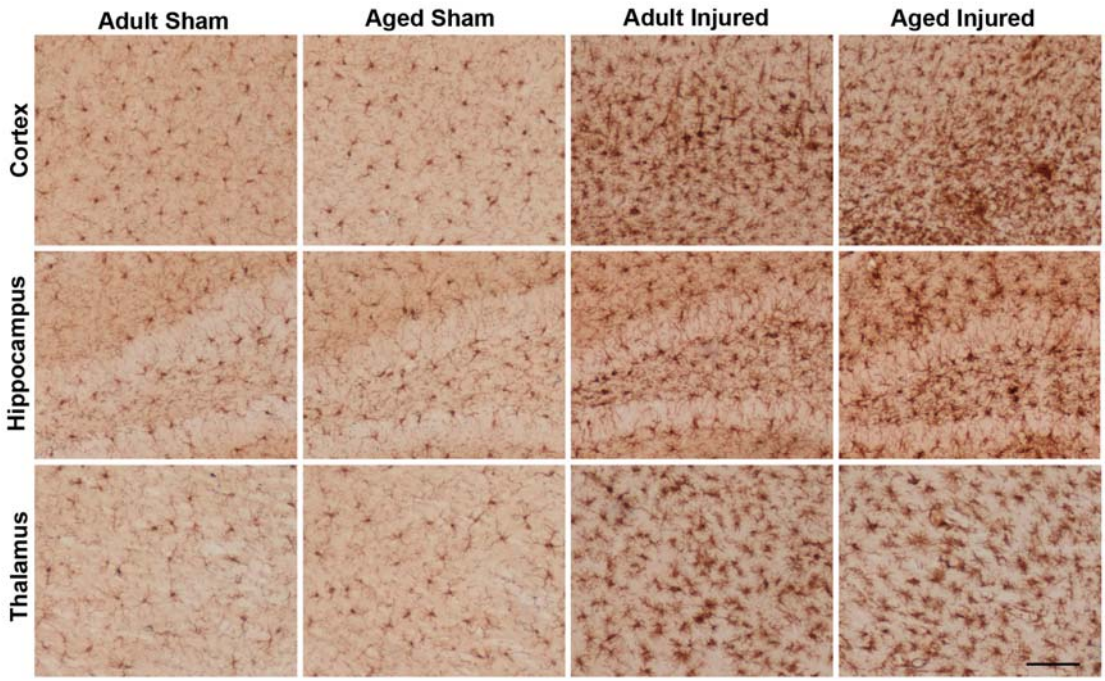

Figure 7: Representative images of anti-Iba1 stained coronal sections, with injured animals at 7 days post injury. Images taken at 100x magnification. Scale bar 0.1mm.

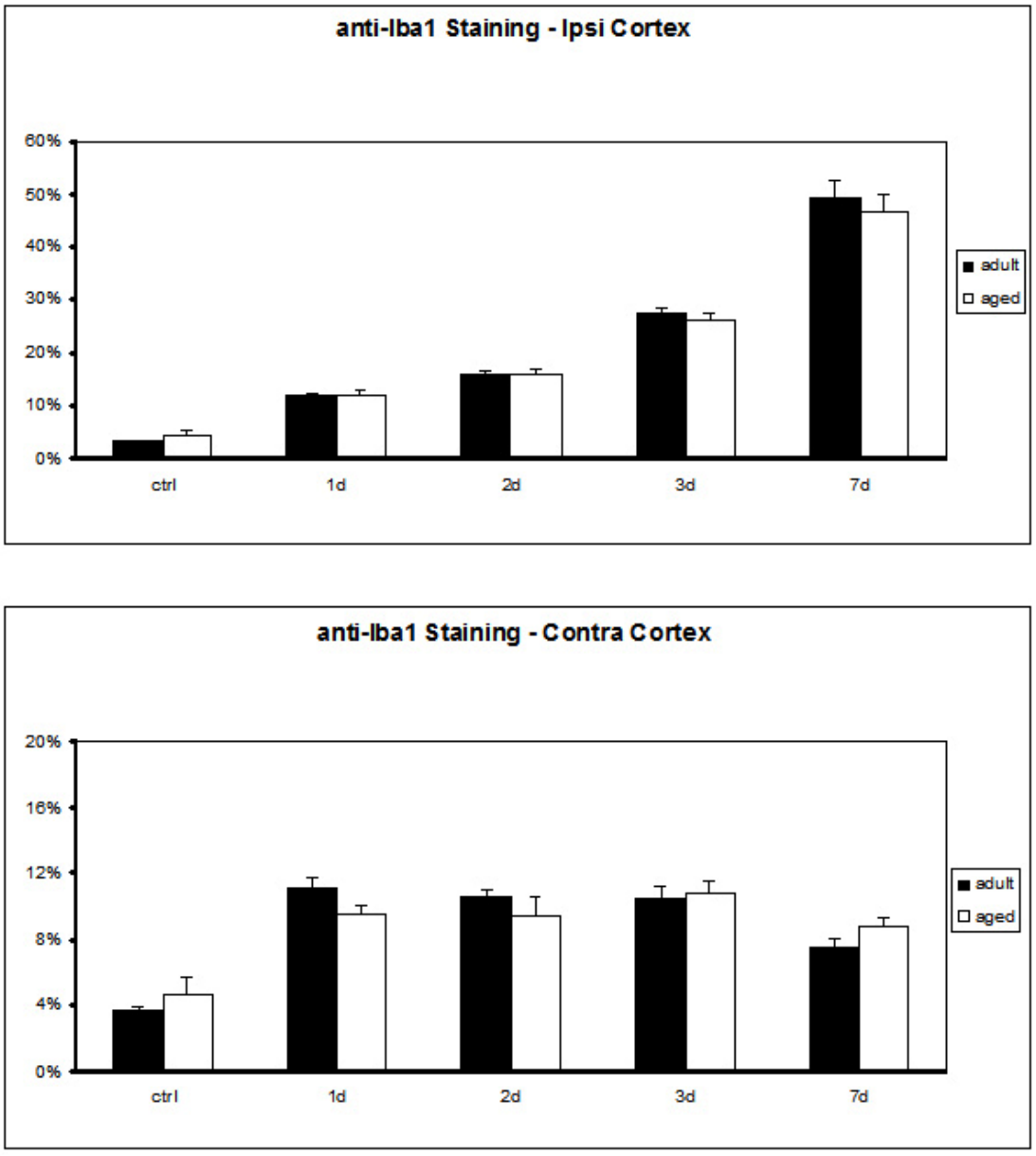

Figure 8: Measurements of anti-Iba1 staining in ipsilateral (A) and contralateral cortex (B). n=4 per group, except at 3 days n=10 per group.

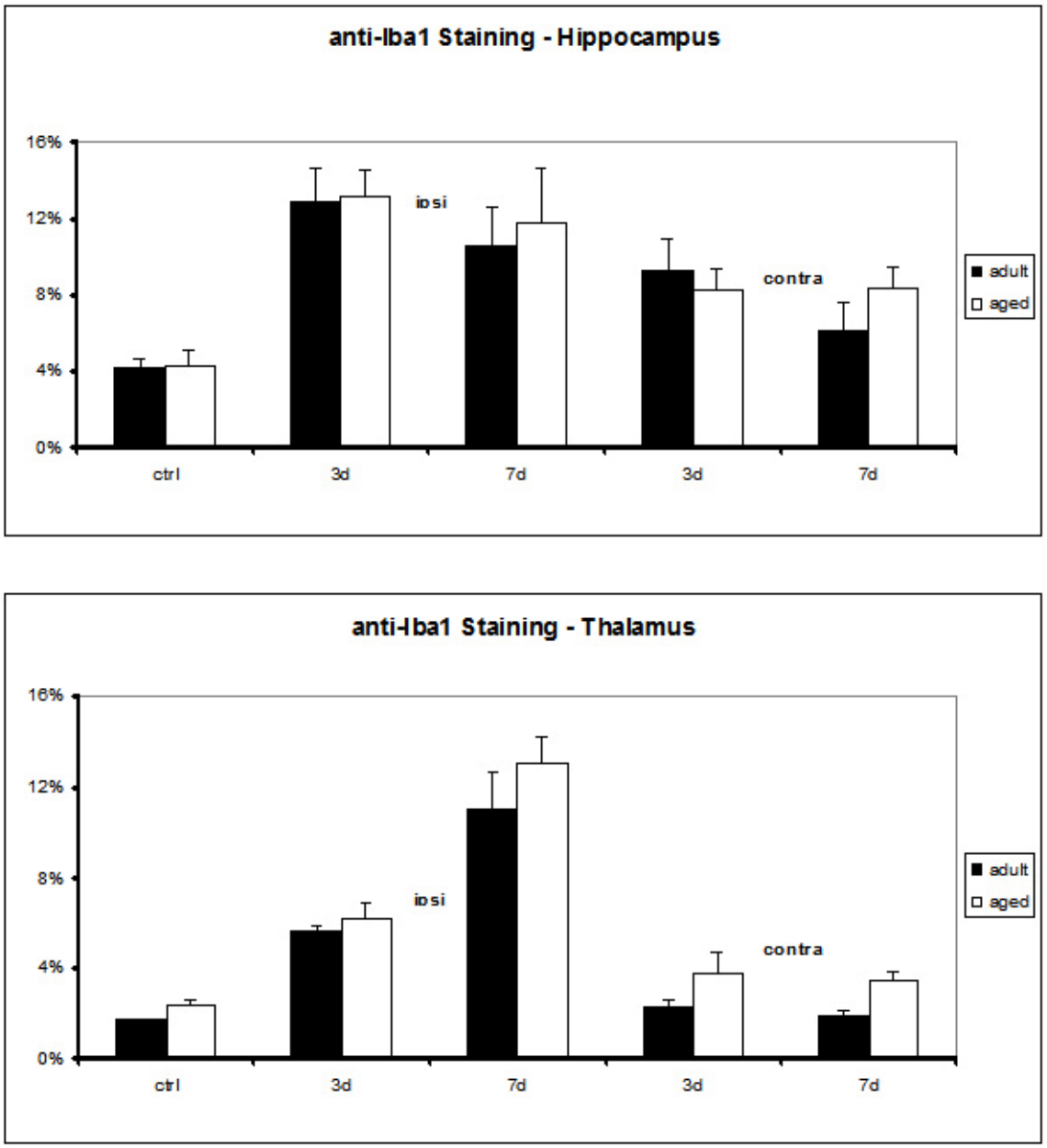

Figure 9: Measurements of anti-Iba1 staining in ipsilateral and contralateral hippocampus (A) and thalamus (B). n=4 per group, except at 3 days n=6 per group.

References

Badan I, Buchhold B, Hamm A, Gratz M, Walker LC, Platt D, Kessler C, Popa-Wagner A (2003) Accelerated glial reactivity to stroke in aged rats correlates with reduced functional recovery. J Cereb Blood Flow Metab 23:845-854.

Bilgen M (2005) A new device for experimental modeling of central nervous system injuries. Neurorehabil Neural Repair 19:219-226.

Bramlett HM, Dietrich WD (2007) Progressive damage after brain and spinal cord injury: pathomechanisms and treatment strategies. Prog Brain Res 161:125-141.

Castejon OJ (1998) Morphological astrocytic changes in complicated human brain trauma. A light and electron microscopic study. Brain Inj 12:409-427; discussion 407.

Deng XH, Bertini G, Xu YZ, Yan Z, Bentivoglio M (2006) Cytokine-induced activation of glial cells in the mouse brain is enhanced at an advanced age. Neuroscience 141:645-661.

Eng LF, Ghirnikar RS (1994) GFAP and astrogliosis. Brain Pathol 4:229-237.

Faden AI (1993) Experimental neurobiology of central nervous system trauma. Crit Rev Neurobiol 7:175-186.

Floyd RA (1999) Neuroinflammatory processes are important in neurodegenerative diseases: an hypothesis to explain the increased formation of reactive oxygen and nitrogen species as major factors involved in neurodegenerative disease development. Free Radic Biol Med 26:1346-1355.

Floyd RA, Hensley K (2002) Oxidative stress in brain aging. Implications for therapeutics of neurodegenerative diseases. Neurobiol Aging 23:795-807.

Fotheringham AP, Davies CA, Davies I (2000) Oedema and glial cell involvement in the aged mouse brain after permanent focal ischaemia. Neuropathol Appl Neurobiol 26:412-423.

Franceschi C, Bonafe M, Valensin S, Olivieri F, De Luca M, Ottaviani E, De Benedictis G (2000) Inflamm-aging. An evolutionary perspective on immunosenescence. Ann N Y Acad Sci 908:244-254.

Franklin KBJ, Paxinos G (1997) The Mouse Brain in Stereotaxic Coordinates: Academic Press.

Fujita K, Yamauchi M, Matsui T, Titani K, Takahashi H, Kato T, Isomura G, Ando M, Nagata Y (1998) Increase of glial fibrillary acidic protein fragments in the spinal cord of motor neuron degeneration mutant mouse. Brain Res 785:31-40.

Galbraith S (1987) Head injuries in the elderly. Br Med J (Clin Res Ed) 294:325.

Gennarelli TA, Graham DI (1998) Neuropathology of the Head Injuries. Semin Clin Neuropsychiatry 3:160-175.

Gentleman SM, Leclercq PD, Moyes L, Graham DI, Smith C, Griffin WS, Nicoll JA (2004) Long-term intracerebral inflammatory response after traumatic brain injury. Forensic Sci Int 146:97-104.

Gomez CR, Boehmer ED, Kovacs EJ (2005) The aging innate immune system. Curr Opin Immunol.

Gong Y, Hua Y, Keep RF, Hoff JT, Xi G (2004) Intracerebral hemorrhage: effects of aging on brain edema and neurological deficits. Stroke 35:2571-2575.

Hall ED, Sullivan PG, Gibson TR, Pavel KM, Thompson BM, Scheff SW (2005) Spatial and temporal characteristics of neurodegeneration after controlled cortical impact in mice: more than a focal brain injury. J Neurotrauma 22:252-265.

Hamm RJ, Jenkins LW, Lyeth BG, White-Gbadebo DM, Hayes RL (1991) The effect of age on outcome following traumatic brain injury in rats. J Neurosurg 75:916-921.

Hamm RJ, White-Gbadebo DM, Lyeth BG, Jenkins LW, Hayes RL (1992) The effect of age on motor and cognitive deficits after traumatic brain injury in rats. Neurosurgery 31:1072-1077; discussion 1078.

Ito D, Tanaka K, Suzuki S, Dembo T, Fukuuchi Y (2001) Enhanced expression of Iba1, ionized calcium-binding adapter molecule 1, after transient focal cerebral ischemia in rat brain. Stroke 32:1208-1215.

Ito D, Imai Y, Ohsawa K, Nakajima K, Fukuuchi Y, Kohsaka S (1998) Microglia-specific localisation of a novel calcium binding protein, Iba1. Brain Res Mol Brain Res 57:1-9.

Kim KY, Ju WK, Neufeld AH (2004) Neuronal susceptibility to damage: comparison of the retinas of young, old and old/caloric restricted rats before and after transient ischemia. Neurobiol Aging 25:491-500.

Koistinaho M, Koistinaho J (2005) Interactions between Alzheimer's disease and cerebral ischemia--focus on inflammation. Brain Res Brain Res Rev 48:240-250.

Kyrkanides S, O'Banion MK, Whiteley PE, Daeschner JC, Olschowka JA (2001) Enhanced glial activation and expression of specific CNS inflammation-related molecules in aged versus young rats following cortical stab injury. J Neuroimmunol 119:269-277.

Laping NJ, Teter B, Anderson CP, Osterburg HH, O'Callaghan JP, Johnson SA, Finch CE (1994) Age-related increases in glial fibrillary acidic protein do not show proportionate changes in transcription rates or DNA methylation in the cerebral cortex and hippocampus of male rats. J Neurosci Res 39:710-717.

Lee JC, Cho GS, Choi BO, Kim HC, Kim YS, Kim WK (2006) Intracerebral hemorrhage-induced brain injury is aggravated in senescence-accelerated prone mice. Stroke 37:216-222.

Lenzlinger PM, Morganti-Kossmann MC, Laurer HL, McIntosh TK (2001) The duality of the inflammatory response to traumatic brain injury. Mol Neurobiol 24:169-181.

Lu L, Li J, Yew DT, Rudd JA, Mak YT (2007) Oxidative stress on the astrocytes in culture derived from a senescence accelerated mouse strain. Neurochem Int.

Lucas SM, Rothwell NJ, Gibson RM (2006) The role of inflammation in CNS injury and disease. Br J Pharmacol 147 Suppl 1:S232-240.

McIntosh TK, Smith DH, Garde E (1996) Therapeutic approaches for the prevention of secondary brain injury. Eur J Anaesthesiol 13:291-309.

McIntosh TK, Saatman KE, Raghupathi R, Graham DI, Smith DH, Lee VM, Trojanowski JQ (1998) The Dorothy Russell Memorial Lecture. The molecular and cellular sequelae of experimental traumatic brain injury: pathogenetic mechanisms. Neuropathol Appl Neurobiol 24:251-267.

Morganti-Kossman MC, Lenzlinger PM, Hans V, Stahel P, Csuka E, Ammann E, Stocker R, Trentz O, Kossmann T (1997) Production of cytokines following brain injury: beneficial and deleterious for the damaged tissue. Mol Psychiatry 2:133-136.

Mosenthal AC, Livingston DH, Lavery RF, Knudson MM, Lee S, Morabito D, Manley GT, Nathens A, Jurkovich G, Hoyt DB, Coimbra R (2004) The effect of age on functional outcome in mild traumatic brain injury: 6-month report of a prospective multicenter trial. J Trauma 56:1042-1048.

Narayana PA, Grill RJ, Chacko T, Vang R (2004) Endogenous recovery of injured spinal cord: longitudinal in vivo magnetic resonance imaging. J Neurosci Res 78:749-759.

Nichols NR, Day JR, Laping NJ, Johnson SA, Finch CE (1993) GFAP mRNA increases with age in rat and human brain. Neurobiol Aging 14:421-429.

Onyszchuk G, Al-Hafez B, He YY, Bilgen M, Berman NE, Brooks WM (2007) A mouse model of sensorimotor controlled cortical impact: characterization using longitudinal magnetic resonance imaging, behavioral assessments and histology. J Neurosci Methods 160:187-196.

Pekny M, Nilsson M (2005) Astrocyte activation and reactive gliosis. Glia 50:427-434.

Pennings JL, Bachulis BL, Simons CT, Slazinski T (1993) Survival after severe brain injury in the aged. Arch Surg 128:787-793; discussion 793-784.

Popa-Wagner A, Badan I, Walker L, Groppa S, Patrana N, Kessler C (2007) Accelerated infarct development, cytogenesis and apoptosis following transient cerebral ischemia in aged rats. Acta Neuropathol (Berl) 113:277-293.

Rapoport MJ, Herrmann N, Shammi P, Kiss A, Phillips A, Feinstein A (2006) Outcome after traumatic brain injury sustained in older adulthood: a one-year longitudinal study. Am J Geriatr Psychiatry 14:456-465.

Ridet JL, Malhotra SK, Privat A, Gage FH (1997) Reactive astrocytes: cellular and molecular cues to biological function. Trends Neurosci 20:570-577.

Rosenberg GA (2002) Matrix metalloproteinases and neuroinflammation in multiple sclerosis. Neuroscientist 8:586-595.

Schmidt OI, Heyde CE, Ertel W, Stahel PF (2005) Closed head injury--an inflammatory disease? Brain Res Brain Res Rev 48:388-399.

Shimamura M, Garcia JM, Prough DS, Hellmich HL (2004) Laser capture microdissection and analysis of amplified antisense RNA from distinct cell populations of the young and aged rat brain: effect of traumatic brain injury on hippocampal gene expression. Brain Res Mol Brain Res 122:47-61.

Streit WJ, Mrak RE, Griffin WS (2004) Microglia and neuroinflammation: a pathological perspective. J Neuroinflammation 1:14.

Sugama S, Yang L, Cho BP, DeGiorgio LA, Lorenzl S, Albers DS, Beal MF, Volpe BT, Joh TH (2003) Age-related microglial activation in 1-methyl-4-phenyl-1,2,3,6-tetrahydropyridine (MPTP)-induced dopaminergic neurodegeneration in C57BL/6 mice. Brain Res 964:288-294.

Susman M, DiRusso SM, Sullivan T, Risucci D, Nealon P, Cuff S, Haider A, Benzil D (2002) Traumatic brain injury in the elderly: increased mortality and worse functional outcome at discharge despite lower injury severity. J Trauma 53:219-223; discussion 223-214.

Switzer RC, 3rd (2000) Application of silver degeneration stains for neurotoxicity testing. Toxicol Pathol 28:70-83.

Topp KS, Faddis BT, Vijayan VK (1989) Trauma-induced proliferation of astrocytes in the brains of young and aged rats. Glia 2:201-211.

Tuppo EE, Arias HR (2005) The role of inflammation in Alzheimer's disease. Int J Biochem Cell Biol 37:289-305.

Uryu K, Giasson BI, Longhi L, Martinez D, Murray I, Conte V, Nakamura M, Saatman K, Talbot K, Horiguchi T, McIntosh T, Lee VM, Trojanowski JQ (2003) Age-dependent synuclein pathology following traumatic brain injury in mice. Exp Neurol 184:214-224.

Weydt P, Moller T (2005) Neuroinflammation in the pathogenesis of amyotrophic lateral sclerosis. Neuroreport 16:527-531.

Whitton PS (2007) Inflammation as a causative factor in the aetiology of Parkinson's disease. Br J Pharmacol 150:963-976.

VI – SUMMARY

A model of controlled cortical impact (CCI) was developed and characterized, for the study of traumatic brain injury (TBI) in mice. Experiments were performed with adult (4-6 months old) and aged (21-24 months old) mice, sham and injured, to study age-related differences in response to TBI. The time course of acute edema formation and resolution and the development of a fluid-filled lesion cavity were studied with high-field magnetic resonance (MR) scanning. Behavior was assessed with pre- and post-injury rotarod, gridwalk and spontaneous forelimb tests. Histological examinations were done to assess neurodegeneration, blood-brain barrier opening, astrocyte activation, microglial activation and total brain tissue loss. In all cases, results from aged animals were compared with results from adult animals to identify age-related differences.

The results for CCI model development and characterization demonstrated that a reliable and repeatable injury can be made with a linear motor-based impact device aimed at sensorimotor cortex. Additionally demonstrated were the value of longitudinal MR imaging as a technique for studying the evolution of damage after CCI in the mouse, and for measuring transient post-injury phenomena such as the formation and resolution of edema. Furthermore, it was shown that the simple battery of rotarod, gridwalk and spontaneous forelimb tests are adequate to record immediate sensorimotor impairment and subsequent recovery.

By comparing the behavioral deficits and recovery patterns of adult and aged mice, the results clearly show that the aged mice have poorer recovery. This is consistent with earlier studies of TBI (Hamm et al., 1992a) and hemorrhage (Gong et al., 2005) in aged rats. It is encouraging that the worsened functional recovery with aging found in the mouse model paralleled the clinical data, in which elderly survivors of TBI were found to have greater functional and cognitive impairments than those found in younger patients (Rapoport et al., 2006; Thompson et al., 2006). This fidelity adds to the credibility of the mouse model, and provides a context for future work to use the model for pre-clinical evaluations of therapeutic approaches devised specifically for the elderly TBI patient population.

MR imaging at 24 and 48 hours post-injury has been used to investigate acute edema at and near the site of injury. The results demonstrate that acute edema, measured by thresholding of T2-weighted spin echo images, is significantly slower to clear in the aged brains than in the adult. There is potentially an important clinical implication of this finding. Given that edema is accepted to play a the major role in the pathophysiology following TBI (Unterberg et al., 2004), and if post-injury edema clearance is slower in the aged human brain than in the adult, then perhaps a more aggressive management of edema in elderly TBI patients will have even more benefit than it does in younger patients.

The results show that neurodegeneration 3 days after CCI, assessed by densitometric measurement of images of aminocupric silver stained tissues, is significantly greater in the aged brains than in the adult. This is shown for measurements over the entire ipsilateral hemisphere and for only in the ipsilateral dorsal cortex. In contrast, total tissue loss at the injury site, assessed by measurement of lesion cavity volume from 3 day histological samples, is not significantly different between adult and aged brains. These measurements are made at a single post-injury time point, and provide only part of the picture of neuron damage and death. If silver staining is viewed as a "leading indicator" of damage, and tissue loss as a "lagging indicator", the results would suggest that the increased silver staining in the aged brains at 3 days post-injury would manifest as increased tissue loss at a later time.

Examining the trends in silver staining over time, in virtually all brain structures examined beyond the ipsilateral cortex, there sharp increases in staining, in the aged brains, at the 7 day post-injury time point. It is possible that there is an identifiable "second wave" of neurodegeneration, beginning between 3 and 7 days post-injury, and continuing for some time later. This would be consistent with recent evidence for prolonged damage processes and "progressive damage" following CNS injury (Bramlett and Dietrich, 2007). A future study of neurodegeneration and tissue loss at several time points beyond 7 days would provide a more complete answer to the question: "is there more neuron death and tissue loss in aged TBI?"

The results also show that there is a significantly greater post-injury increase in the opening of blood-brain barrier – at least to molecules up to 150 kDa in size – in the aged brains compared to the adult ones. The time course of anti-mouse IgG staining also suggests that the increased blood-brain barrier opening is prolonged in the aged brains. This may have important implications for damage processes, since a more open blood-brain barrier can imply increased opportunity for damage-causing cells and molecules to penetrate the brain parenchyma. If a more open blood-brain barrier in the aged brain is an important contributor to ultimate damage, then compounds that act to stabilize this barrier, such as cariporide (Scholz et al., 2007) or interferon beta (Kraus et al., 2004), may prove particularly beneficial in elderly patients.

The difficulty of compounds to cross the blood-brain barrier and reach their targets has been discussed as a possible reason for failure of so many clinical trials in TBI (Tolias and Bullock, 2004). In the aged brain, a greater and prolonged post-injury blood-brain barrier opening may provide a greater opportunity for therapeutic compounds, their downstream signaling molecules, and final effectors to enter into the brain and counteract damage cascades and/or assist repair processes.

The results also show a reduced astrocytic response in the aged brain following injury. The increase in GFAP staining above control levels was significantly less in the ipsilateral hippocampus of the aged animals, and not significantly less in the other brain regions studied. This likely reflects a combination of two effects: activation of

astrocytes in response to injury, and degeneration and demise of astrocytes as a result of the primary and secondary damage cascades. Given the "pro-inflammatory" state of the aged brain, one might expect a more pronounced increased in GFAP staining in the aged brain following CCI, but this was not evident. It may be that the findings reflect a "pro-inflammatory" state in the aged animal brains, with "primed" astrocytes, but in which the astrocytes have an age-related reduction in functional capacity, a concept discussed in the context of ischemia experiments in aged mice (Fotheringham et al., 2000).

The results do show a trend towards increased microglial response in the injured aged brain in the hippocampus and thalamus, remote from the site of cortical impact. The greatest differences in increase of microglial staining above control values between the age groups were found at 7 days post-injury, consistent with a delayed and/or prolonged neuroinflammatory response, not masked by a counteracting effect related to microglial vulnerability. Although a subtle point, the flat trend of microglial staining from 3 to 7 days post-injury in the aged animals contrasts with the falling trend observed in the adult, providing further support to the interpretation of a delayed and/or prolonged neuroinflammatory response. Such a response would be consistent with the results of other investigations in aged mice which demonstrated exaggerated and/or prolonged release of microglial-originated pro-inflammatory cytokines following inflammatory challenge or trauma (Sandhir et al., 2004; Godbout et al., 2005).

It is interesting to compare the results with other pre-clinical studies of aging and brain injury. The CCI-injured aged mouse behavioral results are similar to those of 20-month old rats subjected to a middle cerebral artery occlusion (MCAO) stroke model – greater deficits and less recovery - whereas the immunohistochemistry results differ, in that an accelerated astrocytic and microglial response was not detected, peaking during the first week after injury (Badan et al., 2003). The results are also consistent with those in a study of MCAO in 26-31-month old mice, in which aged mice were found to exhibit greater brain swelling, greater edema at 24 hours, but equal lesion size, compared to 4-6 month old mice (Fotheringham et al., 2000).

To interpret the ensemble of data from these experiments, and especially the possible linkages between events at the molecular, cellular and tissue levels and functional outcomes, it is important to bear in mind additional mechanisms with potentially significant contributions. For example, the contribution of adaptive plasticity to the post-injury recovery from functional impairment was not directly studied in the experiments, but its importance is well-established in clinical and pre-clinical research (Bury and Jones, 2002; Frost et al., 2003; Nudo, 2003; Dancause, 2006). It is possible that part of the behavioral results could be explained by a reduced capacity for plasticity and reorganization in the aged brain. A study with ischemia in aged rats showed that a plasticity-enhancing treatment, anti-Nogo-A therapy, was effective at

improving skilled forelimb reaching scores and at increasing thalamic activation during affected forepaw stimulation (Markus et al., 2005).

Taking the results for edema, blood-brain barrier, and silver staining together, there is strong evidence for increased activation of damage mechanisms and increased acute neurodegeneration in the aged brains compared to the adult. The data for neuroinflammation suggest a reduced astroglial and a trend towards increased microglial response in the aged brains. It is difficult to project what the neurodegeneration and neuroinflammation might be at 14 and 28 days post-injury, but the trends suggest that there may be additional, possibly greater age-related differences at those times.

It is not possible to make cause and effect conclusions from imaging, histological and behavioral data; however the parallel age-related findings in the behavior and histological experiments are not likely coincidental. Experiments with interventions that act to reduce edema, stabilize the blood-brain barrier or support early astrocyte function, would allow for a more definitive investigation of the extent to which these mechanistic elements are causally linked to functional outcomes. This work has laid the foundation for those follow-on studies. If these findings translate to the clinical setting, it may be that some existing experimental treatments that have low or marginal success in younger patients show more significant benefit in elderly patients. It may be that compounds which control edema, support the blood-brain

barrier, or promote astrocyte viability and function show greater effect in elderly than in younger patients, particularly those with focal contusions.

Traumatic brain injury, even with its huge and growing burden, places a distant second to stroke in terms of being understood to have increasing incidence, morbidity and mortality with increasing age. Pre-clinical research activity in TBI mechanisms and outcomes in aged animals is surprisingly low. It is vital that the mechanisms of damage and recovery after injury to the aged brain be more fully described and understood. Only then can successful acute and post-acute interventions and therapies be developed for elderly TBI survivors.

References

Badan I, Buchhold B, Hamm A, Gratz M, Walker LC, Platt D, Kessler C, Popa-Wagner A (2003) Accelerated glial reactivity to stroke in aged rats correlates with reduced functional recovery. J Cereb Blood Flow Metab 23:845-854.

Bramlett HM, Dietrich WD (2007) Progressive damage after brain and spinal cord injury: pathomechanisms and treatment strategies. Prog Brain Res 161:125-141.

Bury SD, Jones TA (2002) Unilateral sensorimotor cortex lesions in adult rats facilitate motor skill learning with the "unaffected" forelimb and training-induced dendritic structural plasticity in the motor cortex. J Neurosci 22:8597-8606.

Dancause N (2006) Neurophysiological and anatomical plasticity in the adult sensorimotor cortex. Rev Neurosci 17:561-580.

Fotheringham AP, Davies CA, Davies I (2000) Oedema and glial cell involvement in the aged mouse brain after permanent focal ischaemia. Neuropathol Appl Neurobiol 26:412-423.

Frost SB, Barbay S, Friel KM, Plautz EJ, Nudo RJ (2003) Reorganization of remote cortical regions after ischemic brain injury: a potential substrate for stroke recovery. J Neurophysiol 89:3205-3214.

Godbout JP, Chen J, Abraham J, Richwine AF, Berg BM, Kelley KW, Johnson RW (2005) Exaggerated neuroinflammation and sickness behavior in aged mice following activation of the peripheral innate immune system. Faseb J 19:1329-1331.

Gong Y, Xi GH, Keep RF, Hoff JT, Hua Y (2005) Aging enhances intracerebral hemorrhage-induced brain injury in rats. Acta Neurochir Suppl 95:425-427.

Hamm RJ, White-Gbadebo DM, Lyeth BG, Jenkins LW, Hayes RL (1992) The effect of age on motor and cognitive deficits after traumatic brain injury in rats. Neurosurgery 31:1072-1077; discussion 1078.

Kraus J, Ling AK, Hamm S, Voigt K, Oschmann P, Engelhardt B (2004) Interferon-beta stabilizes barrier characteristics of brain endothelial cells in vitro. Ann Neurol 56:192-205.

Markus TM, Tsai SY, Bollnow MR, Farrer RG, O'Brien TE, Kindler-Baumann DR, Rausch M, Rudin M, Wiessner C, Mir AK, Schwab ME, Kartje GL (2005) Recovery and brain reorganization after stroke in adult and aged rats. Ann Neurol 58:950-953.

Nudo RJ (2003) Adaptive plasticity in motor cortex: implications for rehabilitation after brain injury. J Rehabil Med:7-10.

Rapoport MJ, Herrmann N, Shammi P, Kiss A, Phillips A, Feinstein A (2006) Outcome after traumatic brain injury sustained in older adulthood: a one-year longitudinal study. Am J Geriatr Psychiatry 14:456-465.

Sandhir R, Puri V, Klein RM, Berman NE (2004) Differential expression of cytokines and chemokines during secondary neuron death following brain injury in old and young mice. Neurosci Lett 369:28-32.

Scholz M, Cinatl J, Schadel-Hopfner M, Windolf J (2007) Neutrophils and the blood-brain barrier dysfunction after trauma. Med Res Rev 27:401-416.

Thompson HJ, McCormick WC, Kagan SH (2006) Traumatic brain injury in older adults: epidemiology, outcomes, and future implications. J Am Geriatr Soc 54:1590-1595.

Tolias CM, Bullock MR (2004) Critical appraisal of neuroprotection trials in head injury: what have we learned? NeuroRx 1:71-79.

Unterberg AW, Stover J, Kress B, Kiening KL (2004) Edema and brain trauma. Neuroscience 129:1021-1029.